從蛋白質微陣列晶片至單一分子奈米陣列-應用於癌症篩檢

From Protein Micro Array to Protein Single Molecule Array-for early cancer detection

Prof. Fan-Gang Tseng

曾繁根 教授

Engineering and System Science Dept./
Institute of NEMS
National Tsing Hua University, Taiwan
國立清華大學 工科系/奈微所
Institute of Applied Science, Academia Sinica, Taiwan
中研院應科中心

03.27.2008

Outline

- Surface tension dominate Micro/Nano Fluidic Systems
- 3-in-1 Protein Chip
  - Micro filling chip
  - Micro stamper chip
  - Micro bio-reaction chip
- Single Protein Molecule Array

微奈米流體系統Micro/Nano fluidic systems

類比(連續)式微流體系統
Continuous Fluidic Systems

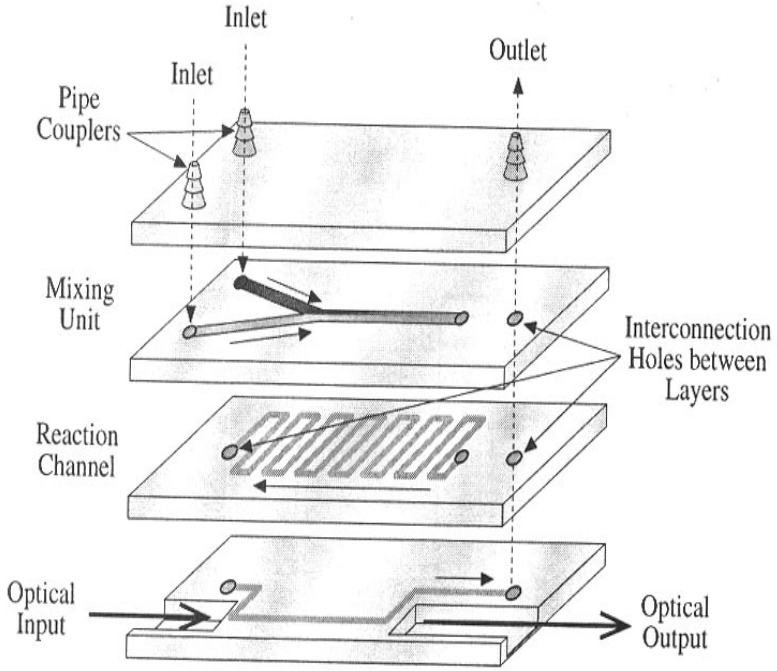

μTransducers sourcebook, 98

液珠控制系統⇔ 連續流體系統

1. 計量精確控制 (metering issue)
2. 較少因接觸所產生之摩擦阻力、表面反應、及氣泡阻塞問題(surface tension, friction, surface interaction issues)
3. 較簡單之流體系統 (System integration)

數位式微流體系統
Digital Fluidic Systems

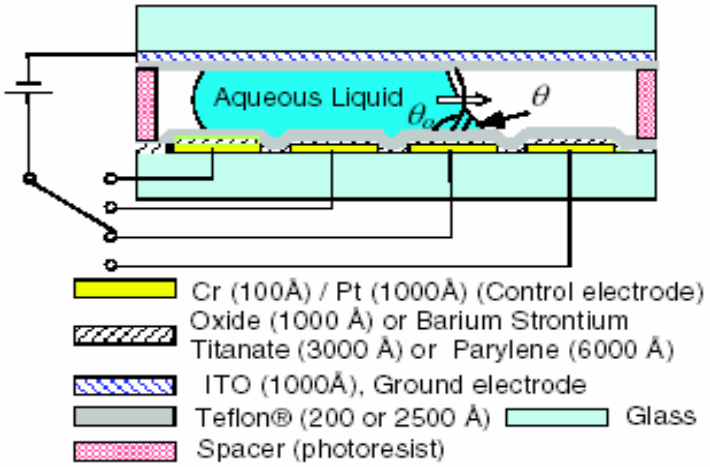

EWOD, CJ Kim, UCLA

Introduction

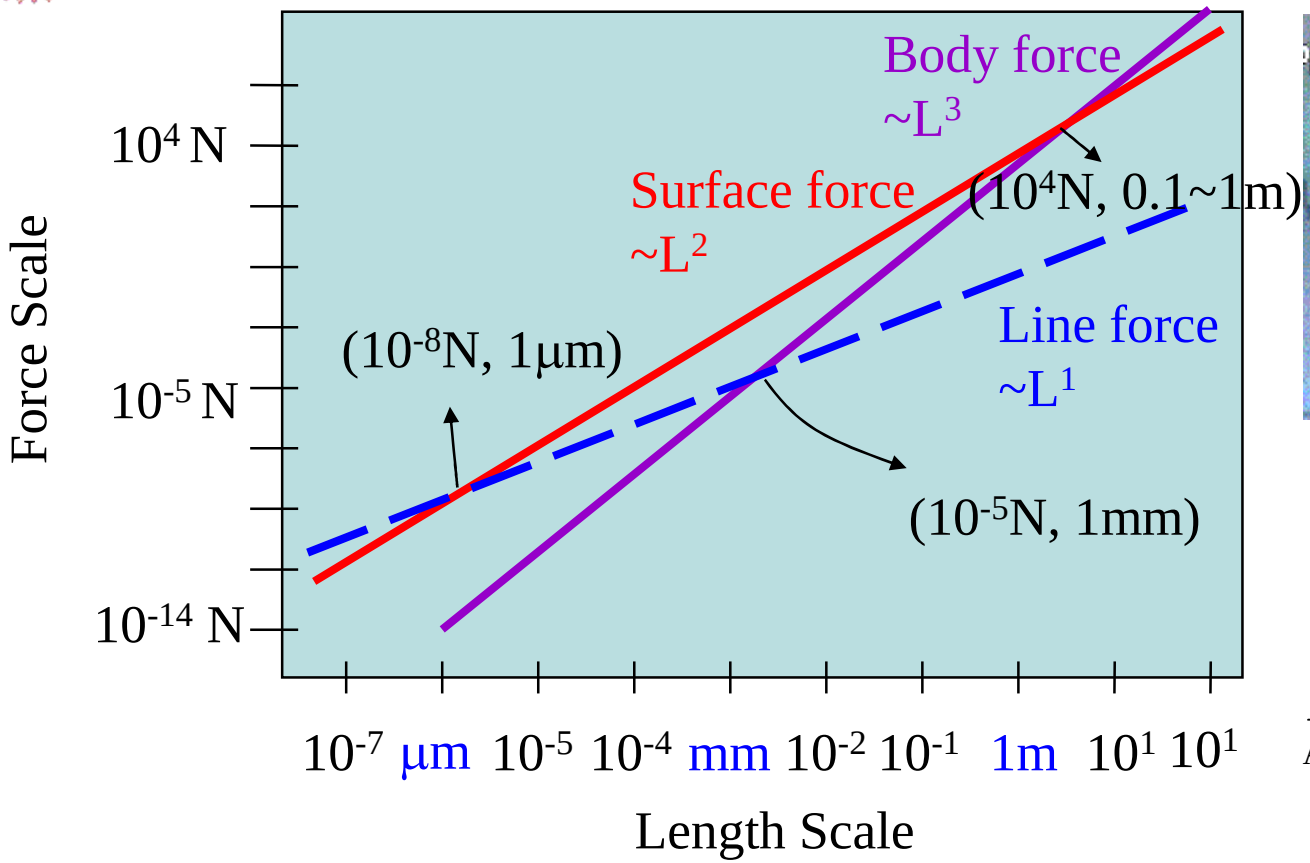

Mercury motor

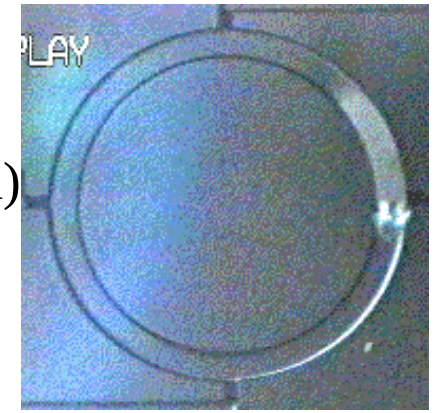

J. Lee, and C.-J. Kim,
J of MEMS, June 2000

Slug flow

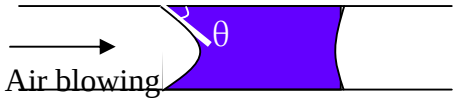

Surface tension force (line force) is dominate in nano scale and important in micro scale!!

F. Tseng, Nanomechanics 04, ACPOT'06

Role of Surface Tension in Micro/nano Scale

Line force/body force

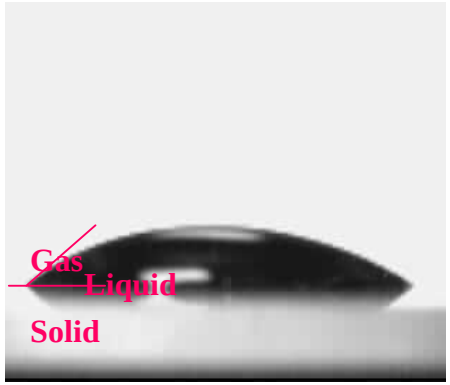

$F_s = \sigma(\pi D)\sin\theta$

$F_b \sim \pi D^3$

$F_s/F_b = 1/D^2$

Drug delivery or bio-sample transportation

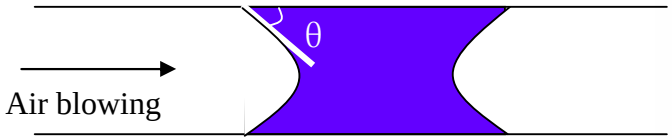

1. Air blowing to provide clean actuation
2. Precise dosage control
3. Less distance limitation
4. Surface tension is one of the dominate forces
5. Dynamic contact angle between liquid and channel wall

Surface Tension Driven Hg slug

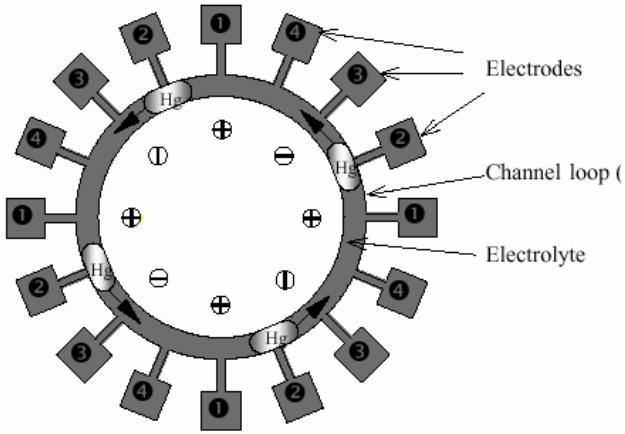

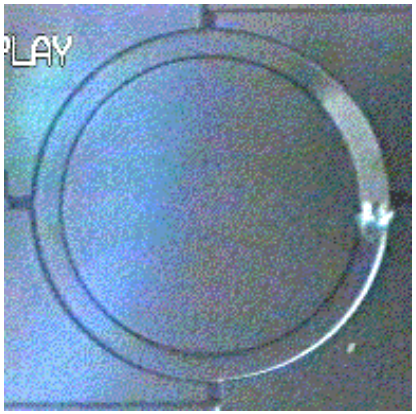

J. Lee, and C.-J. Kim,
J of MEMS, June 2000

Capillary stop valve

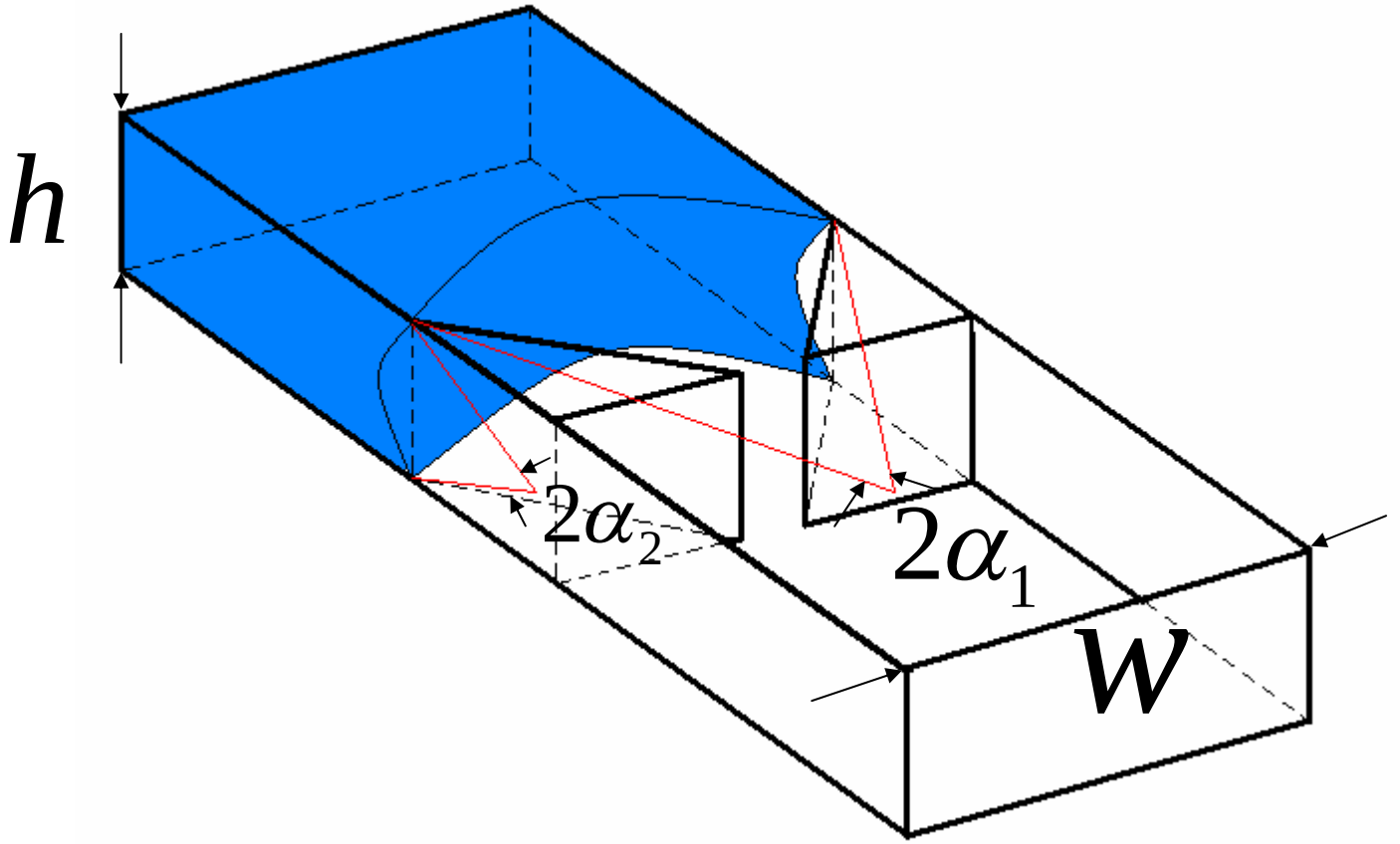

Pressure Barrier Calculation

- **U_T is the total interfacial energy of the system and Young's equation**

$$\begin{cases} U_T = A_{sl}\gamma_{sl} + A_{sa}\gamma_{sa} + A_{la}\gamma_{la} \\ \gamma_{sa} = \gamma_{sl} + \gamma_{la}\cos\theta_c \end{cases}$$

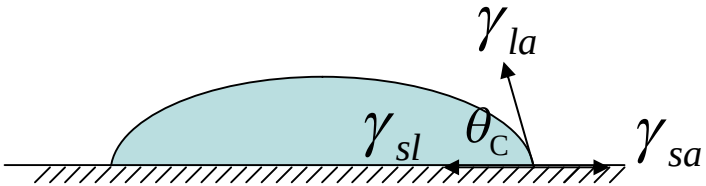

$$\Rightarrow U_T = (A_{sl} + A_{sa})\gamma_{sa} - A_{sl}\gamma_{la}\cos\theta_c + A_{la}\gamma_{la}$$
$$= U_o - A_{sl}\gamma_{la}\cos\theta_c + A_{la}\gamma_{la}$$

U_o is constant since the sum $A_{sl}+A_{sa}$ remains invariant

$$P = -\frac{dU_T}{dV_l} = \gamma_{la}\left(\cos\theta_c \frac{dA_{sl}}{dV_l} - \frac{dA_{la}}{dV_l}\right)$$

In order to stop the flow, we have to make P become negative.

- **contact angle $\theta_c \geqq 90°$ (stop in channel flow)**
- **A_{la} increase more than A_{sl} for given volume change**

Process of capillary flow

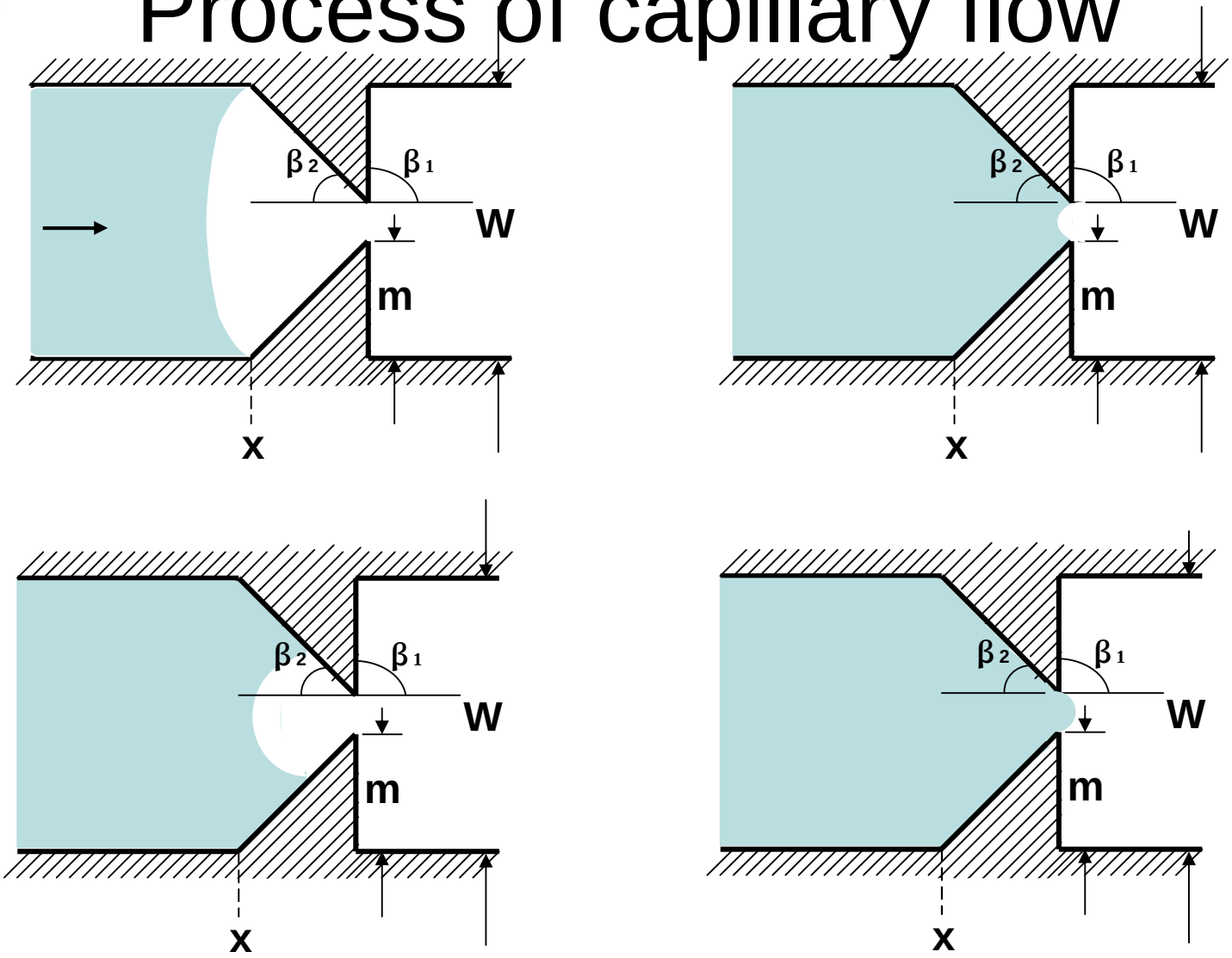

B1=45 °and B2=90 °

hn is the height of the channel and 2α is the curvature of the meniscus

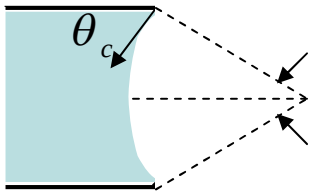

$$2\alpha_1 \Rightarrow \alpha_1 = \frac{\pi}{2} - \theta_c$$

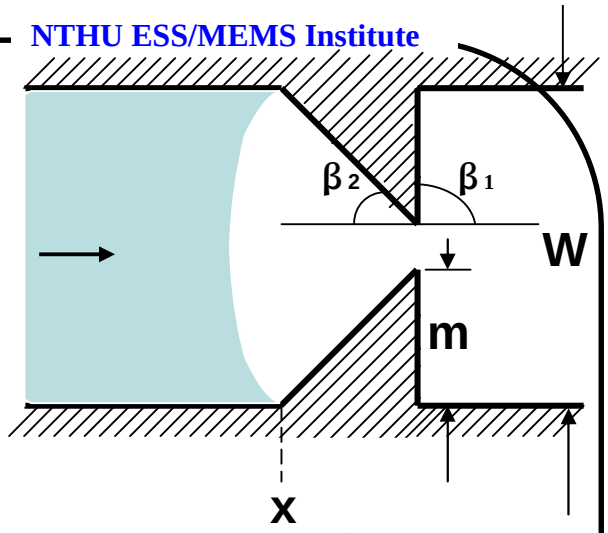

$$\begin{cases} A_{sl} = 2x(w+h) - \frac{1}{2}w^2\left(\frac{\alpha_1}{\sin^2\alpha_1} - \frac{\cos\alpha_1}{\sin\alpha_1}\right) - \frac{1}{2}h^2\left(\frac{\alpha_2}{\sin^2\alpha_2} - \frac{\cos\alpha_2}{\sin\alpha_2}\right) \\ A_{la} = wh\frac{\alpha_1\alpha_2}{\sin\alpha_1\sin\alpha_2} \end{cases}$$

$$\Rightarrow U_T = U_o - \gamma_{la}\cos\theta_c\left[2x(w+h) - \frac{1}{2}w^2\left(\frac{\alpha_1}{\sin^2\alpha_1} - \frac{\cos\alpha_1}{\sin\alpha_1}\right) - \frac{1}{2}h^2\left(\frac{\alpha_2}{\sin^2\alpha_2} - \frac{\cos\alpha_2}{\sin\alpha_2}\right)\right] + wh\gamma_{la}\frac{\alpha_1\alpha_2}{\sin\alpha_1\sin\alpha_2}$$

$$V_l = wxh - \frac{w^2h}{4\sin\alpha_1}\left(\frac{\alpha_1}{\sin\alpha_1} - \cos\alpha_1\right) - \frac{wh^2\alpha_2}{4\sin\alpha_1\sin\alpha_2}\left(\frac{\alpha_2}{\sin\alpha_2} - \cos\alpha_2\right)$$

$$\Rightarrow P = -\frac{dU_T}{dV_l} = \gamma_{la}\left(\cos\theta_c\frac{dA_{sl}}{dV_l} - \frac{dA_{la}}{dV_l}\right) > 0 \text{ if } \theta_c < 90^0 \text{ (straight channel flow)}$$

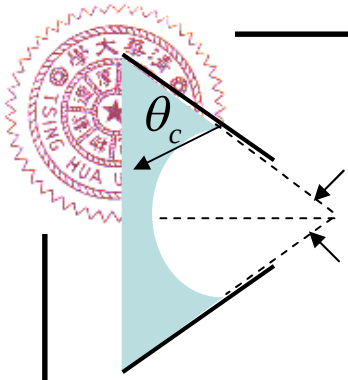

$$\Rightarrow \alpha_1' = \frac{\pi}{2} - \beta_2 - \theta_c$$

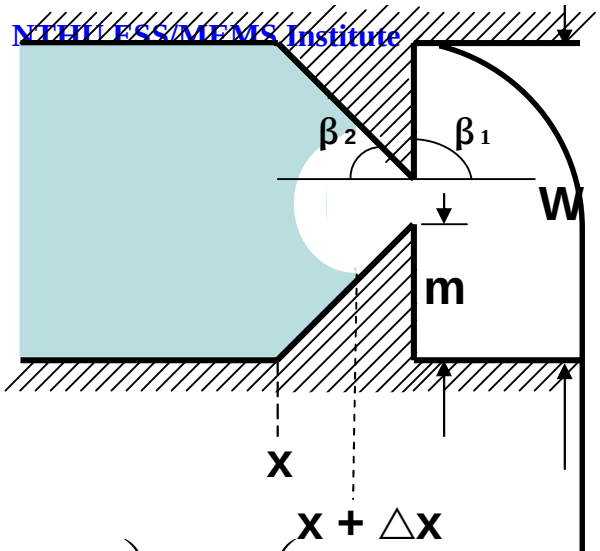

$$\begin{cases} A_{la} = \left(w - 2\Delta x \tan\beta_2\right) h \dfrac{\alpha_1'\alpha_2}{\sin\alpha_1' \sin\alpha_2} \\ A_{sl} = 2\left(x+\Delta x\right) w - 2\Delta x^2 \tan\beta_2 - \dfrac{1}{2} w^2 \left(\dfrac{\alpha_1'}{\sin^2\alpha_1'} - \dfrac{\cos\alpha_1'}{\sin\alpha_1'} \right) + 2h\left(x + \dfrac{\Delta x}{\cos\beta_2} \right) - \dfrac{1}{2} h^2 \left(\dfrac{\alpha_2}{\sin^2\alpha_2} - \dfrac{\cos\alpha_2}{\sin\alpha_2} \right) \end{cases}$$

$$\Rightarrow U_T = U_o - \gamma_{la}\cos\theta_c [2\left(x+\Delta x\right) w - 2\Delta x^2 \tan\beta_2 - \frac{1}{2} w^2 \left(\frac{\alpha_1'}{\sin^2\alpha_1'} - \frac{\cos\alpha_1'}{\sin\alpha_1'} \right) + 2h\left(x + \frac{\Delta x}{\cos\beta_2} \right) - \frac{1}{2} h^2 \left(\frac{\alpha_2}{\sin^2\alpha_2} - \frac{\cos\alpha_2}{\sin\alpha_2} \right)] + \gamma_{la} \left[\left(w - 2\Delta x \tan\beta_2\right) h \frac{\alpha_1'\alpha_2}{\sin\alpha_1' \sin\alpha_2} \right]$$

$$V_l = wh\left(x+\Delta x\right) - \Delta x^2 \tan\beta_2 h - \frac{\left(w - 2\Delta x \tan\beta_2\right)^2 h}{4\sin\alpha_1'} \left(\frac{\alpha_1'}{\sin\alpha_1'} - \cos\alpha_1' \right) - \frac{\left(w - 2\Delta x \tan\beta_2\right) h^2 \alpha_2}{4\sin\alpha_1' \sin\alpha_2} \left(\frac{\alpha_2}{\sin\alpha_2} - \cos\alpha_2 \right)$$

$$\Rightarrow P = -\frac{dU_T}{dV_l} = \gamma_{la}\left(\cos\theta_c \frac{dA_{sl}}{dV_l} - \frac{dA_{la}}{dV_l} \right) > 0 \quad \textbf{if } \theta_c < \frac{\pi}{2} - \beta_2 \text{(contract channel flow)}$$

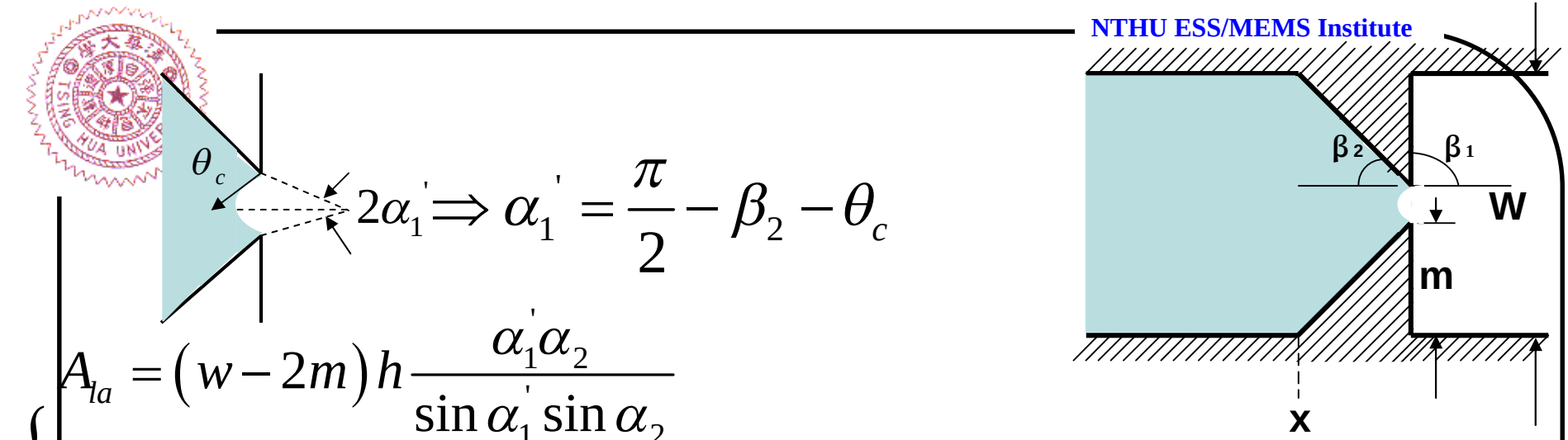

$$2\alpha_1' \Rightarrow \alpha_1' = \frac{\pi}{2} - \beta_2 - \theta_c$$

$$A_{la} = (w-2m)\,h\,\frac{\alpha_1'\alpha_2}{\sin\alpha_1'\sin\alpha_2}$$

$$\begin{cases} A_{sl} = 2\left(x+\dfrac{m}{\tan\beta_2}\right)w - \dfrac{2m^2}{\tan\beta_2} - \dfrac{1}{2}(w-2m)^2\left(\dfrac{\alpha_1'}{\sin^2\alpha_1'} - \dfrac{\cos\alpha_1'}{\sin\alpha_1'}\right) + 2h\left(x+\dfrac{m}{\sin\beta_2}\right) - \dfrac{1}{2}h^2\left(\dfrac{\alpha_2}{\sin^2\alpha_2} - \dfrac{\cos\alpha_2}{\sin\alpha_2}\right) \\ \Rightarrow U_T = U_o - \gamma_{la}\cos\theta_c\left[2\left(x+\dfrac{m}{\tan\beta}\right)w - \dfrac{2m^2}{\tan\beta_2} - \dfrac{1}{2}(w-2m)^2\left(\dfrac{\alpha_1'}{\sin^2\alpha_1'} - \dfrac{\cos\alpha_1'}{\sin\alpha_1'}\right) + 2h\left(x+\dfrac{m}{\sin\beta_2}\right) - \dfrac{1}{2}h^2\left(\dfrac{\alpha_2}{\sin^2\alpha_2} - \dfrac{\cos\alpha_2}{\sin\alpha_2}\right)\right] + \gamma_{la}\left[(w-2m)\,h\,\dfrac{\alpha_1'\alpha_2}{\sin\alpha_1'\sin\alpha_2}\right] \end{cases}$$

$$V_l = wh\left(x+\frac{m}{\tan\beta_2}\right) - \frac{m^2h}{\tan\beta_2} - \frac{(w-2m)^2\,h}{4\sin\alpha_1'}\left(\frac{\alpha_1'}{\sin\alpha_1'} - \cos\alpha_1'\right) - \frac{(w-2m)\,h^2\alpha_2}{4\sin\alpha_1'\sin\alpha_2}\left(\frac{\alpha_2}{\sin\alpha_2} - \cos\alpha_2\right)$$

$$\Rightarrow P = -\frac{dU_T}{dV_l} = \gamma_{la}\left(\cos\theta_c\,\frac{dA_{sl}}{dV_l} - \frac{dA_{la}}{dV_l}\right) > 0 \quad \text{if } \theta_c < \frac{\pi}{2} - \beta_2 \text{ (contract channel flow)}$$

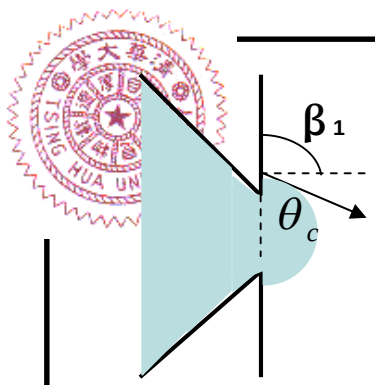

$$\Rightarrow \alpha_1'' = \frac{\pi}{2} - \theta_c - \beta_1$$

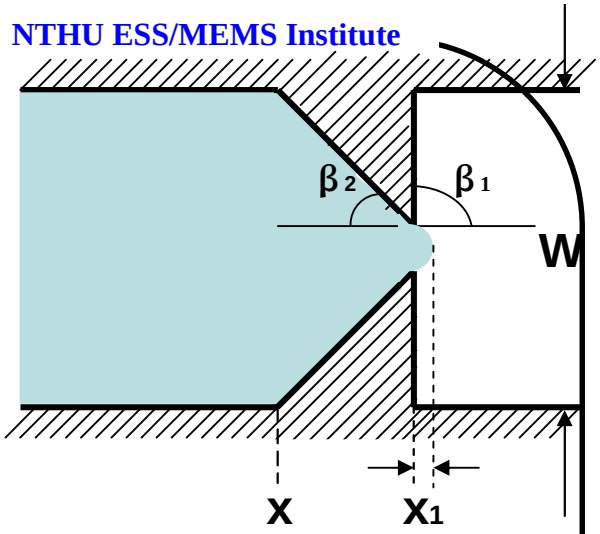

$$\begin{cases} A_{la} = \left(w - 2m + 2x_1 \tan\beta_1\right) h \dfrac{\alpha_1'' \alpha_2}{\sin\alpha_1'' \sin\alpha_2} \\ A_{sl} = 2\left(x + \dfrac{m}{\tan\beta_2}\right) w - \dfrac{2m^2}{\tan\beta_2} + 2\left(w - 2m + x_1\tan\beta_1\right) x_1 - \dfrac{1}{2}\left(w - 2m + 2x_1\tan\beta_1\right)^2 \left(\dfrac{\alpha_1''}{\sin^2\alpha_1''} - \dfrac{\cos\alpha_1''}{\sin\alpha_1''}\right) \\ \qquad + 2h\left(x + \dfrac{m}{\sin\beta_2} + \dfrac{2x_1}{\cos\beta_1}\right) - \dfrac{1}{2}h^2\left(\dfrac{\alpha_2}{\sin^2\alpha_2} - \dfrac{\cos\alpha_2}{\sin\alpha_2}\right) \end{cases}$$

$$\Rightarrow U_T = U_o - A_{sl}\gamma_{la}\cos\theta_c + A_{la}\gamma_{la}$$

$$V_l = wh\left(x + \frac{m}{\tan\beta_2}\right) - \frac{m^2 h}{\tan\beta_2} + hx_1\left(w - 2m + x_1\tan\beta_1\right) - \frac{\left(w - 2m + 2x_1\tan\beta_1\right)^2 h}{4\sin\alpha_1''}\left(\frac{\alpha_1''}{\sin\alpha_1''} - \cos\alpha_1''\right)$$
$$- \frac{\left(w - 2m + 2x_1\tan\beta_1\right) h^2 \alpha_2}{4\sin\alpha_1''\sin\alpha_2}\left(\frac{\alpha_2}{\sin\alpha_2} - \cos\alpha_2\right)$$

For $\alpha_2 \Rightarrow \dfrac{\pi}{2} - \theta_c \geq \alpha_2 \geq \theta_c - \dfrac{\pi}{2}$

To stop the flow, make $P \leq 0 \Rightarrow$ **The critical angle** $\beta_{1c} \geq \dfrac{\pi}{2} - \theta_c$ (Stop flow)

Capillary barrier_3D modeling

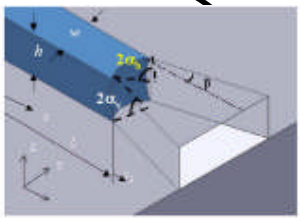

(a)

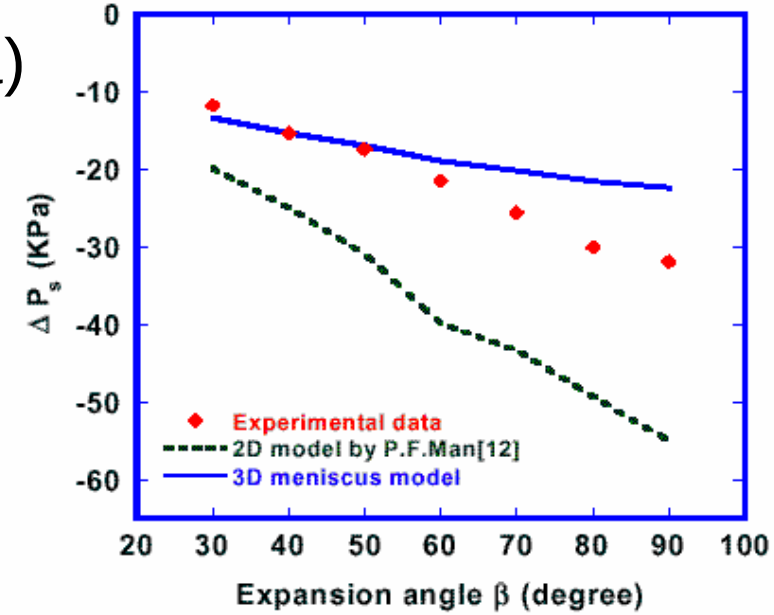

(b)

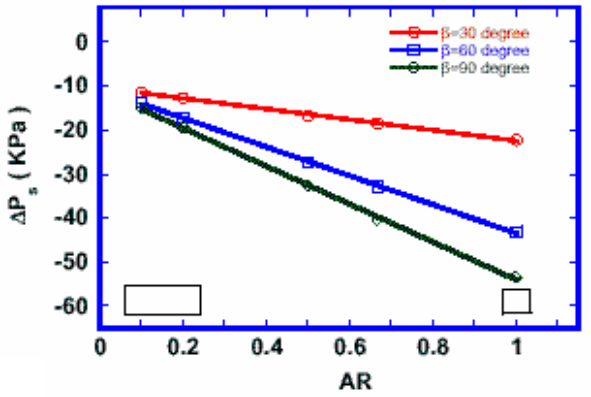

(c)

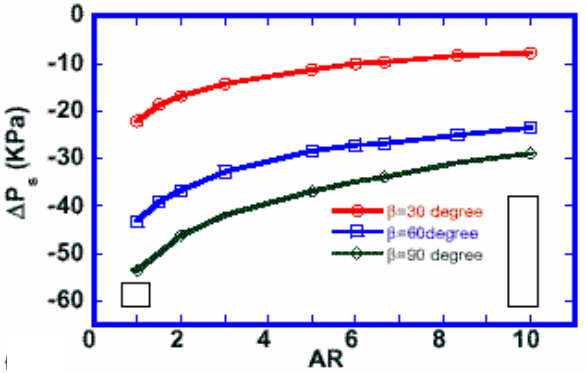

(a) 流道擴張角越大, 壓力屏障越大

(b) when AR<1, 流道越寬, 壓力屏障越小

(c) when AR>1, 流道厚度越厚, 壓力屏障越小

$$AR = \frac{channel\ Height}{channel\ Width}$$

(T.S. Leu; Sensors and Actuators A vol.115, 2004, p508-515)

Capillary burst valve_ Experiment

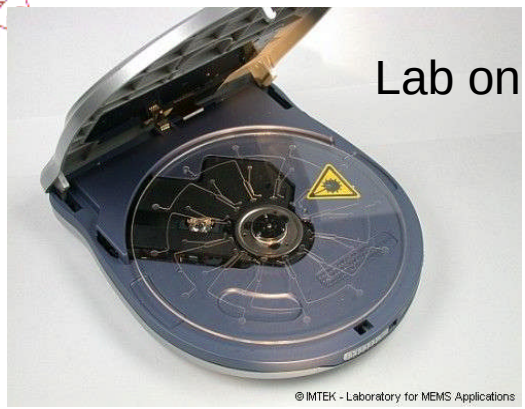

Lab on a CD

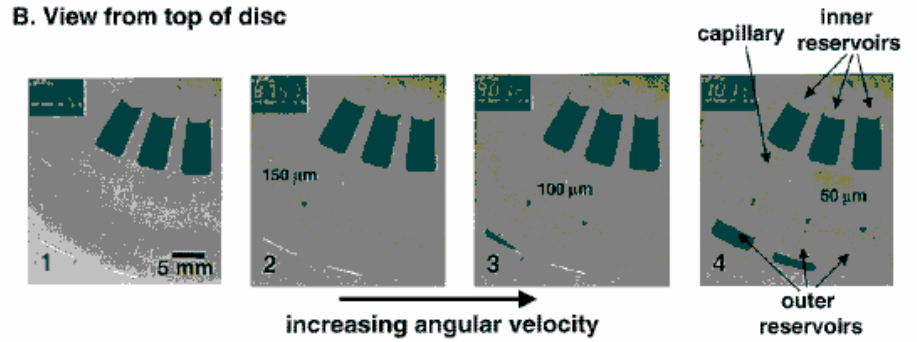

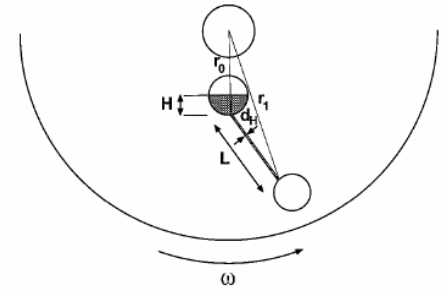

利用離心力來得知要破出此屏障所需壓力值

當轉速加快後 較細的流道才有液體流出
(流道寬度越小時 壓力屏障越大)

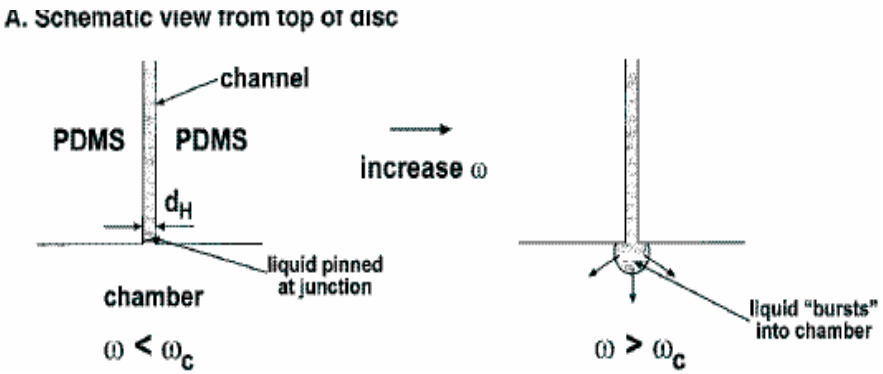

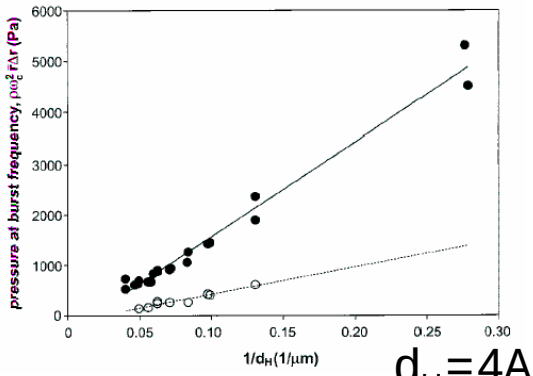

A: the cross-section area of the channel

P: perimeter of the channel

$d_H = 4A/P$

d_H 值越小, 壓力屏障越大

(D.C. Duffy; Anal. Chem. vol.71 1999, p4669)

Surface tension energy of the interface

(a) 疏水性流道管壁

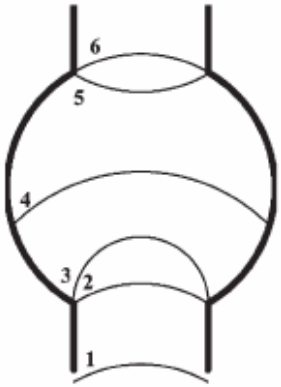

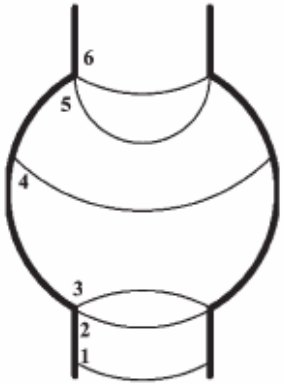

(b) 親水性流道管壁

要填滿此valve在各階段所需能量

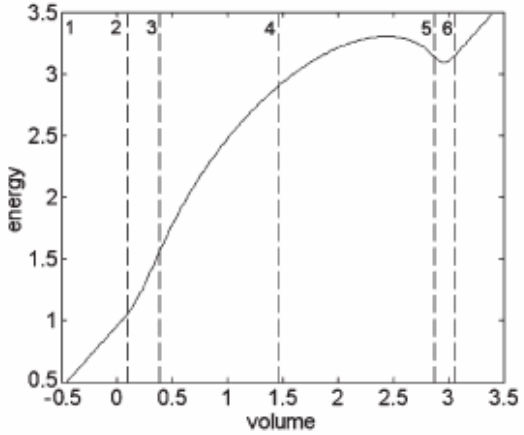

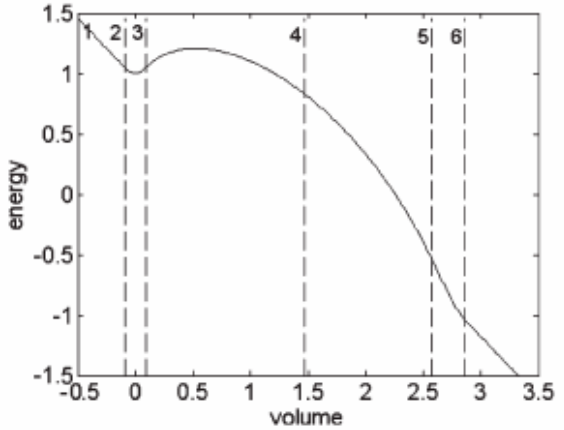

該階段的表面能

Simulation of the filling

(I. Treise; Lab on a chip, vol.5, 2005, p285-297)

數位微流體系統
(Digital Micro Fluidic Systems)

1. 液珠產生

2. 液珠懸浮控制

3. 液珠平面控制

Droplet generators

HP

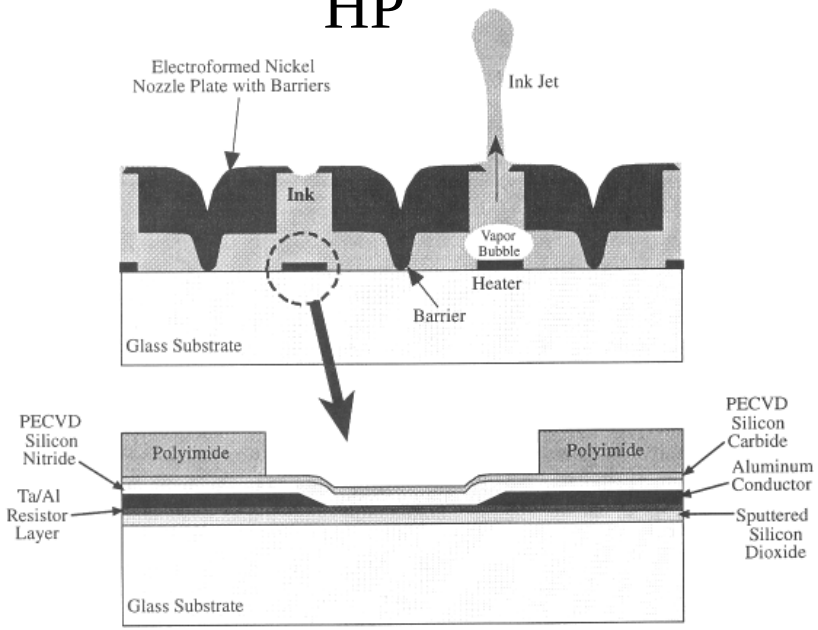

Epson

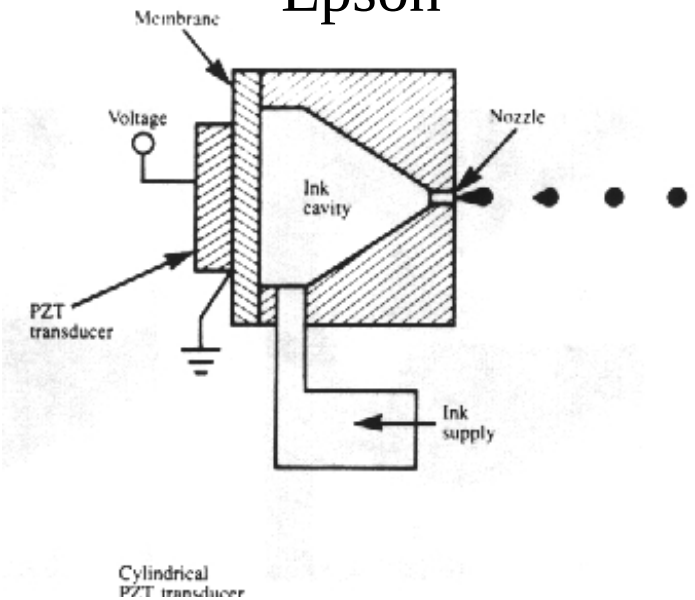

Sharp, Inc, MEMS 96

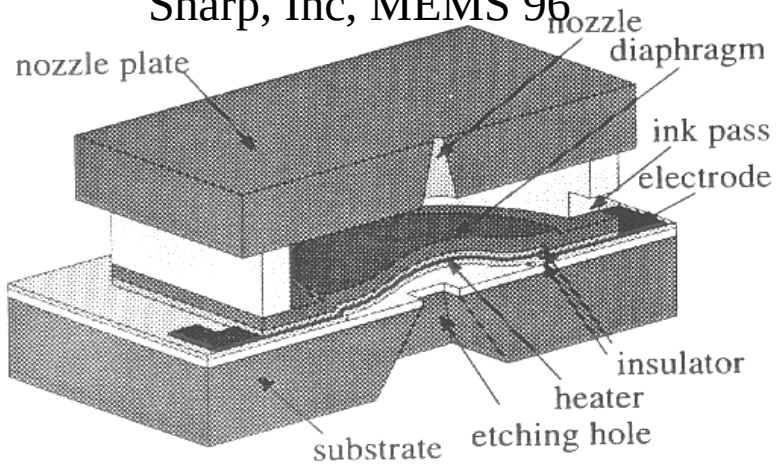

E.S. Kim, USC, MEMS98

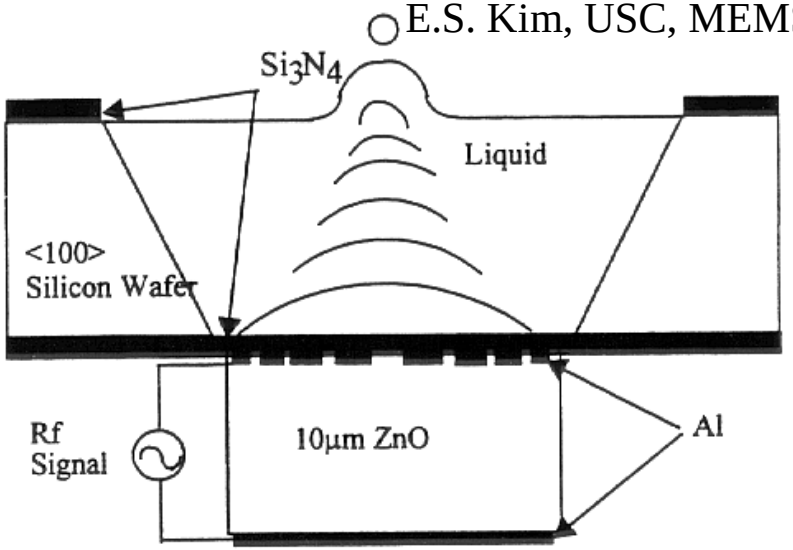

微液珠產生器

HP

F. G. Tseng

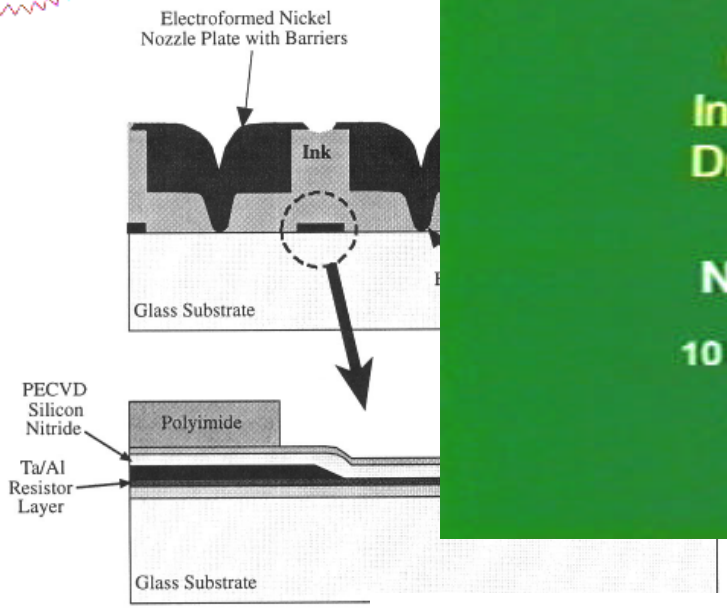

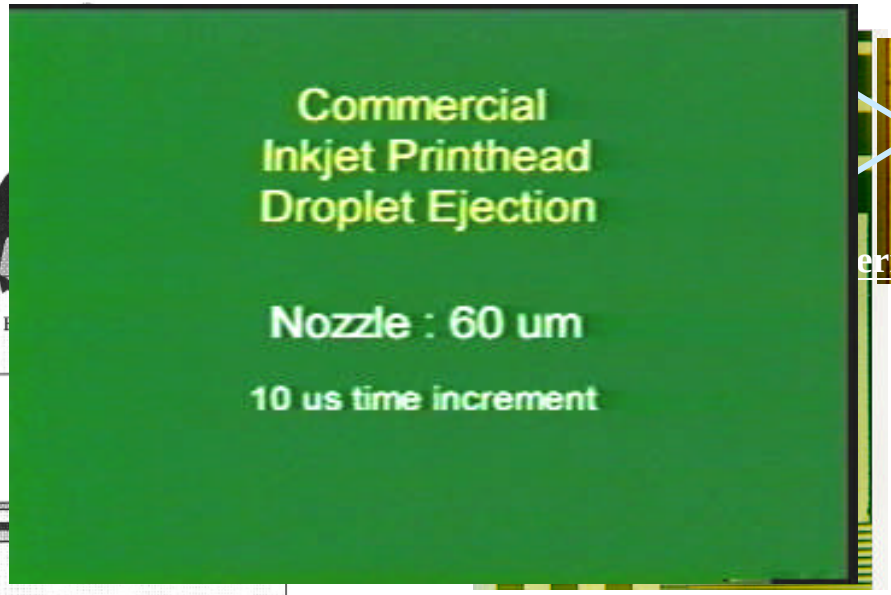

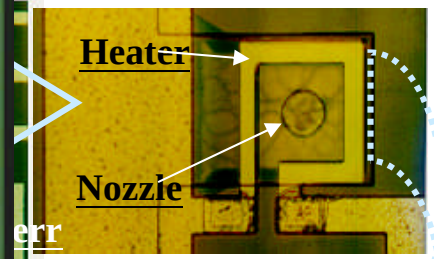

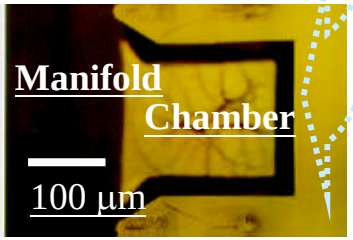

Nozzle: 60 µm
Droplet: 50 µm
Frequency: 8 kHz

Fastest one in market
Nozzle: 20 µm
Droplet: (5 pl)
Frequency: 12 kHz
Speed: 10 m/s

HP 51626A Printhead

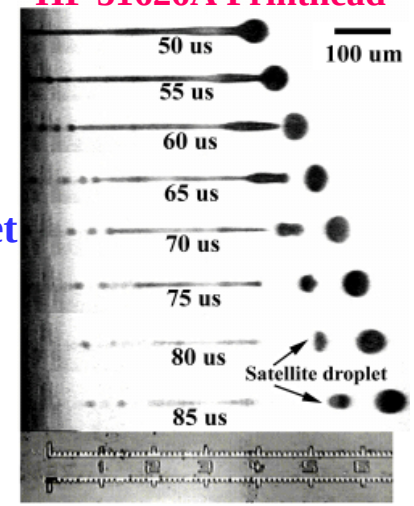

Microinjector

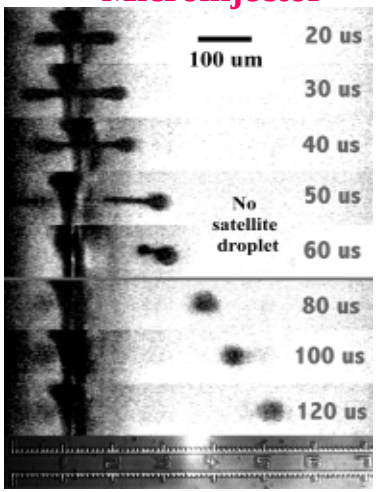

Nozzle: 40 µm
Droplet: 45µm
Frequency: 18 kHz

Fastest one
Nozzle: 10 µm
Droplet: 12 µm (0.9pl)
Frequency: 33 kHz
Speed: 10 m/s

Droplet Tail Cutting

Microinjector

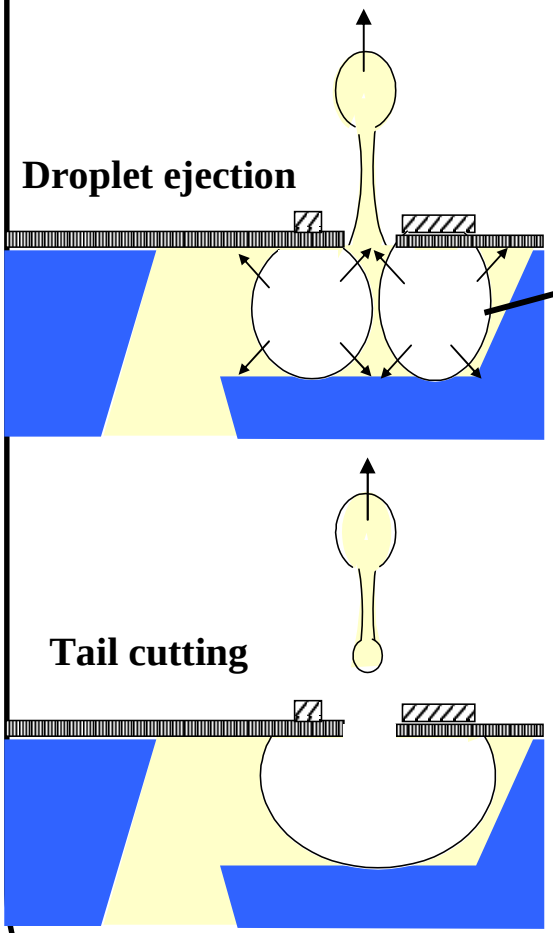

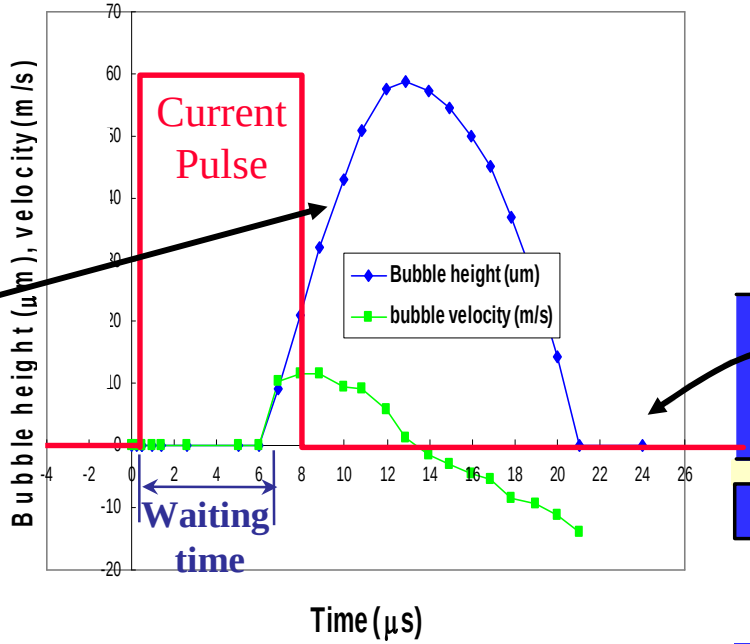

(Lee and Tirumala, IBM, 1988)

Commercial Inkjet

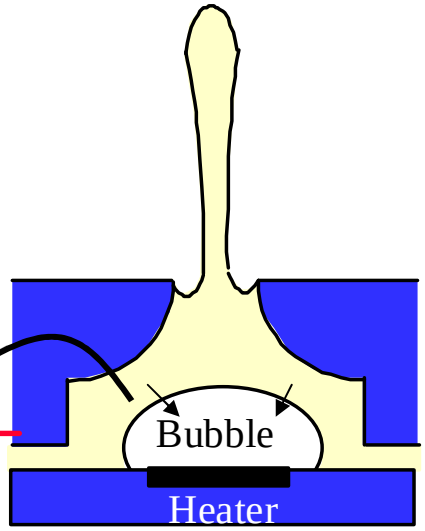

(a) Top shooter

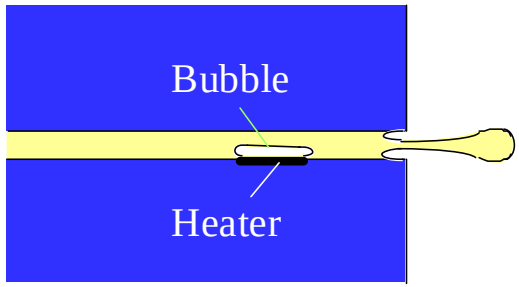

(b) Side shooter

Bubble Merging for Tail Cutting

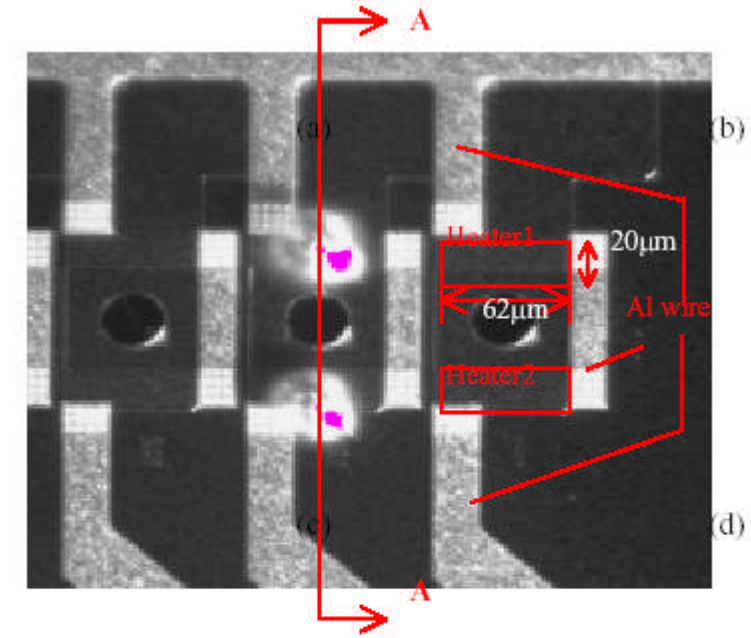

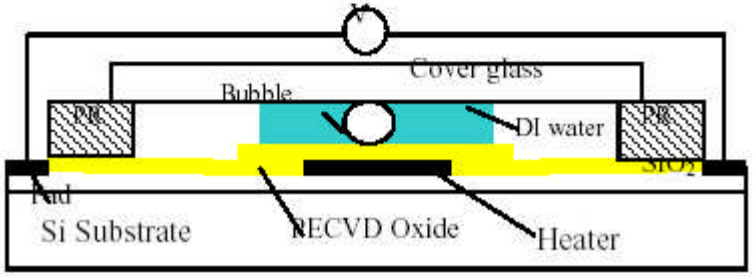

Bubble formation sequence (1 μs interval)

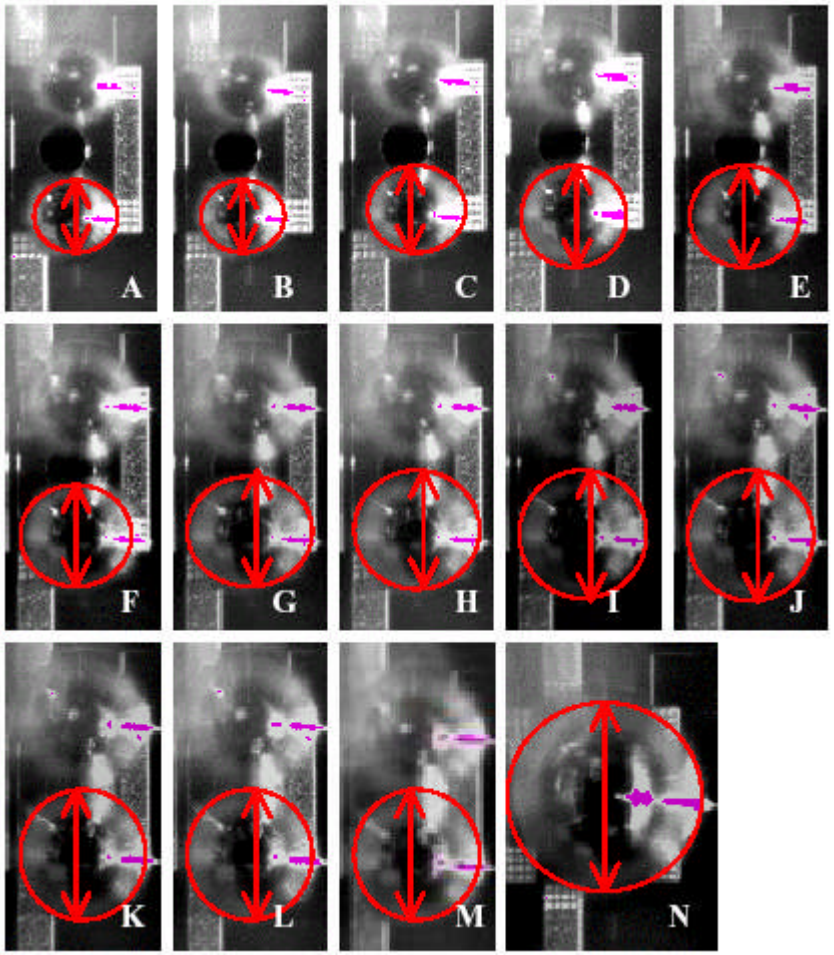

液珠懸浮控制

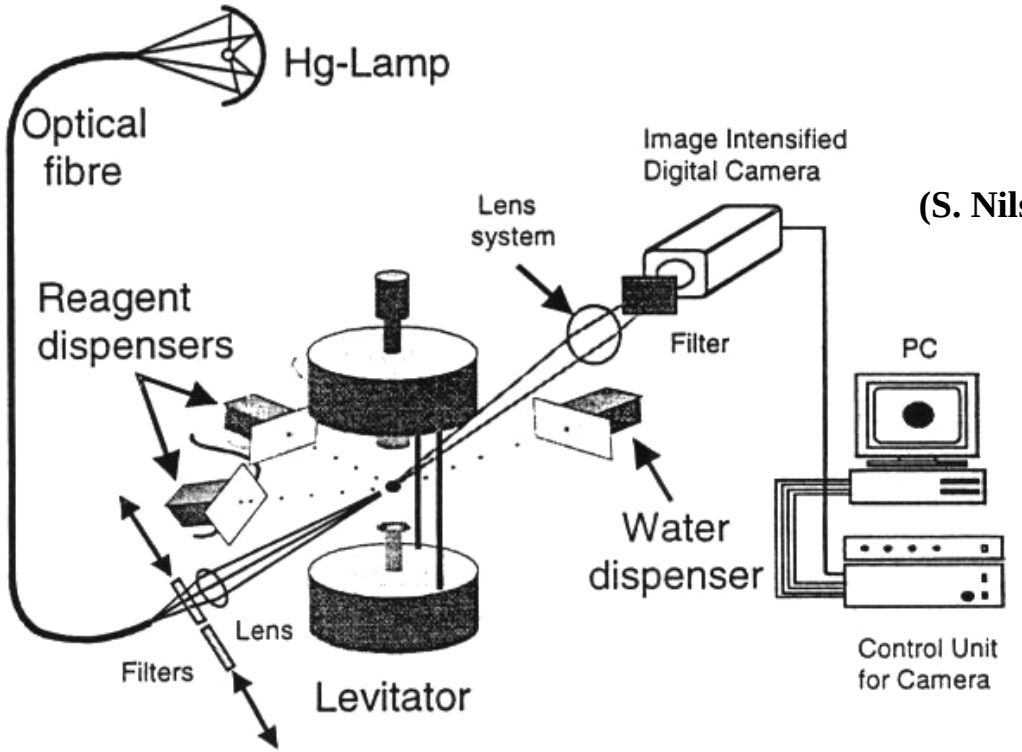

(S. Nilsson, et. al., μTas'00)

1. Instrumental set-up for levitation cell experiments with fluorescence imaging detection, consisting of a Hg-lamp, an optical fibre, two alternating interference filters (405 and 435 nm), a cylindrical lens, an acoustic levitator, a lens system, and another interference filter (510 nm). A CCD camera is used to collect images of the levitated droplets, which are then analysed by a specially designed, in-house developed computer program for image analysis of the levitated droplets. Three continuous flow-through pico litre dispensers are used for additions to the levitated droplet, one for the addition of water and two for the addition of reagents (isoprenaline and insulin).

微液珠平面驅動方式

- 微液珠驅動方式:
  1. 靜電及電潤濕［2-4］2. 光驅動法［5］
  4. 固態液體珠［6］
  5. 非對稱結構［8］
  6. 熱毛細力［9］
  7. 結合Marangoni效應，熱毛細力，凝結及成核　效應[7]
  8.表面奈米分子操縱

Most of them are employing surface tension gradient!!!

Lee. J, Sensors and Actuators 2002

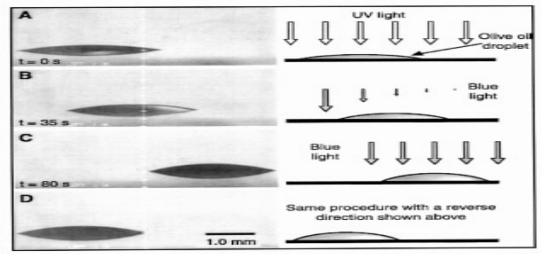

K. Ichimura, Science, 2002

P. Aussllous, Nature, 2001

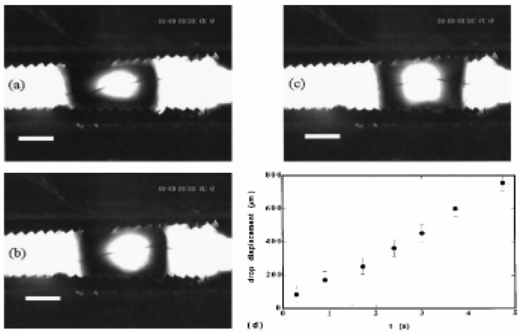

O. Sandre, Physical Review E, 1999

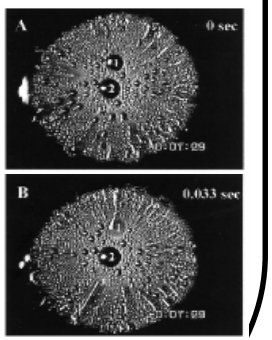

J. C. Chen, Science, 2001

Electrostatic

- **Very high voltage,**
- **electrolysis problem,**
- **charged bio-molecules may be attracted by electrical field**

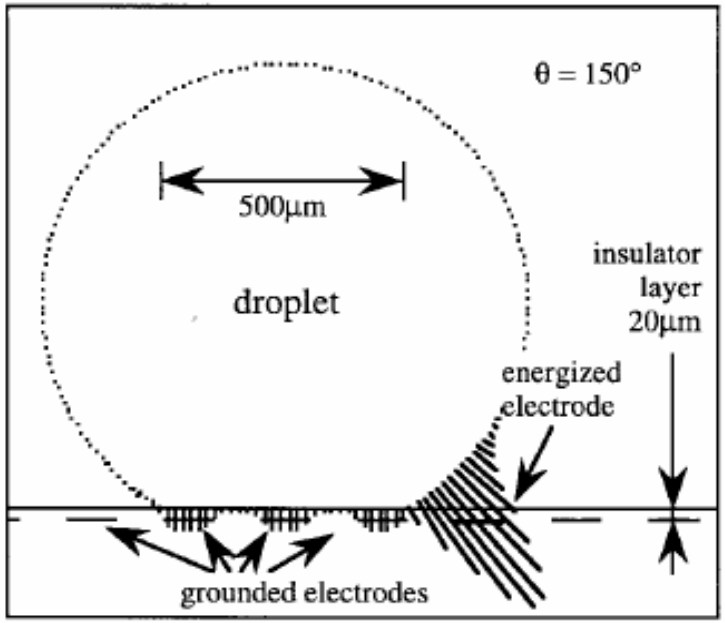

(Masao Washizu, *IEEE* 1998)

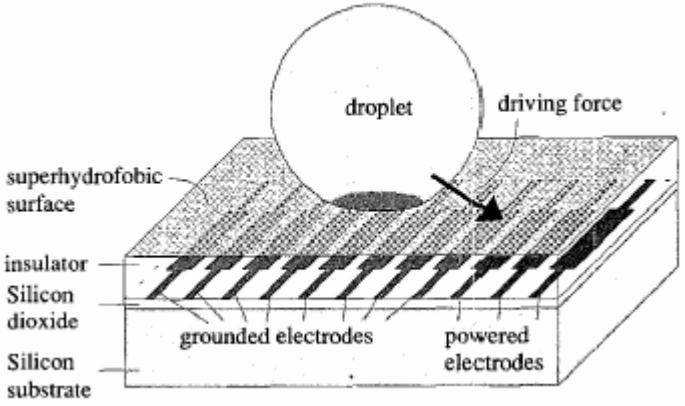

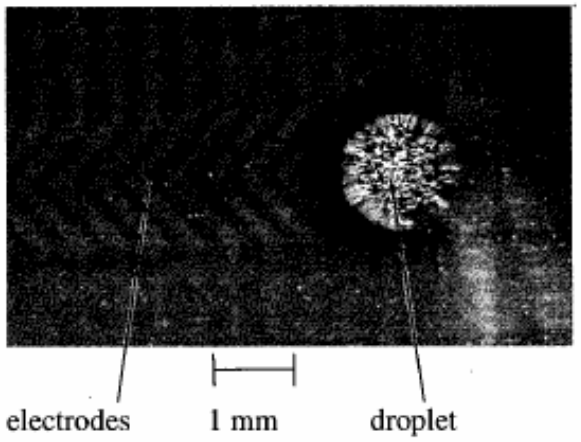

(Altti Torkkeli, *IEEE* 2001)

Electrowetting

EWOD
(ElectroWetting on Dielectric)

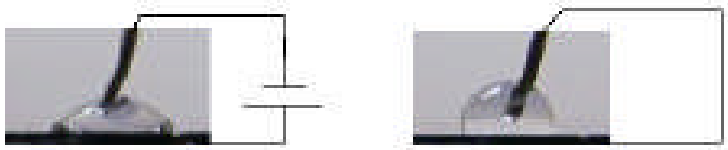

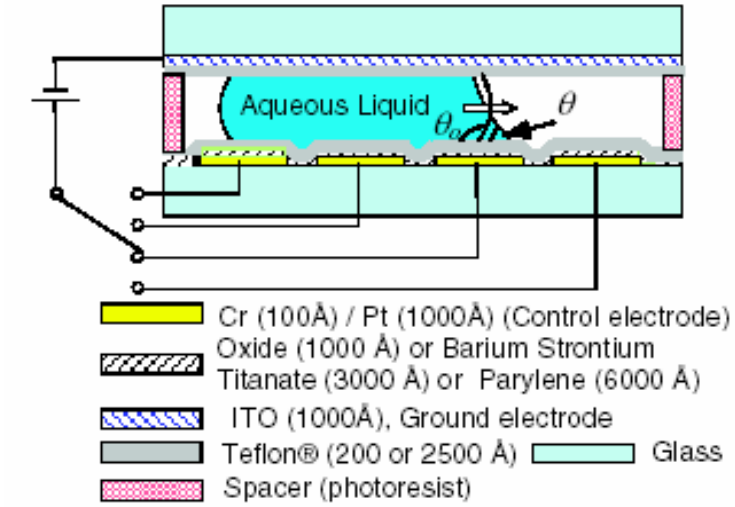

(Sung Kwon Cho, *IEEE* 2002)

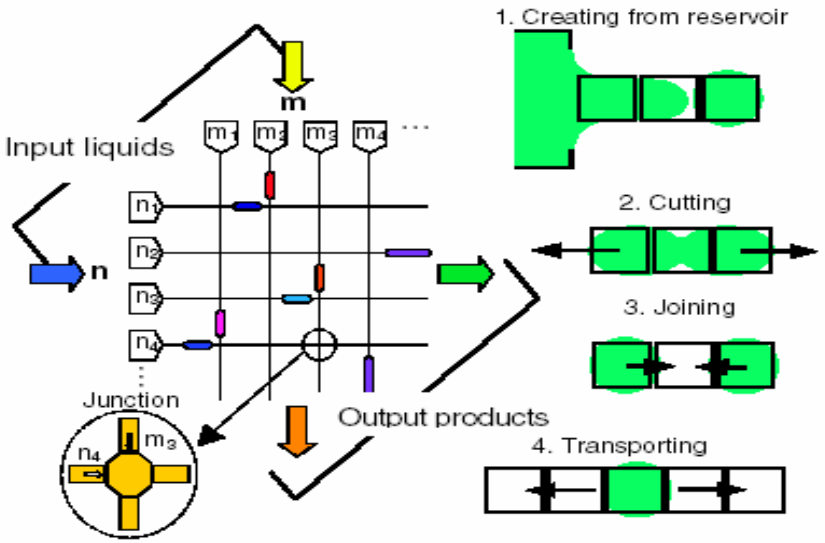

Fig. 1 Envisioned digital microfluidic circuit and the four fundamental droplet operations necessary

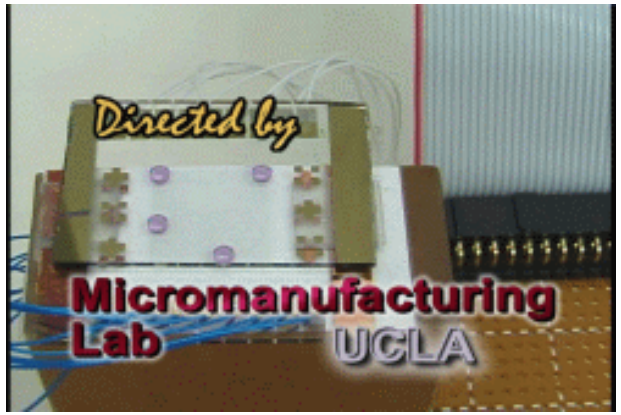

CJ Kim, UCLA

Electrowetting

OWE (Opto-Electrowetting)

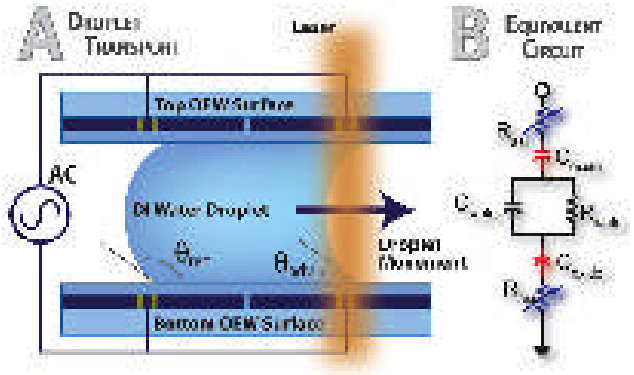

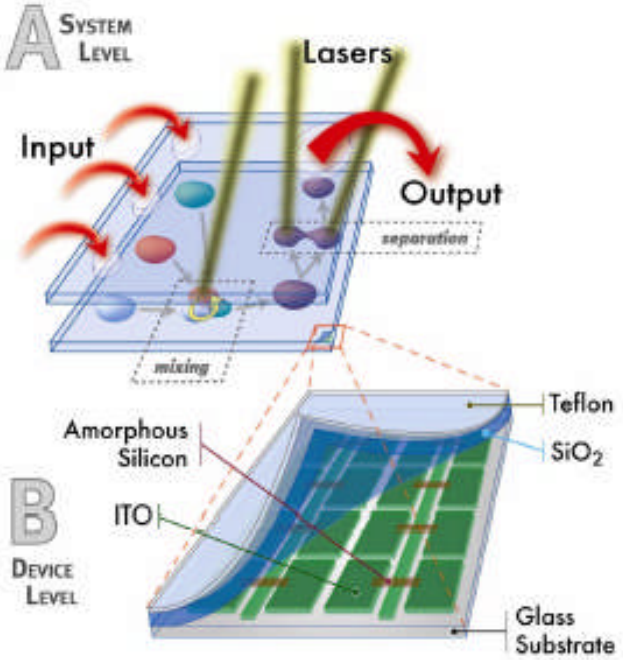

(Pei Yu Chiou, *IEEE* 2003)

Creating

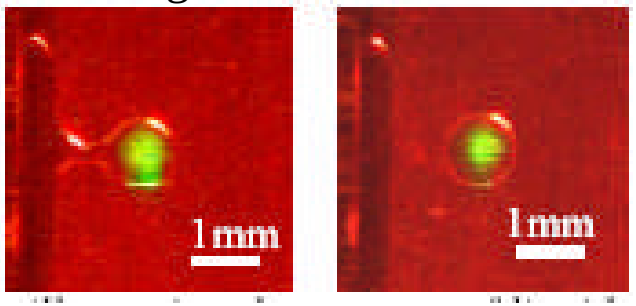

Moving

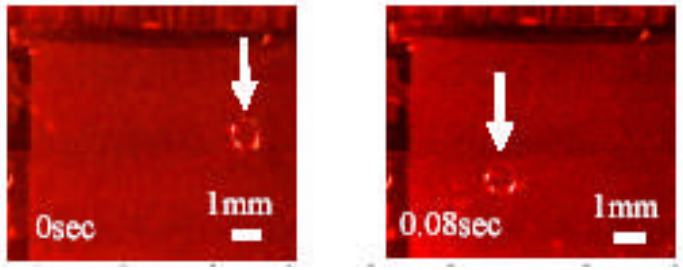

Separation

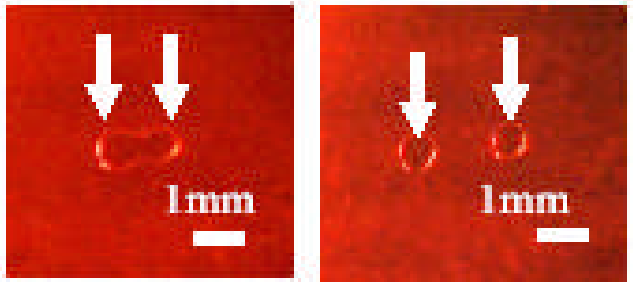

Marangoni Effect

- **Droplets Moving Behavior**

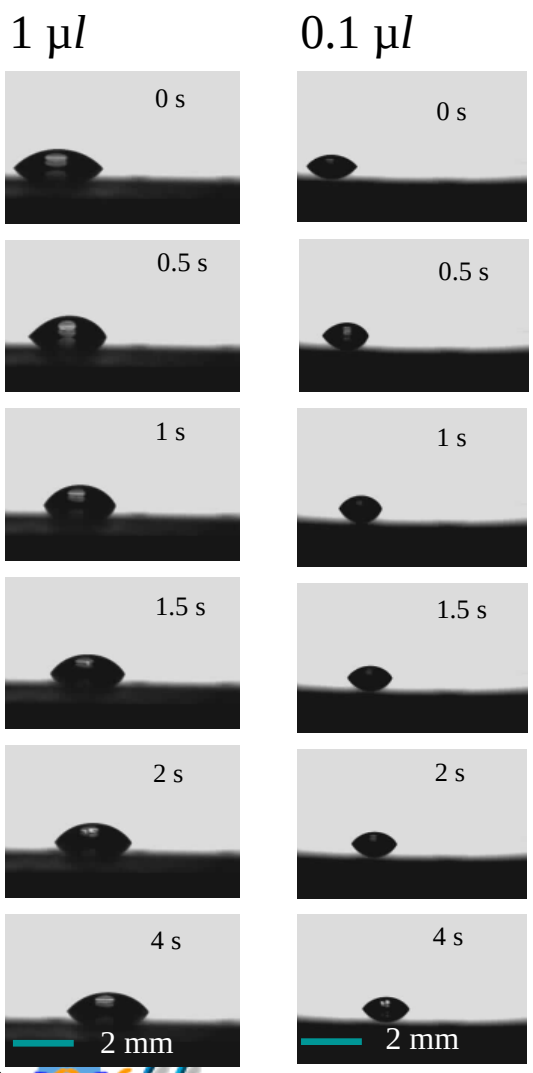

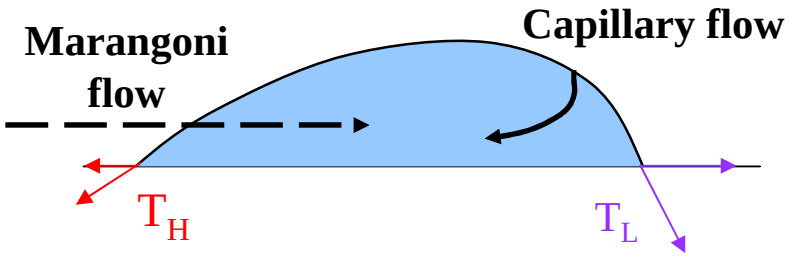

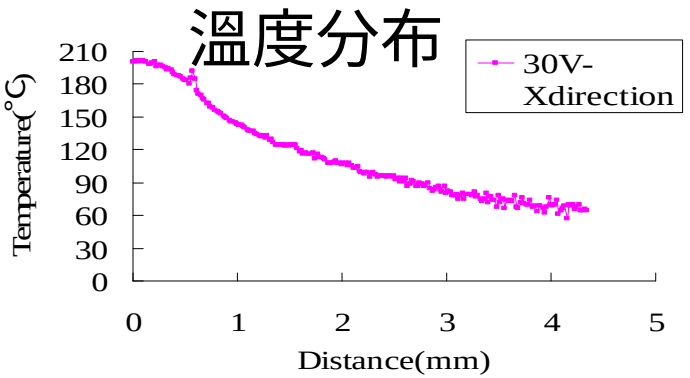

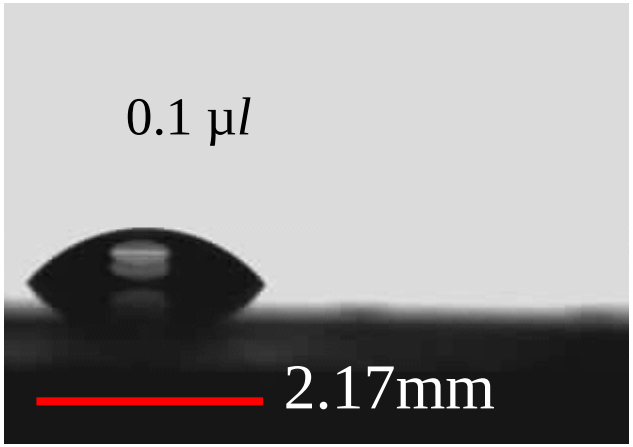

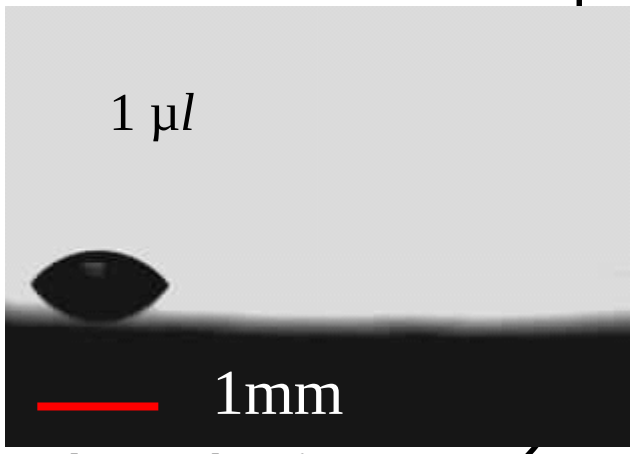

F. G. Tseng et al, Transducer'03

Thermal Capillary Actution

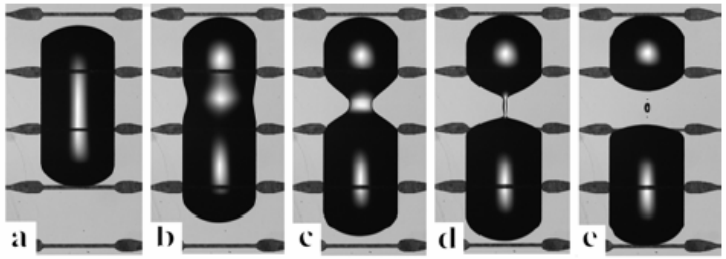

Figure 3. (a)-(e) Thermally induced splitting of a dodecane drop on a partially wetting stripe (droplet width = 1000 μm). Resistive heaters are defined by the light gray regions. The voltage applied to the 155 Ω resistor was 2.5 V. The images were recorded at t = 0, 6.0, 7.5, 8.0, and 8.5 s.

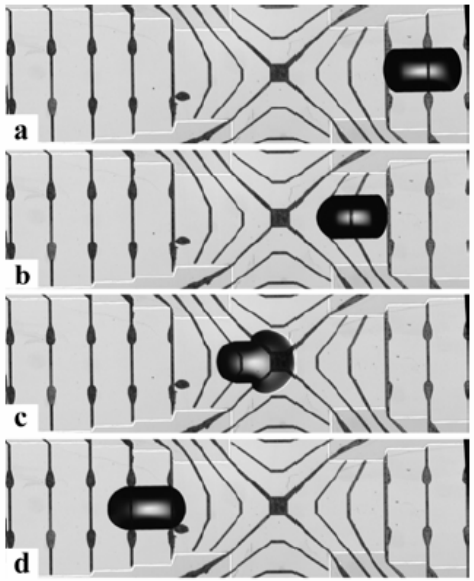

Figure 4. (a)-(d) Thermocapillary actuation of dodecane drop through intersection (droplet width = 1000 μm, time lapse = 104 s).

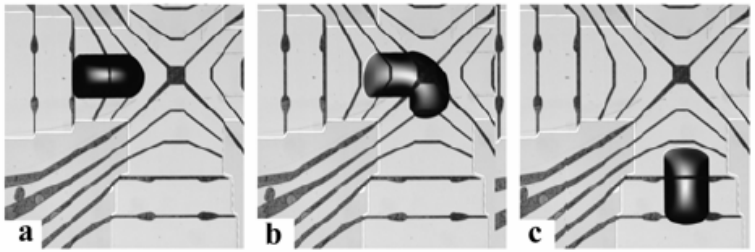

Figure 5. (a)-(c) Dodecane drop turning 90° corner. Power applied to each resistor ≤ 40 mW (Time lapse = 164 s).

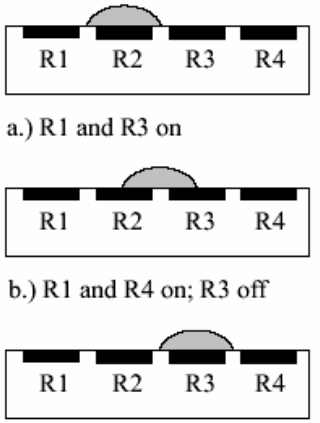

Figure 6. Cross-section of device showing sequential heating of resistors, R1, R2, R3, R4: a.) Voltage applied to R1 and R3: the drop is confined on top of R2. b.) Turn off R3 and apply voltage to R4: drop moves away from R1. c.) Apply voltage to R2 and turn off R1: drop is positioned above R3.

J. P. Valentinoa, A. A. Darhuberb, and S. M. Troian, Transducers'03

Marangoni +capillary+ coalesces Effect

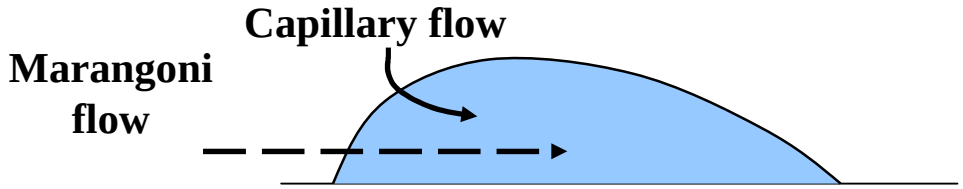

Hydrophobic T_H → T_L Hydrophilic

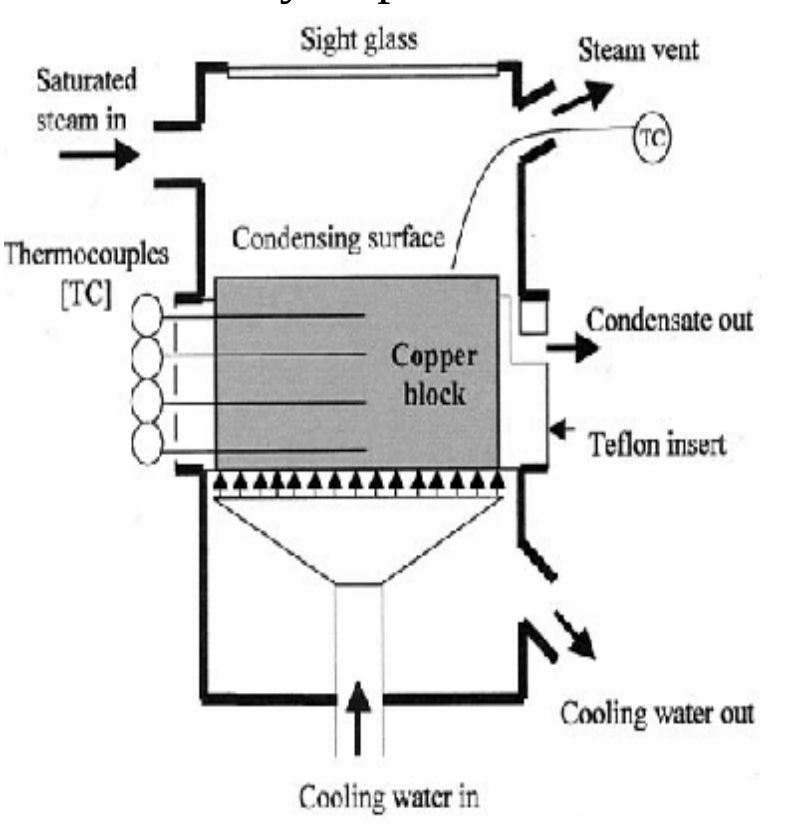

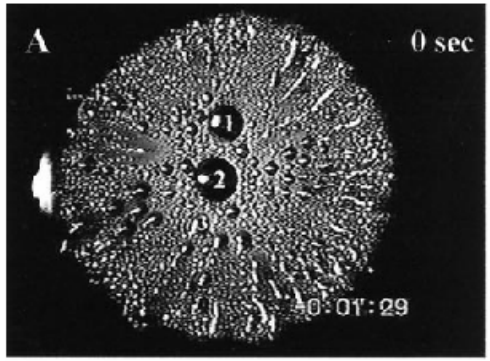

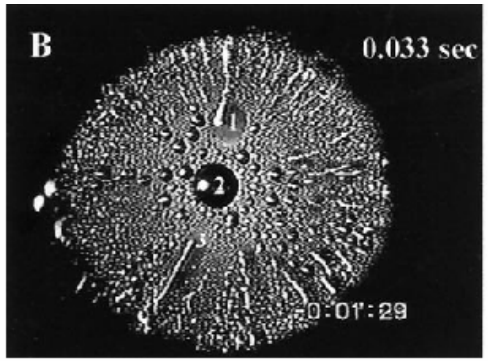

Droplet movement ~10 cm/s, 10 times faster

(Susan Daniel, *Science* 2001)

Surface Roughness

Winzel

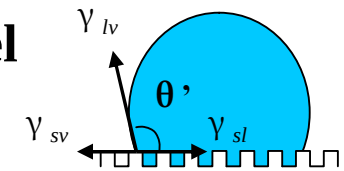

$$\cos\theta' = \frac{r(\gamma_{sv} - \gamma_{sl})}{\gamma_{lv}} = r\cos\theta$$

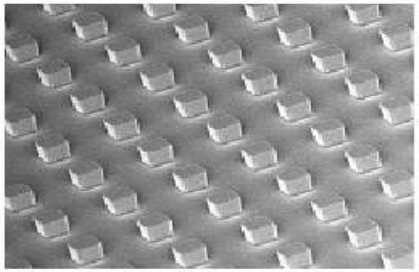

(a) PDMS pillars (SEM)

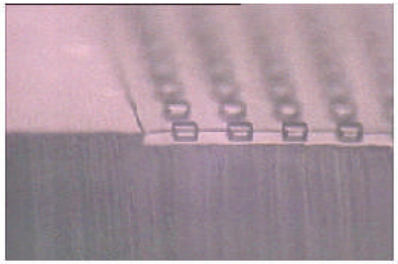

(b) Suspended PDMS membranes (optical microscopy)

Cassie

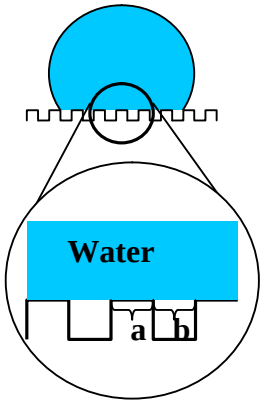

$$\cos\theta' = f\cos\theta + f - 1$$

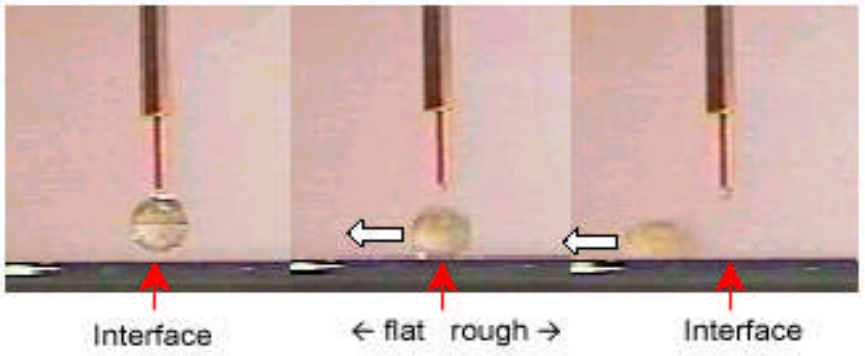

Wettability Switching by Surface Roghness Effect (Bo He, *IEEE* 2003)

Temperature Responsive Surface

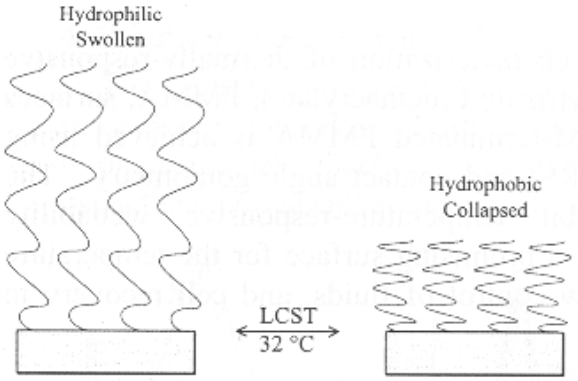

Figure 1. Depiction of temperature effects on pNIPAAM. Below the LCST pNIPAAM is hydrophilic and swollen. The reverse is true above the LCST.

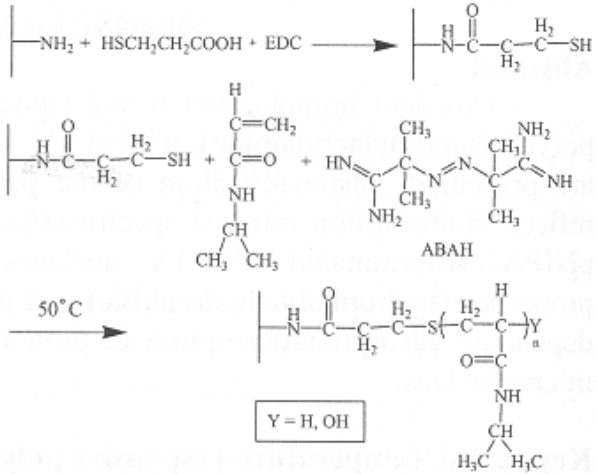

Figure 2. Reaction sequence leading to the free-radical polymerization of pNIPAAM from modified PMMA surfaces. All reactions were performed in aqueous medium.

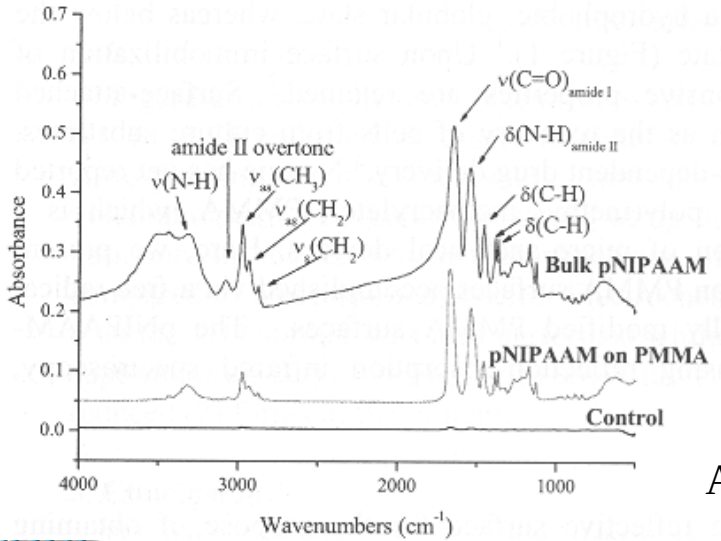

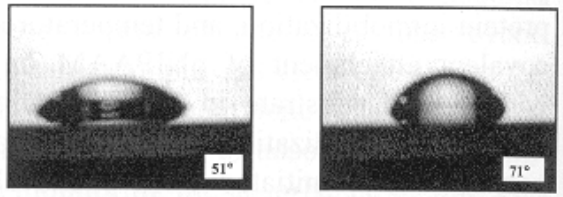

A. F. Smith, R. L. McCarley, μTAS 2002

Photonic & SAMs

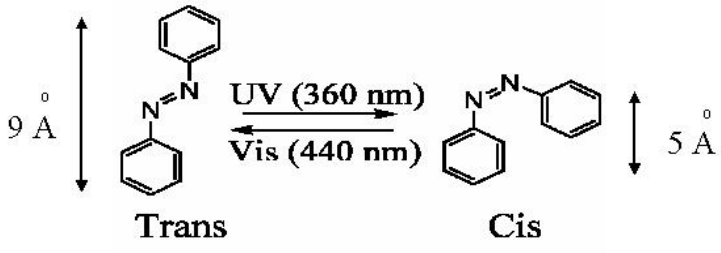

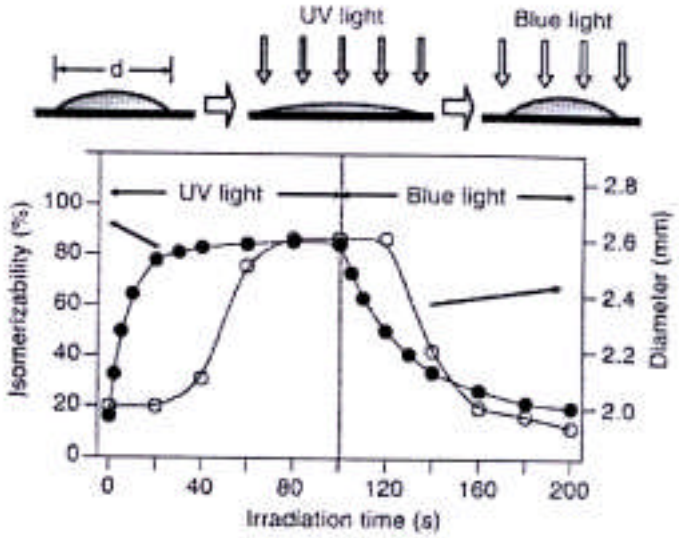

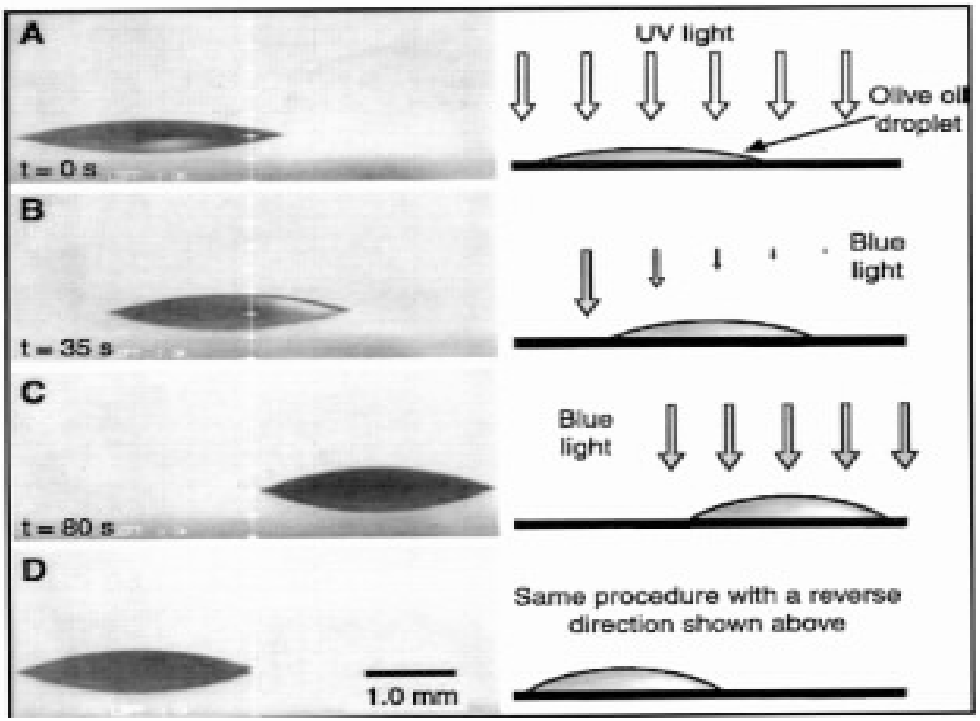

(K. Ichimura, *Science* 2000)

Bending molecules by Electrical Potential

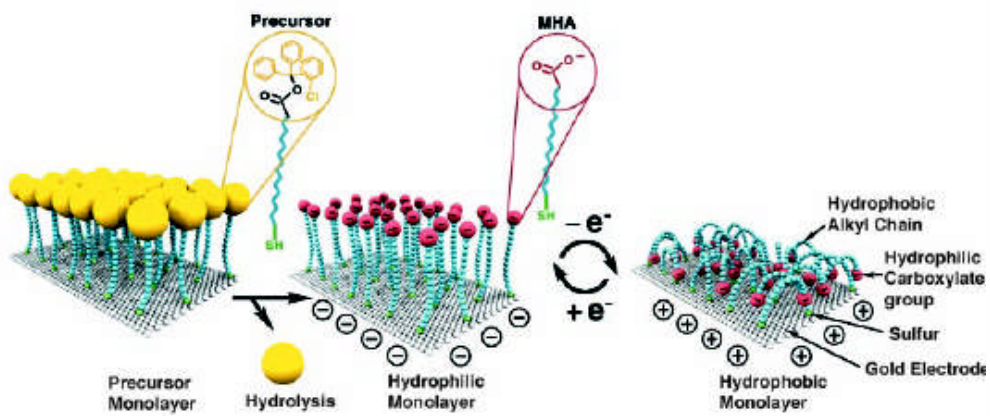

Fig. 1. Idealized representation of the transition between straight (hydrophilic) and bent (hydrophobic) molecular conformations (ions and solvent molecules are not shown). The precursor molecule MHAE, characterized by a bulky end group and a thiol head group, was synthesized from MHA by introducing the (2-chlorophenyl)diphenylmethyl ester group.

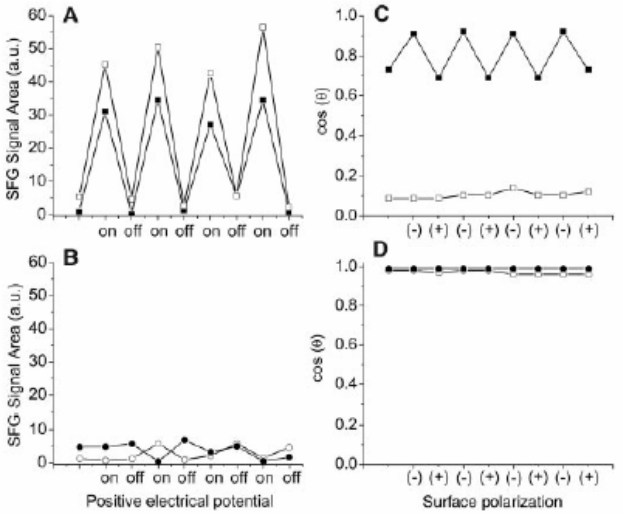

Fig. 4. Microscopic and macroscopic responses of the low-density SAM to an electrical potential as monitored by SFG spectroscopy and contact angle measurements. Relative SFG intensities (peak areas) of the methylene modes at wavelengths of 2855 cm^{-1} (solid symbols) and 2925 cm^{-1} (open symbols) are shown for the low-density (**A**) and the dense (**B**) SAMs measured in d^3-acetonitrile (0.1 M CT) when a potential of +25 mV w.r.t. SCE was repeatedly applied to the system. Cosine of the advancing (open symbols) and receding (solid symbols) contact angles for the low-density (**C**) and the dense (**D**) SAMs were determined while applying either +80 or −300 mV w.r.t. SCE to the underlying gold electrode. Four switch cycles were conducted, and contact angles were measured with an aqueous solution (0.1 M CT, pH = 11.5) at air using a goniometer (VCA-2500XE, Advanced Surface Technology) equipped with an electrometer (6517A, Keithley Instruments) and platinum and carbon fiber microelectrodes (Kation Scientific). Contact angles averaged at least 100 data points from nine samples with maximum errors of ±3°. The SAMs were examined for chemical integrity and deprotonation by IR spectroscopy after an electrical potential was applied. The lines are drawn as a guide to the eye.

J. Lahann et al, Science 2003.

Superhydrophobic & Gravity

Superhydrophobic Surface (SAMs)

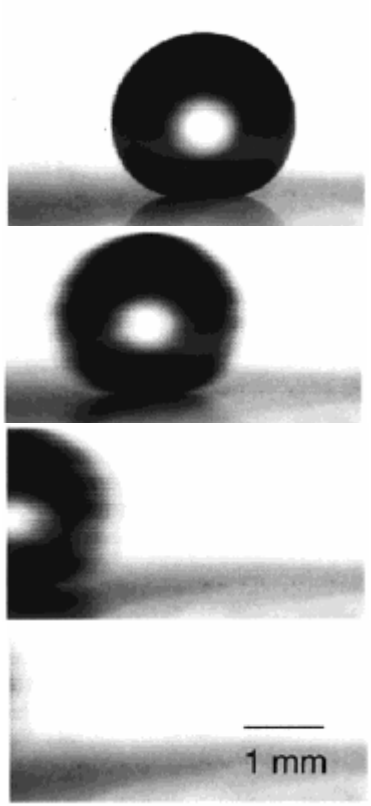

Water Droplet Weight 7mg with tilt angle of surface 1° (Masashi Miwa, *Langmuir* 2000)

Liquid Marble (Powder coating)

Hydropphobic powder (20μm) coating (Pascale Aussillous, *Nature* 2001)

Comparasion

Principle	Max. Velocity (mm/s)	Droplet Size (μl)	Power
Electrstatic (Altti Torkkeli, *IEEE* 2001)	10	2 ~ 50	Yes($124V_{AC}$)
Electrowetting (S. K. Cho, *IEEE* 2002)	250	1	Yes($100V_{AC}$)
Optic (K. Ichimura, *Science* 2000)	0.035	2	Yes
Temperature Gradient (Susan Daneil, *Science* 2001)	~ 20	0.001 ~ 1	Yes
Roughness (Bo He, *IEEE* 2003)	?	7	No
Gravity (P. Aussillous, *Nature* 2001)	?	1 ~ 10	No

Conventional array machine system

機械手臂點針法

- Robotic machine and steel pin

- Serial process: long running time
- Need wash: (cross contamination)
- Expansive: position control system
- Sample dry out: not good for protein

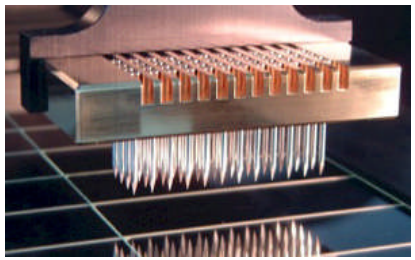

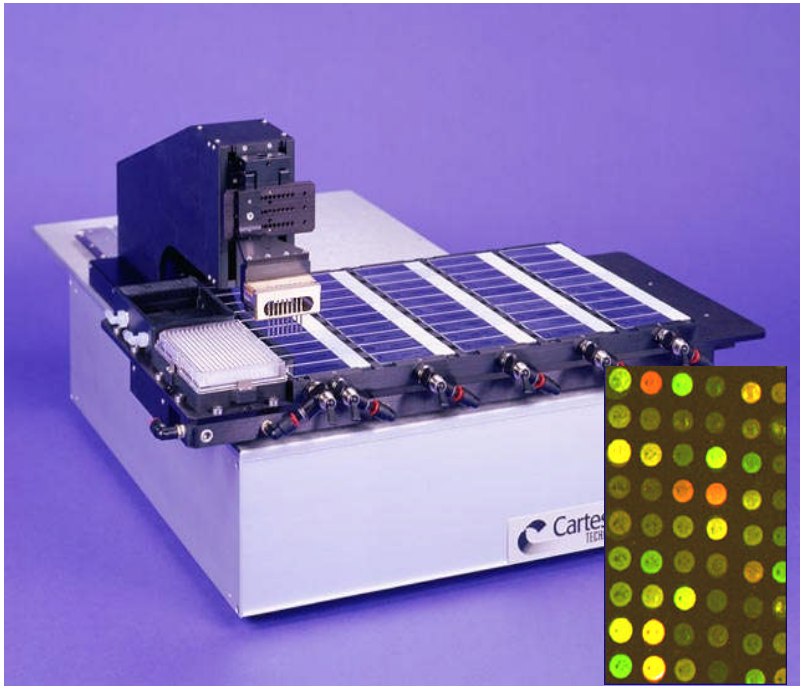

光學微影法

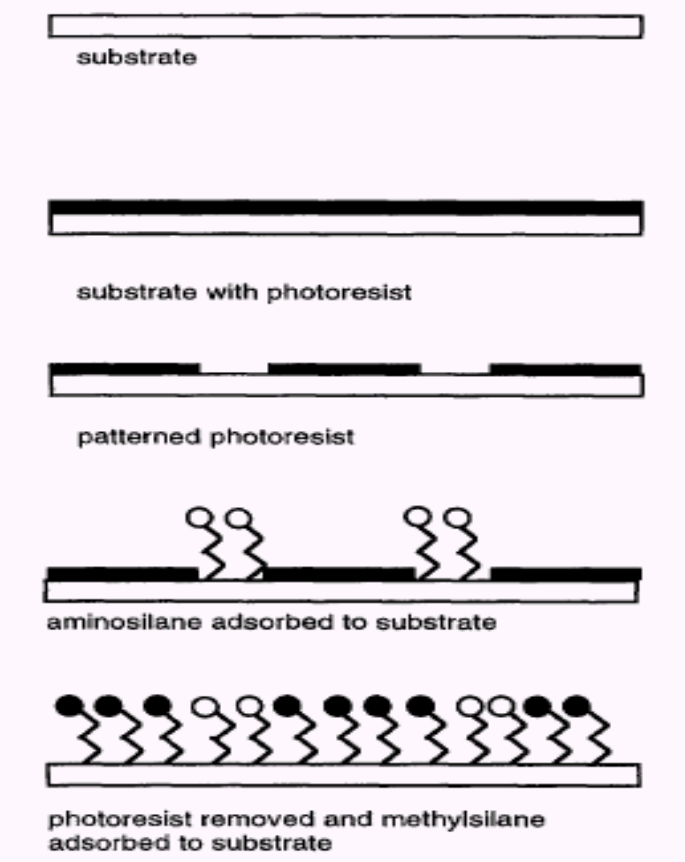

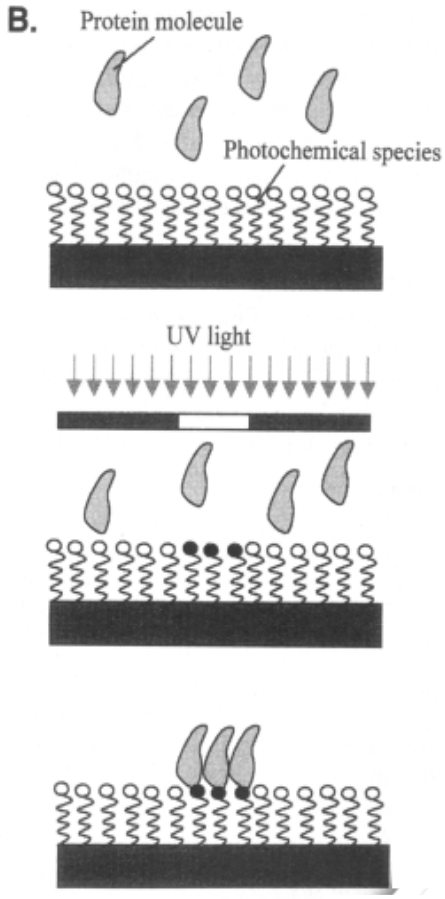

Blawas, *Biomaterials*, 1998

缺點： 化學藥品可能傷害檢體、不適合多種檢體

微噴墨法

壓電式

(Piezoelectric)

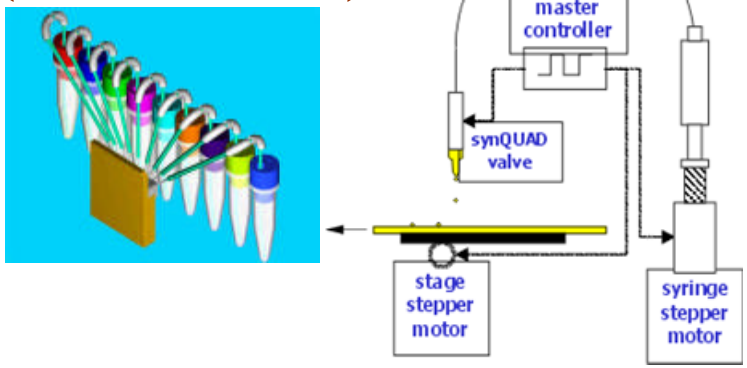

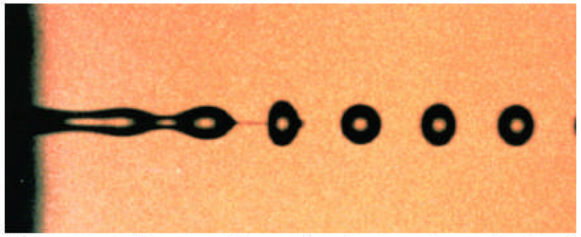

Figure 1: A 50μm jet of water breaking up due to Rayleigh instability into 100μm droplets at 20kHz.

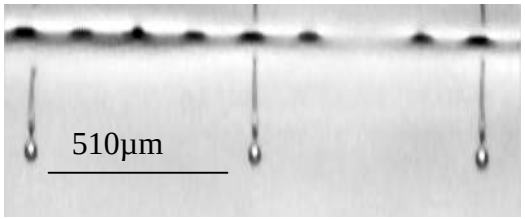

Spot size: 80~50μm

(SPIE Microfluidics and BioMEMS 2001)

缺點

❑噴嘴及管路重復使用需清洗

❑致動器須控制良好以使產生的液珠體積均勻且避免衛星液珠

Nozzle:50 μ m

Pizeo stroke: 3~9 μ m

Droplet volume: 200~1400pl

氣動式微噴墨法

氣動式

(Piezoactuator)

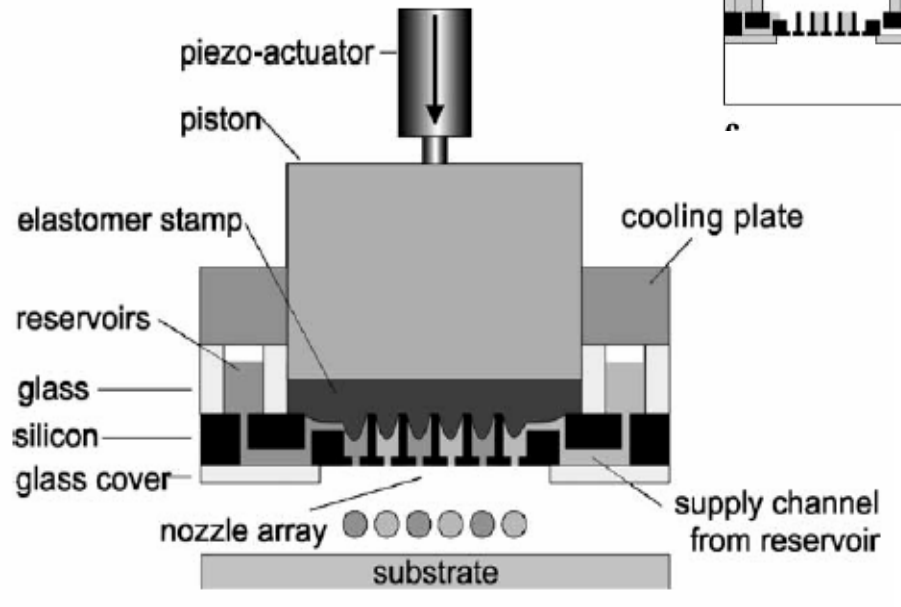

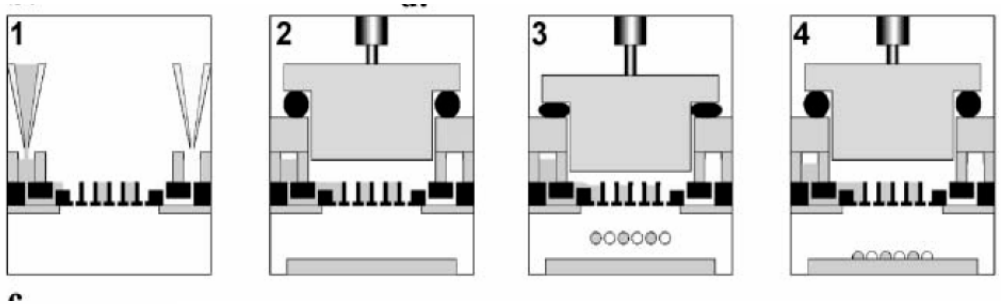

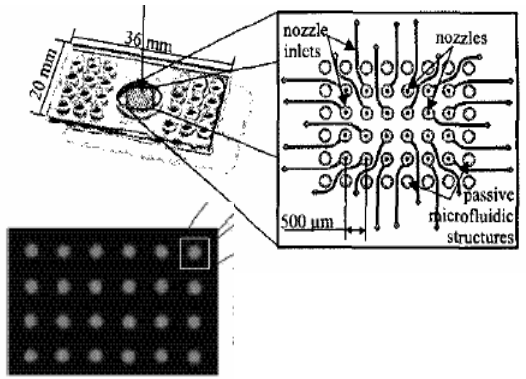

Spot size: 400~50µm

(Gustmann, Germany Transducer, 2003)

氣壓需要控制良好

間距大

電噴灑法

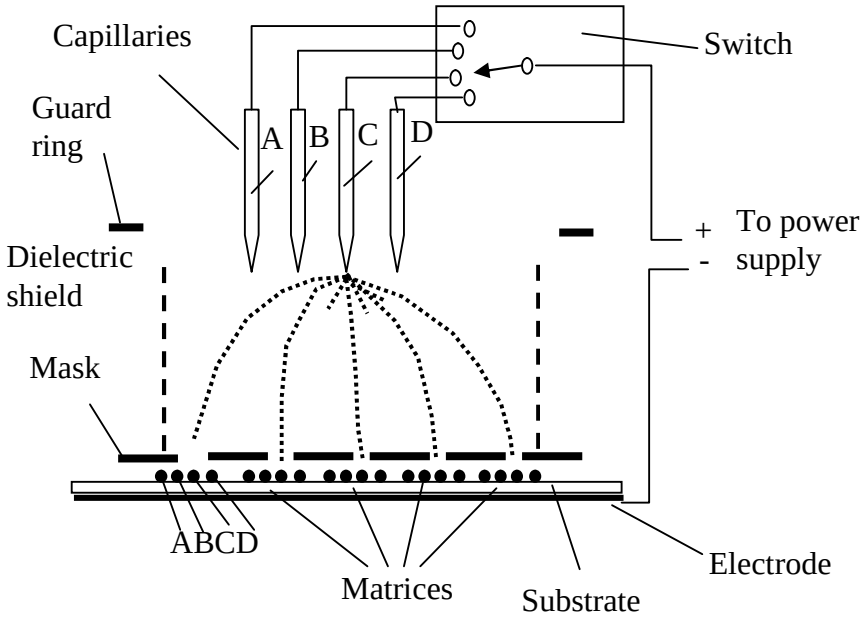

(Electrospray Mozorov 1999)

以電噴灑法沉積蛋白質及DNA的主要問題在於蛋白質及DNA在電噴灑沉積後，並在接續的帶電電噴灑生成物撞擊下，是否仍能保存本身的活性。電噴灑法需要使用極高的電壓，以噴灑蛋白質為例，需要高達3-4kV的電壓，安全上的考量不可不慎。再者，以電噴灑法形成的點形狀並不均勻，需要再配合其他的設計才能解決，增加製程上的麻煩。

雷射法加熱法 Biological laser printing

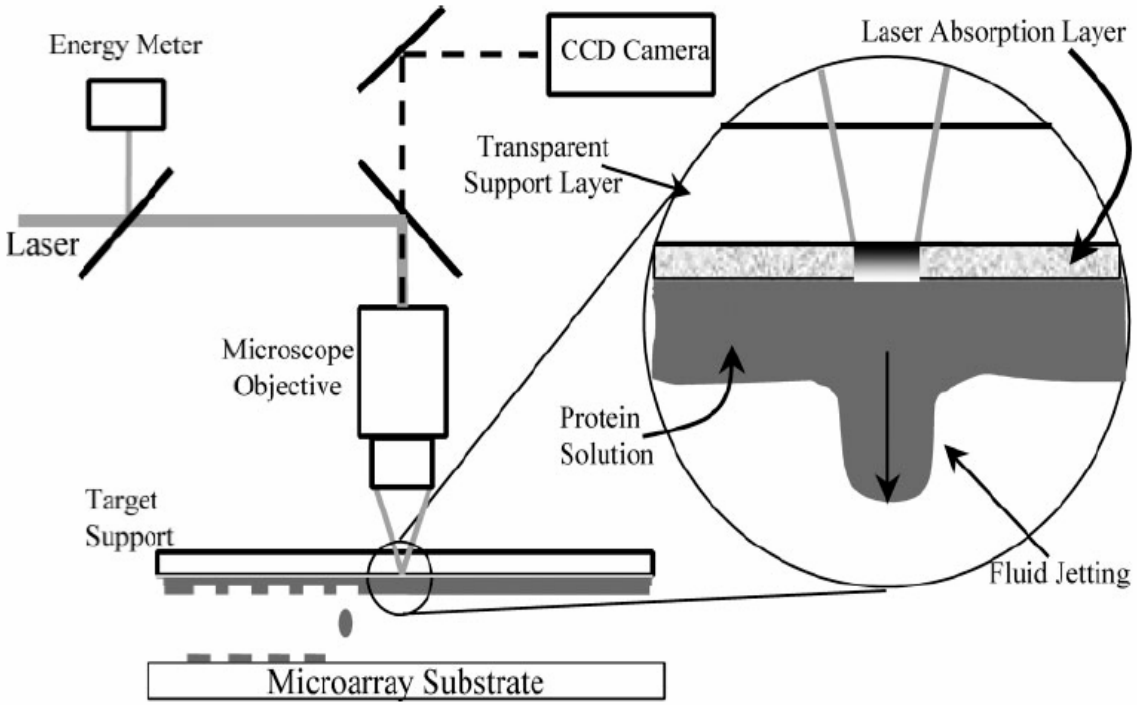

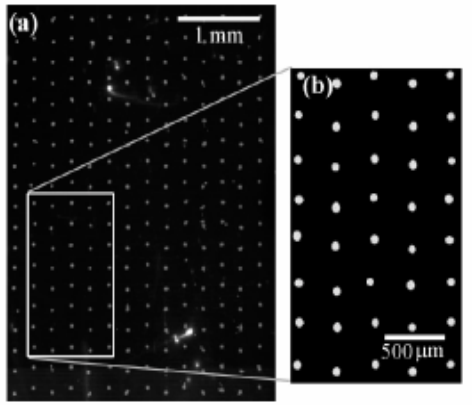

Figure 5. (a) A 2000-spot BSA microarray after immunoassay with anti-BSA (imaged with fluorescent detection; 266 spots shown). Standard deviation is 10% of the average spot size of 60 µm. (b) Higher magnification of one portion of the microarray.

(J.A. Barron Proteomics2005)

- Microscope objective to focus the laser beam
- Quartz substrate and metal or metal oxide absorption layer

需考量能量對檢體所造成的影響

AFM沾水筆微影法

AFM tip

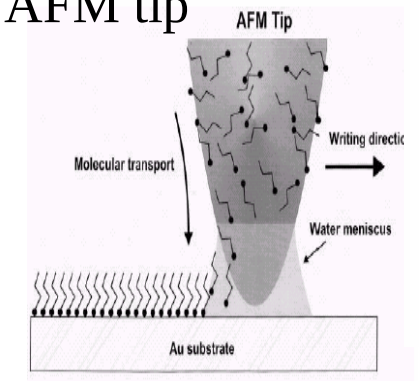

(Piner, Science 1999)

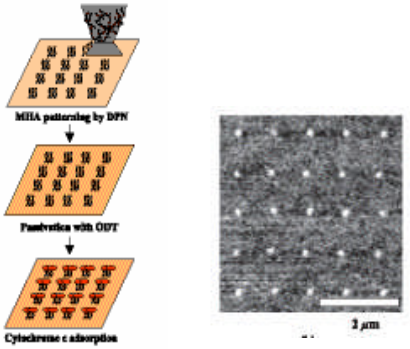

(J. W. Choi, 2004)

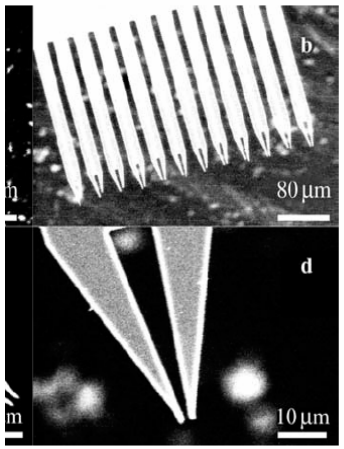

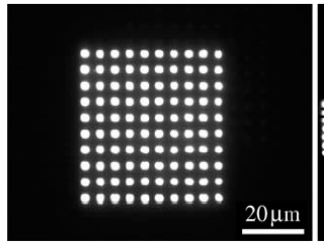

Spot size: 2~3µm

Space :5µm

缺點

- **需AFM移動軸筒做精密移動控制及施力下針控制以行成陣列**
- **機台成本高且打印3000點需1小時**
- **蛋白質點讀取分析不易**

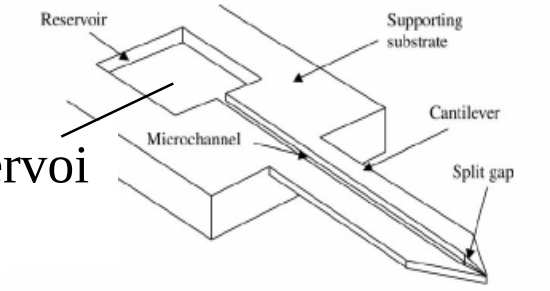

Reservoir

(Henderson, Biomedical Microdevice 2004)

用PDMS微流道作蛋白質陣列

(a) 微流道通檢體在玻片上

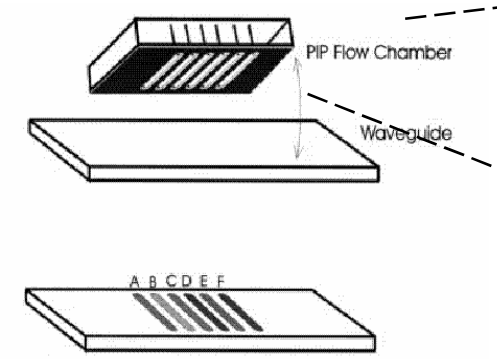

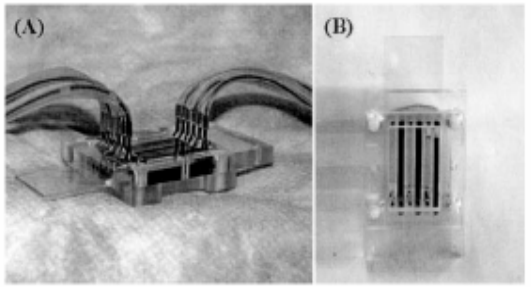

(b) 微流道晶片轉90度, 通檢體在玻片上

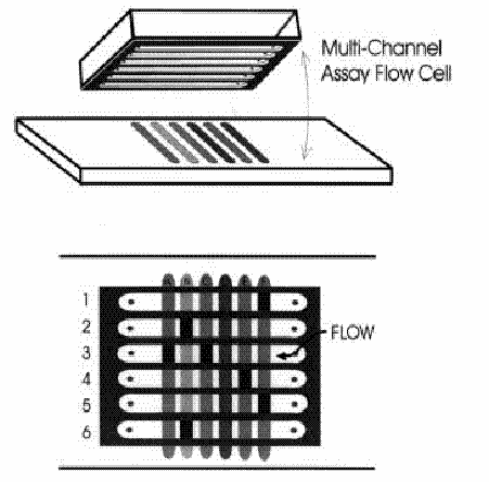

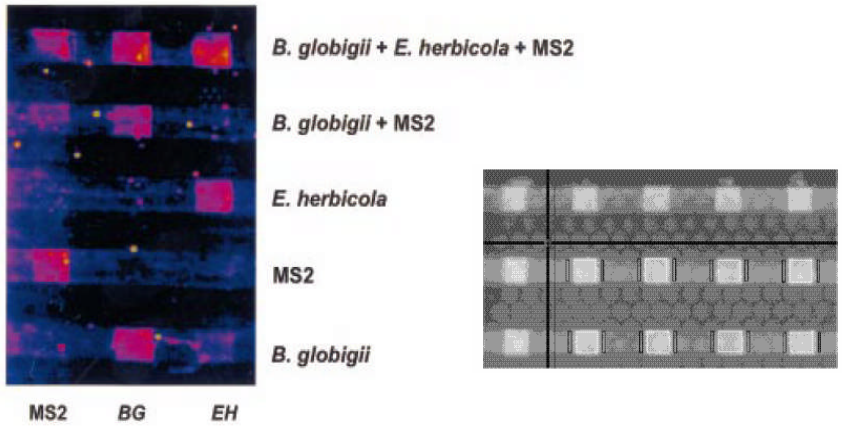

Size 尺寸間距大 (400~1500μm) 怕交互污染

(Ligler, Biosensor & Bioelectronics 02)

各微陣列技術比較

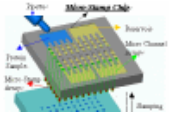
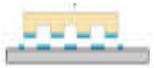


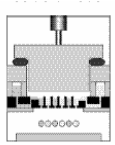
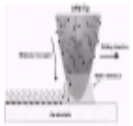


	液珠尺寸(um)	時間	一次可上種類	點體積(pl)	成本	拋棄式
微壓印法 (Lin) (Bernard)	50-100 5	快 200點/次	>100 1	400	低	Yes
點針法 (P.O.Brown 2001)	100~65	慢	48	500	高	No
噴墨法(壓電式)	150~50	快 100~4kHz	10	120	中	No
噴墨法(氣壓式) (C.P. Steineret 2003)	400~50	中	24(96)	125~1700	中	Yes
沾水筆法 AFM	0.1 2	慢 3000點/1hr	1 12	(0.01)	高	Yes
奈米壓印法	1~0.25	快	1	(0.05)	低	Yes

Force in Scale

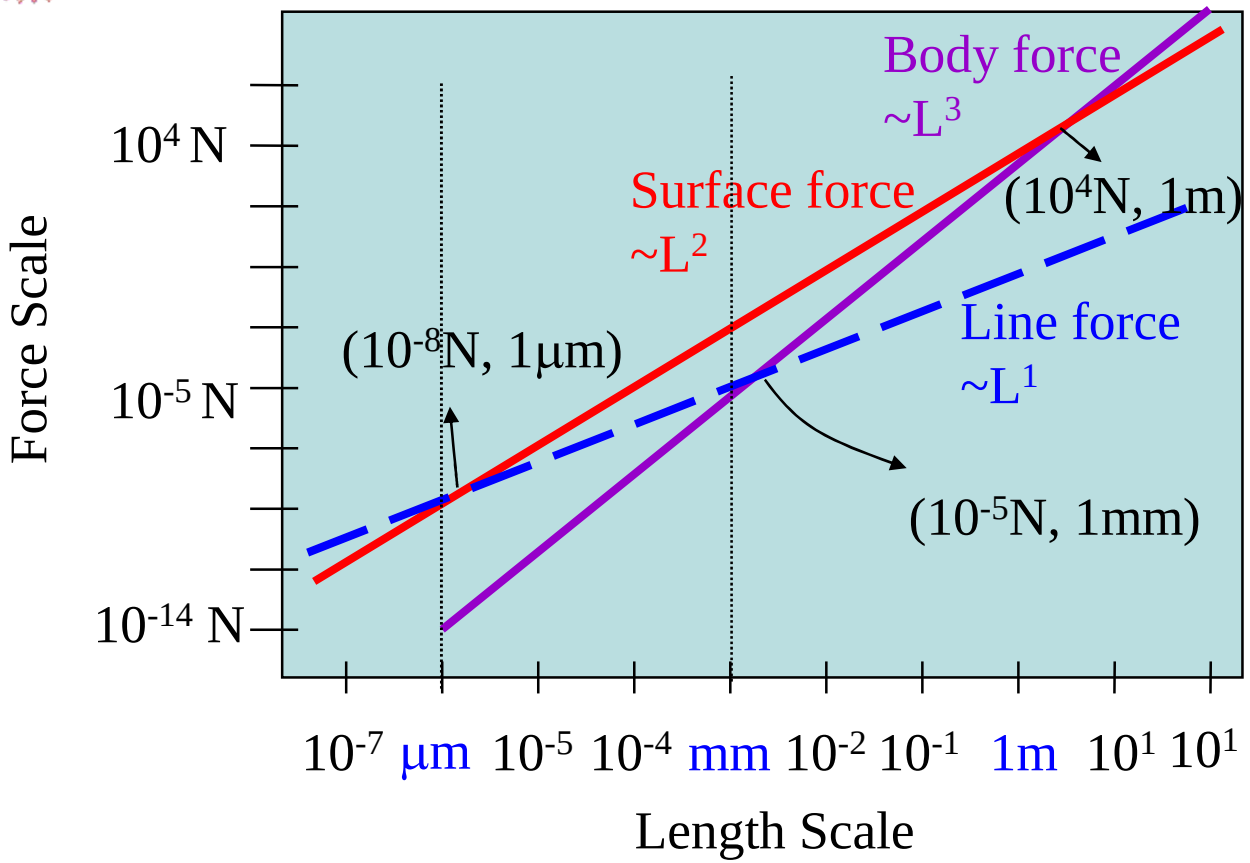

Mercury motor

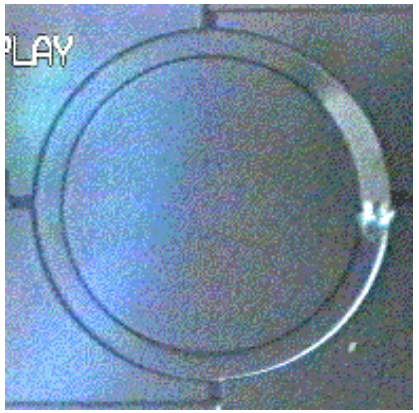

J. Lee, and C.-J. Kim,
J of MEMS, June 2000

Slug flow

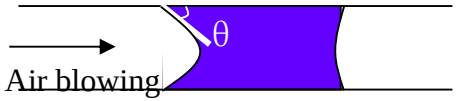

Surface tension force (line force) is dominate in nano scale and important in micro scale!!

❑3-in-1 Protein Chip

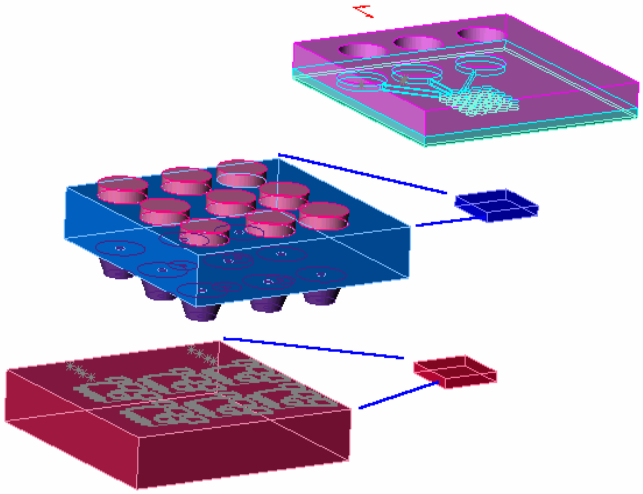

- ➢Micro filling chip
- ➢Micro stamper chip
- ➢Micro bio-reaction chip

Chip System Integration

- Filling, Stamping, Detection

1. Micro Filling Chip

Hand-Fill-in Reservoir

Micro-Fill-in Reservoir

Micro Needle connector

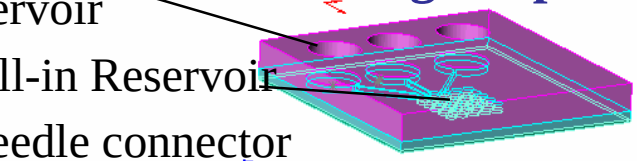

2. Micro Array Stamper

Micro Stamper

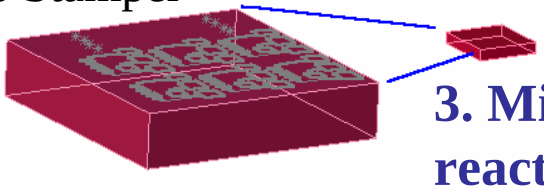

3. Micro Bio-reaction Chip

Bio-reaction surface

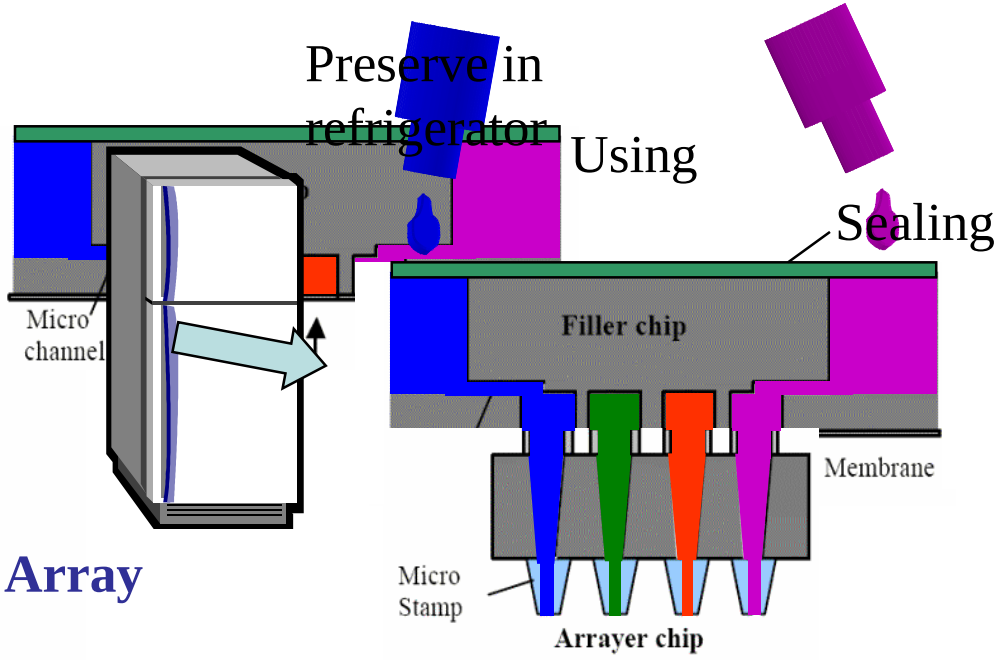

SAM coating

Protein Array

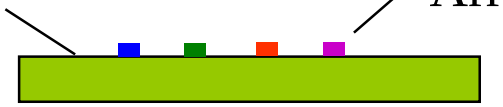

Bio-reaction chip

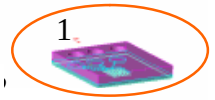

1. Micro Filling Chip

- Hand fill in
- Micro flow channel to micro filling reservoir
- PDMS membrane sealed. Conserved in refrigerator

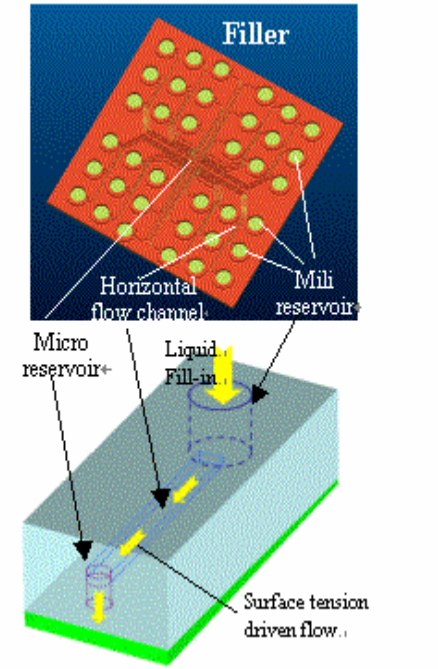

a. μ flow channel connect the Hand fill-in reservoir and μ-reservoir

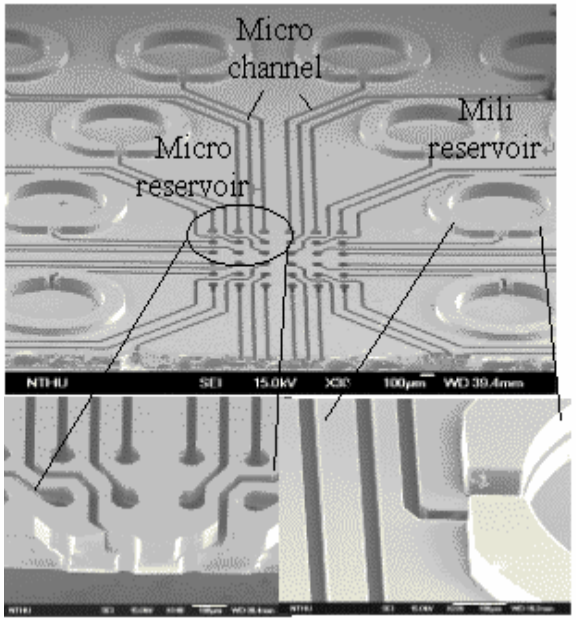

b. Micro flow channel cross section

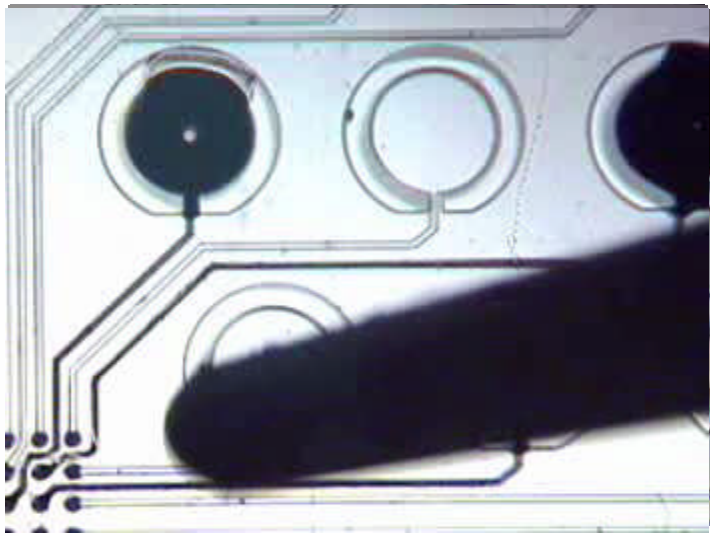

c. Filling testing. From hand-fill reservoir to micro reservoir

1. Micro Filling Chip

- Sample fluid filled parallel from micro reservoir into the micro stamper.
- Filling the micro stamper by the capillary force.

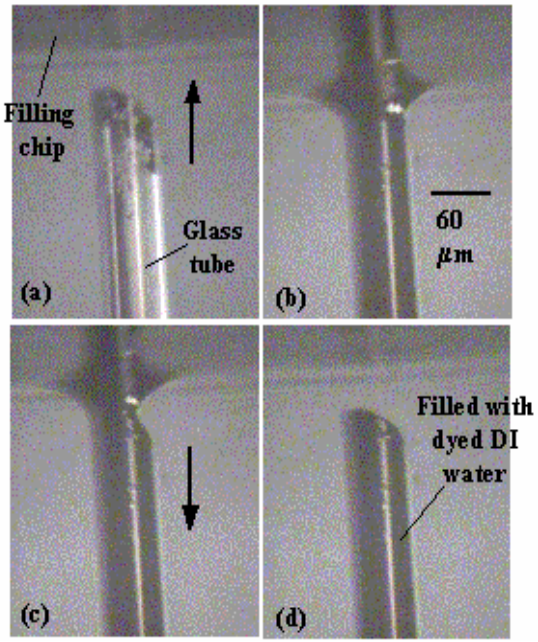

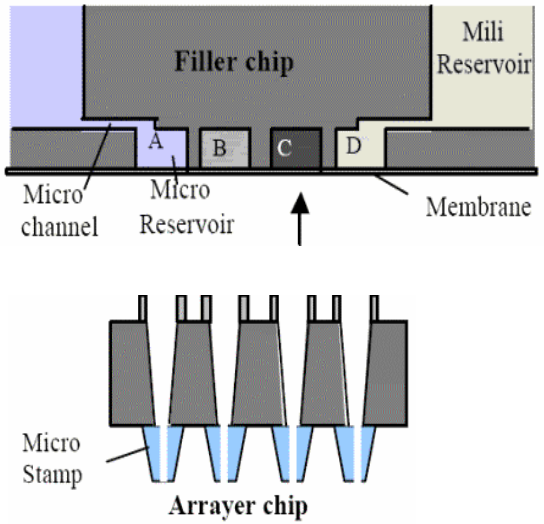

Filling Process

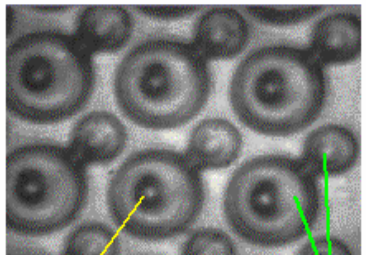

Su8 post

Well

Liqui

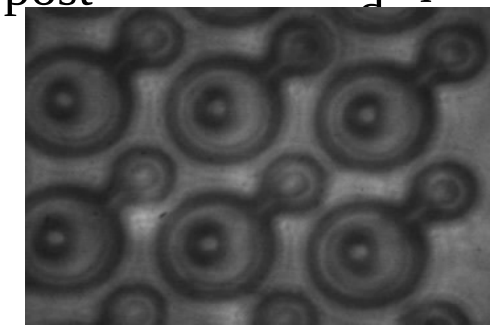

2. Stamp different types soluti simultaneously

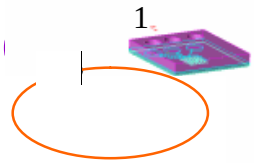

Stamp two types solution

Cy3 anti-rabbit IgG, Cy5 anti-mouse IgG

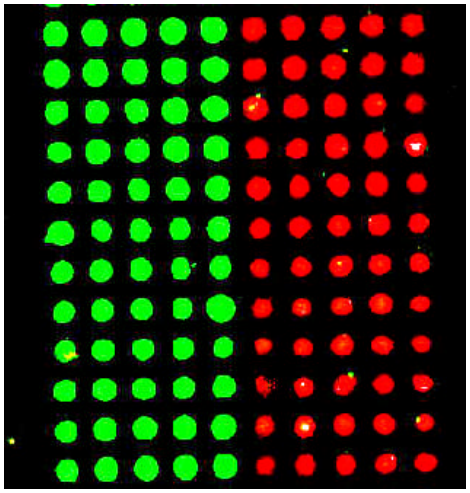

120 points array

Cy3 10^{-3}; Cy5 10^{-1}

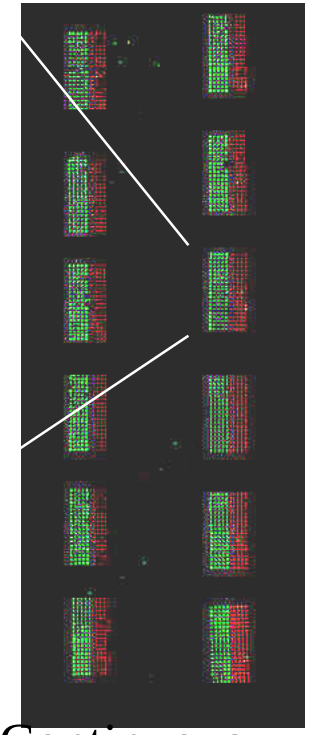

Continuous printing12 times

Stamp 4 types solution

Concentration: Cy5 10^{-1}; Cy3 10^{-3}

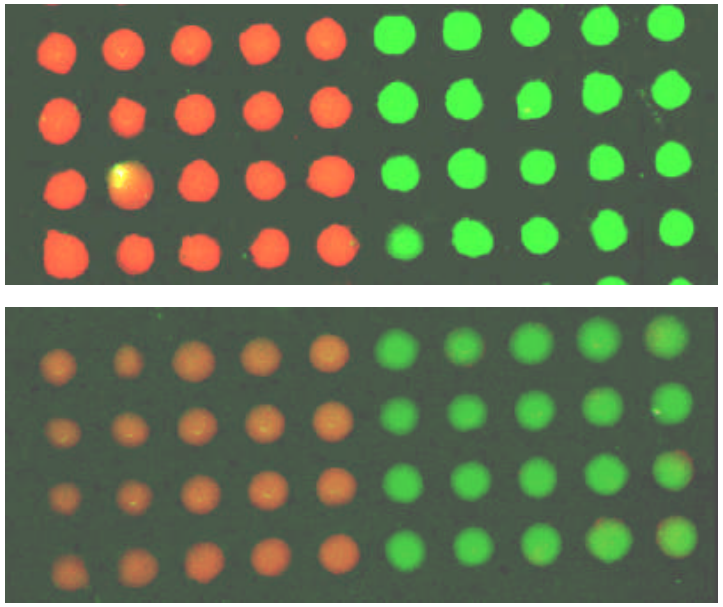

Cy5 10^{-2}; Cy3 10^{-4}

PBS solution with 30% glycerol

C Lin, F. Tseng, and C. Chieng, S&A B, 2004.

Protein Stamp result on substrates with different wettability

- The drop size increases with the wettablity of the chip surface. Observed from fluorescent scanner and optical microscope.

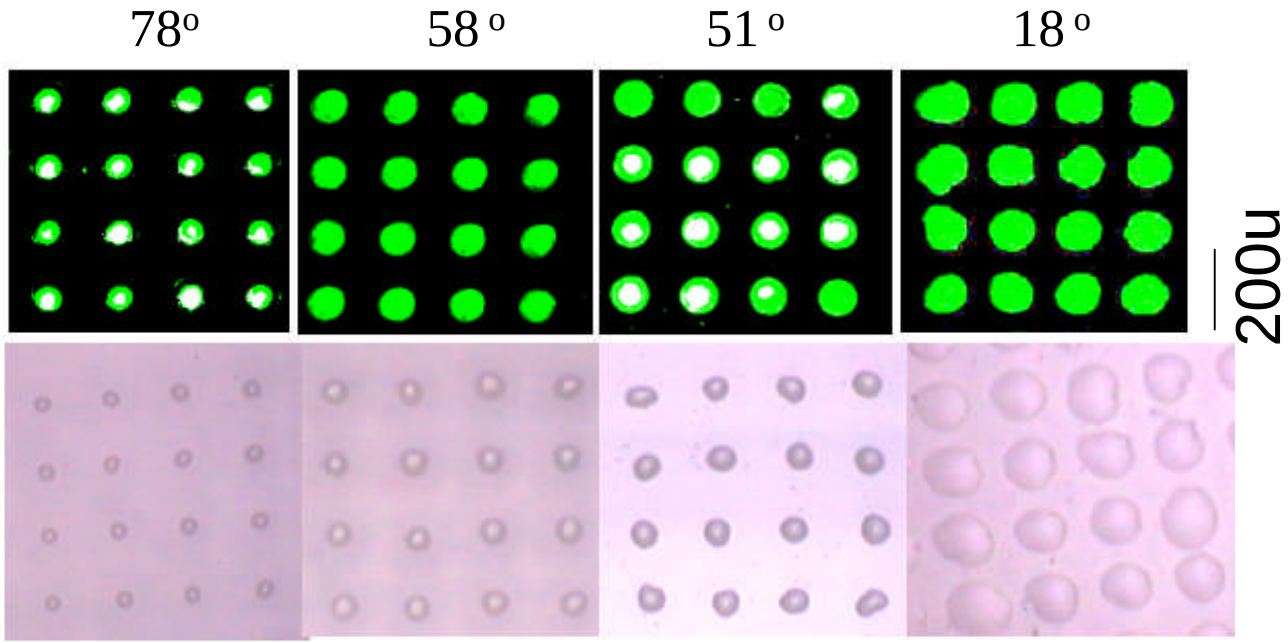

C. Ho, F. Tseng, and C. Chieng, J MM, 2005.

Simulation of drop formation process

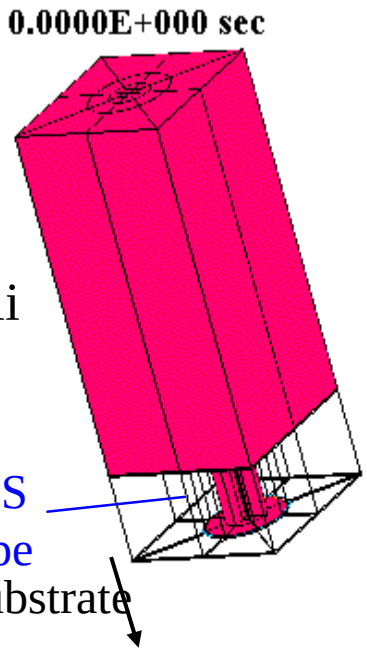

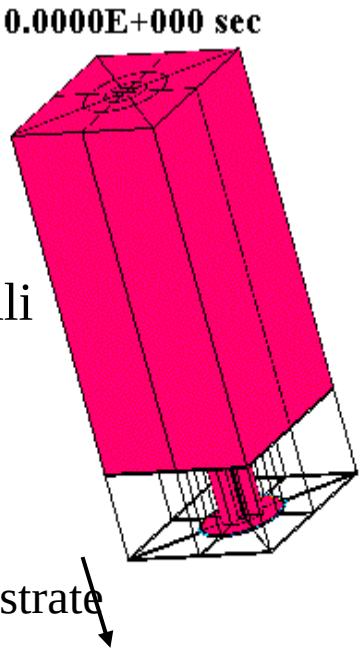

- Substrate wettability effect the drop size

Experiment

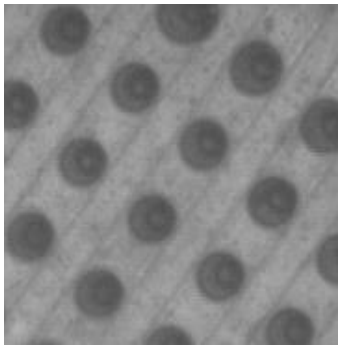

Flow channel filled with sample fluid

Drop formation

PDMS stamper

Substrate

Y. Chen, F. Tseng, and C. Chieng, J CIS, 2005.

Comparison of Computed and Measured Spotsizes on various SubstrateSurfaces

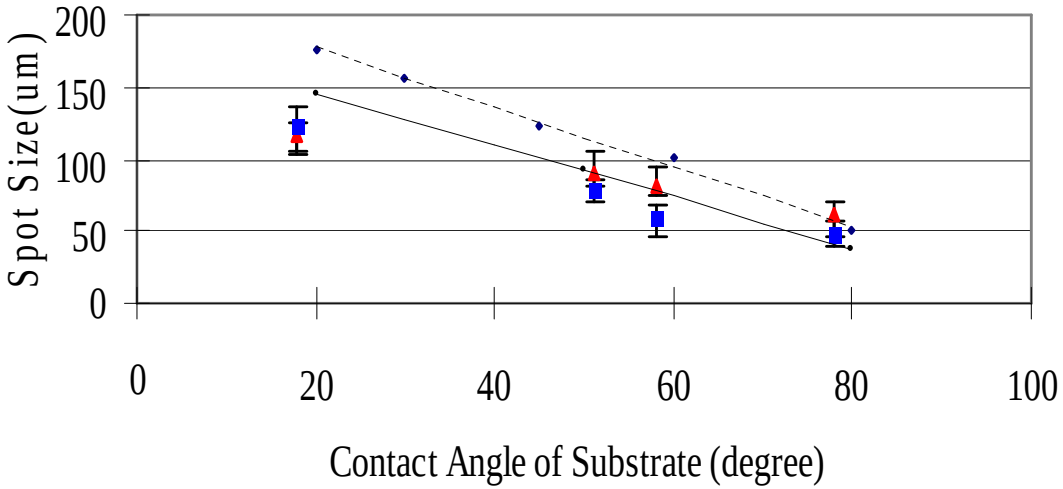

On different wettability of surface, the spot size of soft printing decrease with the decreasing of the surface wettability.

Simulation

---- solution viscosity (1.02cp)

—— solution viscosity (3.20cp)

Experiment

▲ fluorescent observation spot

■ optical microscope observed spot

PBS+30%glycerol solution(viscosity 3.20)

C. Ho, F. Tseng, and C. Chieng, J MM, 2005.

Bio-fluid 微陣列填充與壓印晶片系統

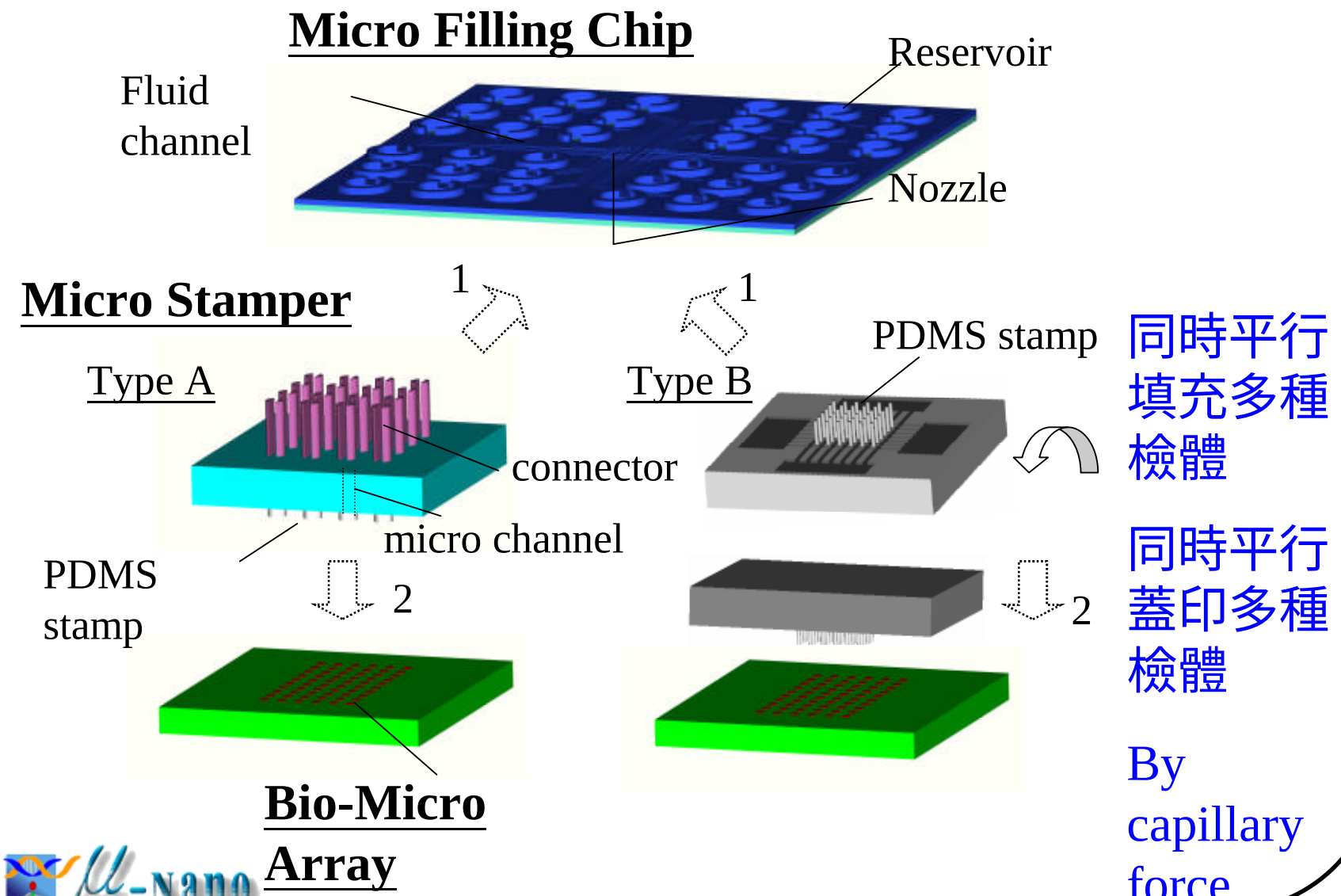

Teflon溶液轉印於導棒周圍

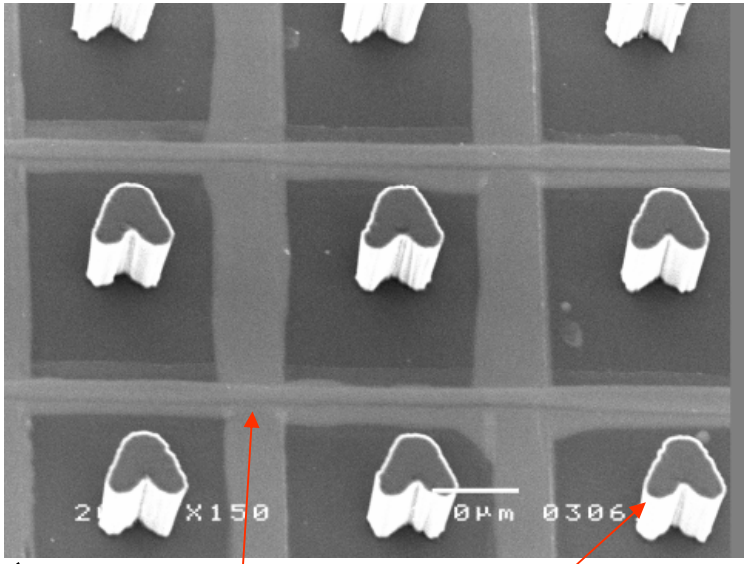

Teflon　　Su8 導棒

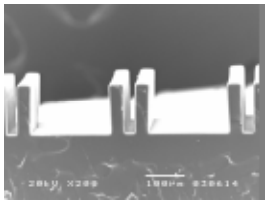

轉印Teflon用的PDMS

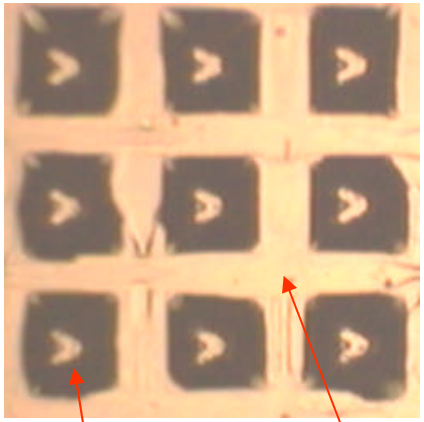

水珠　　Teflon 疏水區

液珠被Teflon限制住,區隔分離良好

微陣列壓印晶片

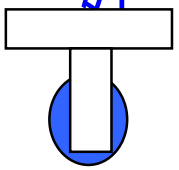

傳統的單支PDMS轉印溶液易擴散. 太乾則轉印上去的量不夠

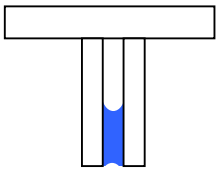

改良式的PDMS印章轉印溶液

(可適用於轉印其他溶液)

微陣列壓印晶片

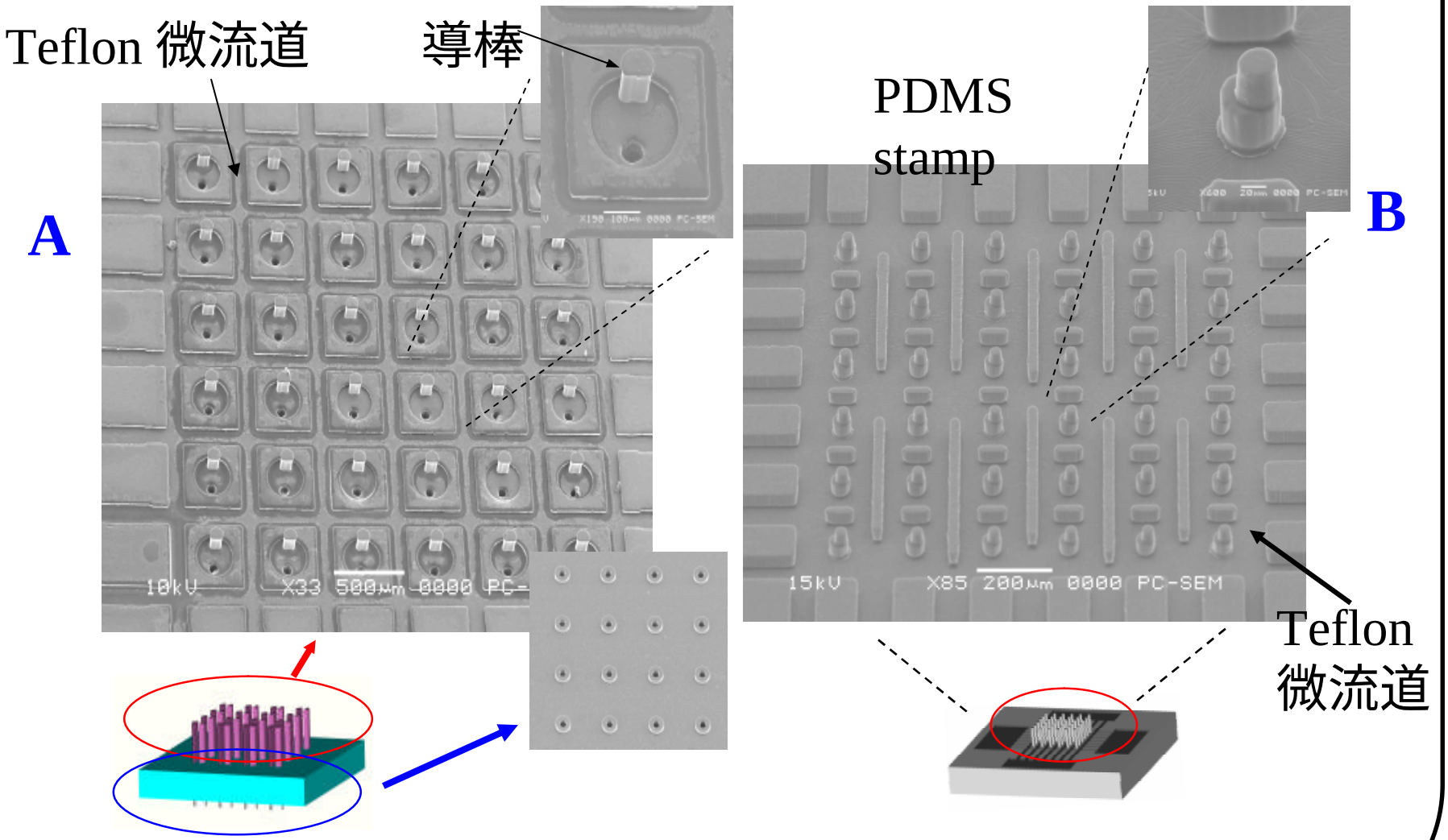

Type A Connector-filling micro stamper

Type B PDMS stamp-filling

Teflon疏水區隔防止填充時側向擴散

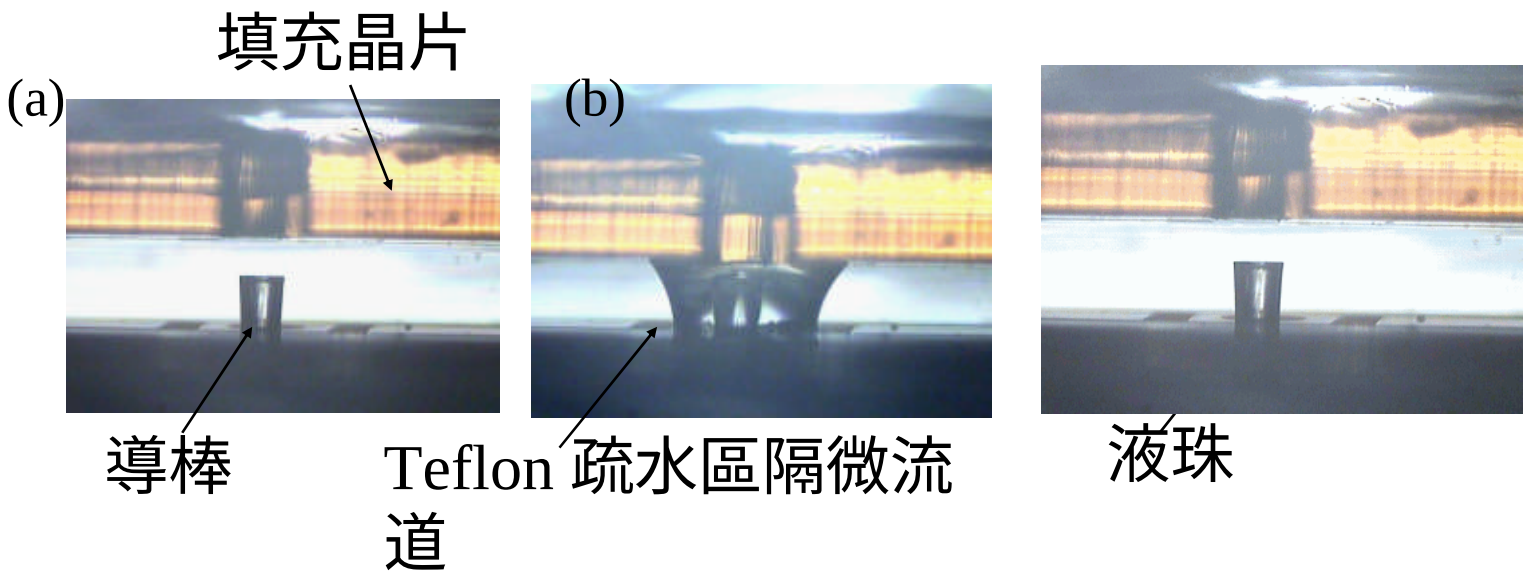

有Teflon作疏水區隔

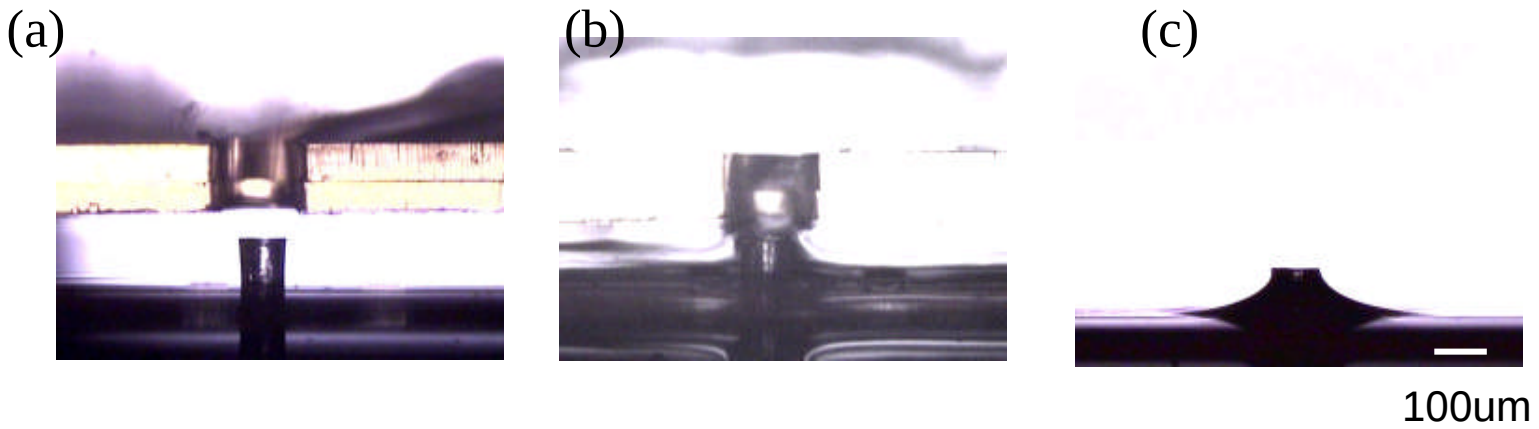

無Teflon作疏水區隔

晶片結合填充過程

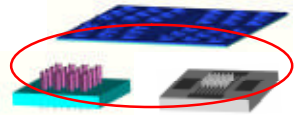

填充晶片之填充孔液面被限制住無擴散液體留在導棒上

Type A

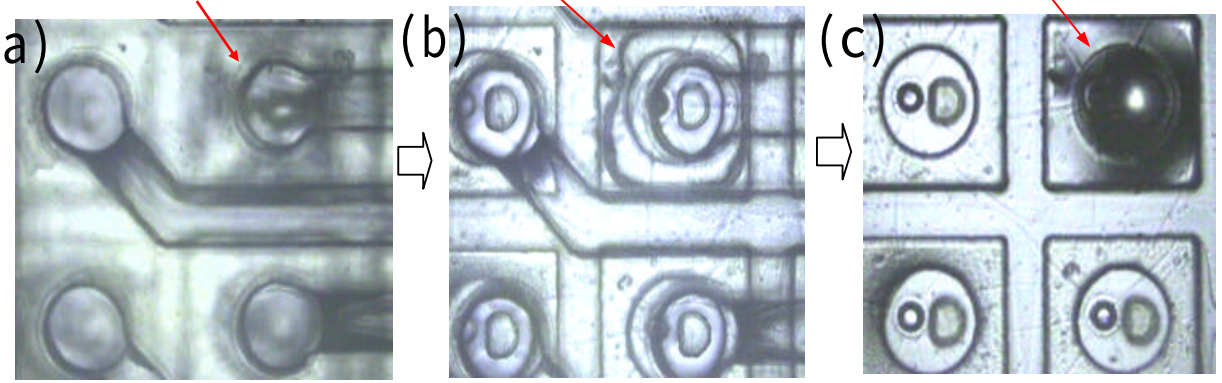

Type B

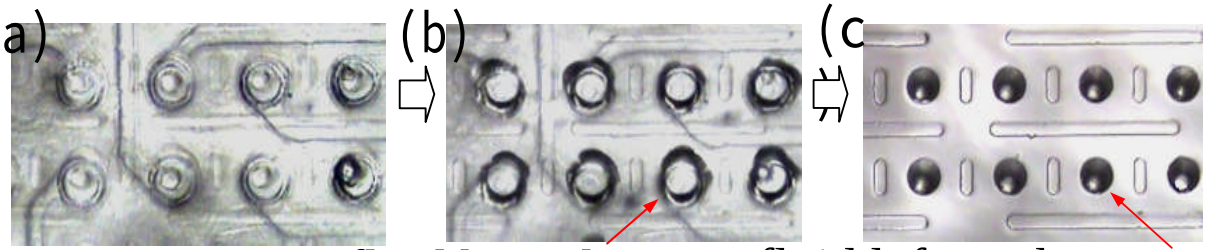

fluid boundary

fluid left on the PDMS stamper

填充晶片與壓印晶片結合填充時

液體被週遭Teflon 所限制住，無擴散

填完後 移開填充晶片，液珠留在壓印晶片上

PDMS同時平行一次蓋印多種之結果

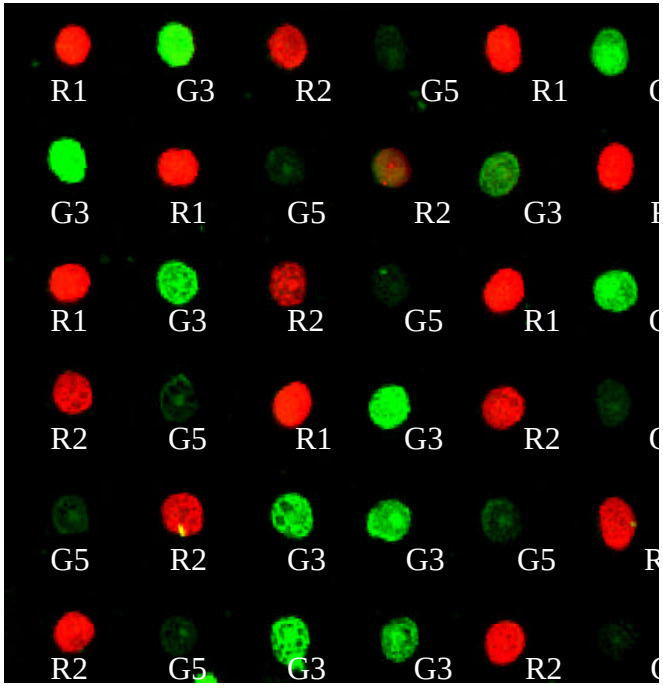

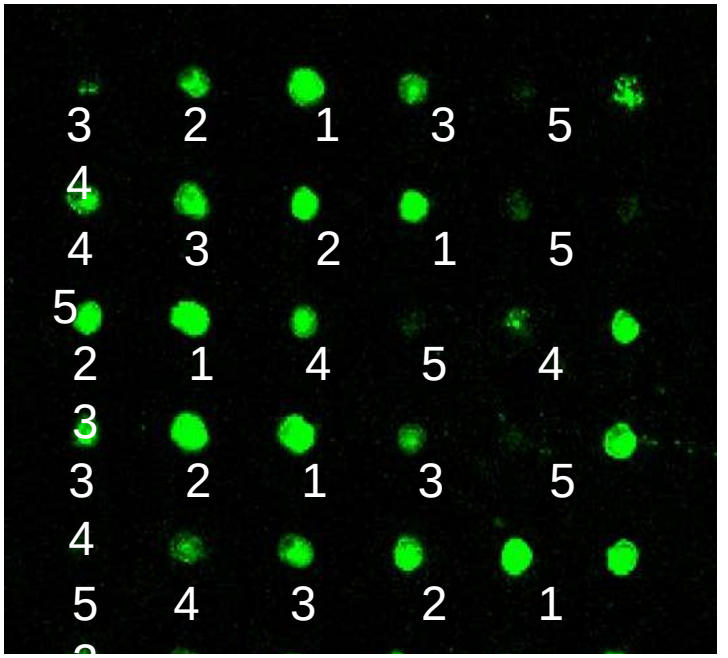

R1: anti-mouse IgG cy5 0.6mg/mL,

R2: anti-mouse IgG cy5 0.1 mg/mL,

G1: anti-rabbit IgG cy3 1.0mg/mL

G2: anti-rabbit IgG cy3 0.8mg/mL,

G3: anti-rabbit IgG cy3 0.4mg/mL,

G4: anti-rabbit IgG cy3 0.2mg/mL

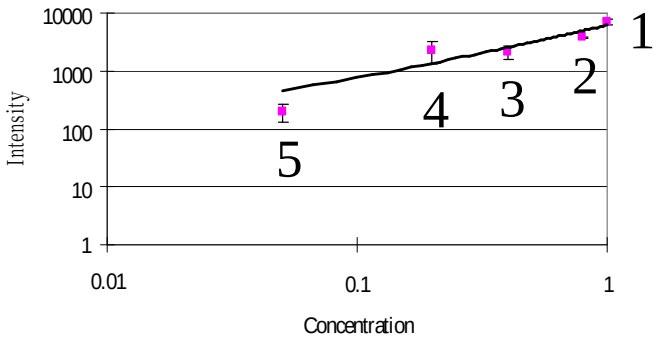

Self-Directed Movements of Droplets on Radially Patterned Surfaces Based on Self-Assembled Monolayers (Cont'd)

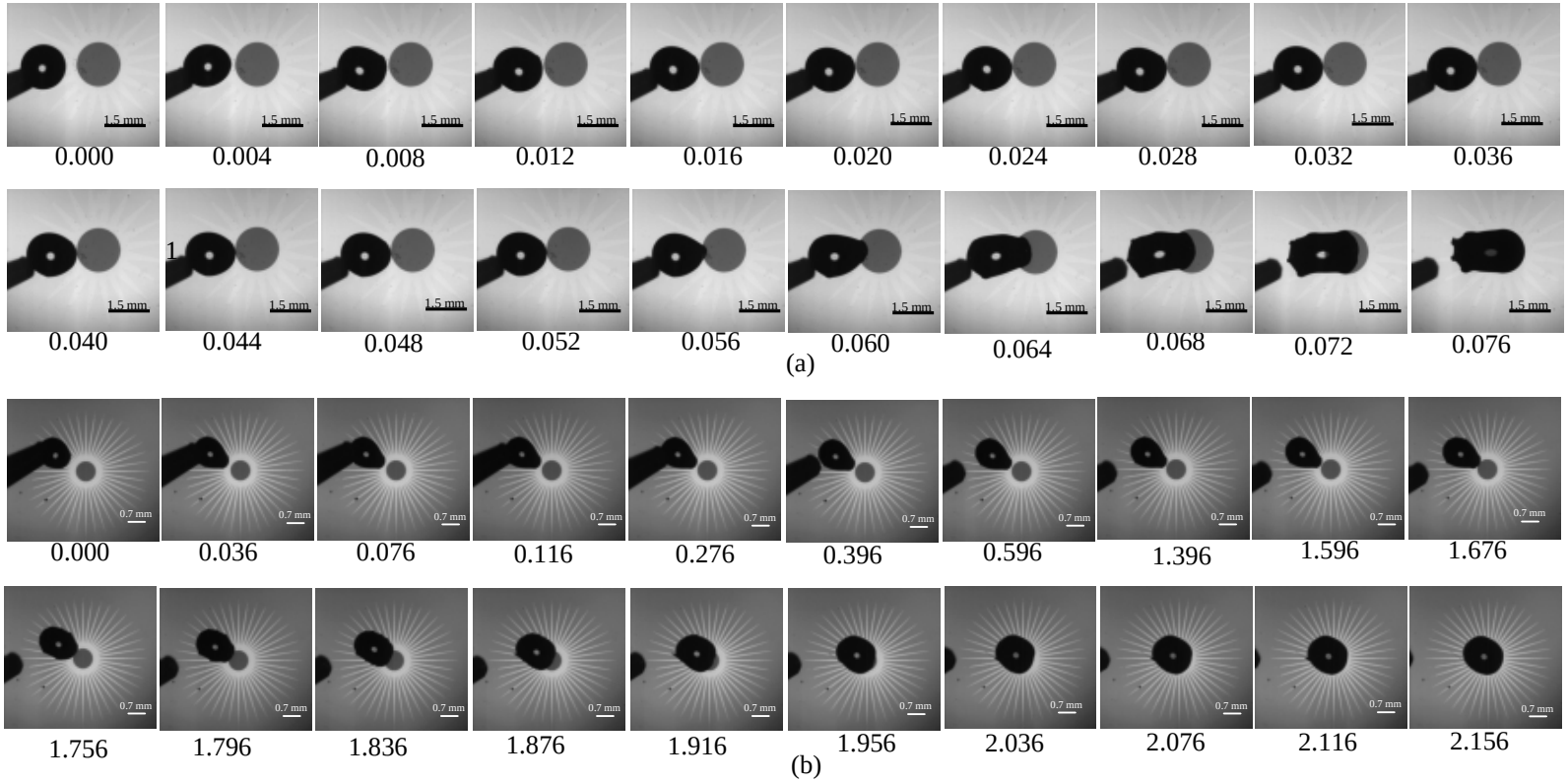

The motions of (a) 1.1 μL DI water droplet on the **dual SAMs** and (b) 0.4 μL DI water droplet on the **single SAM** systems taken using high speed CCD camera with a speed of 250 frames/sec (units in sec).

5. Bio-detection Chip

Micro Bio-Optics

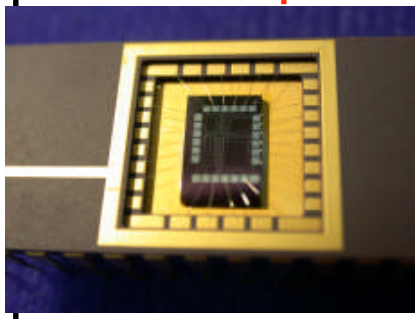

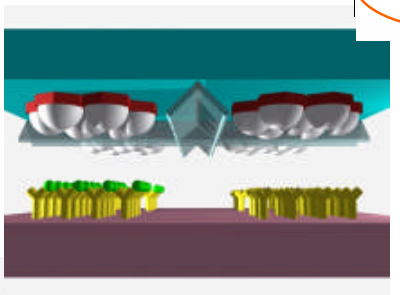

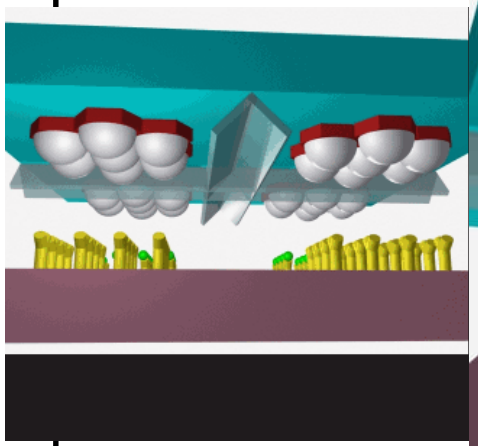

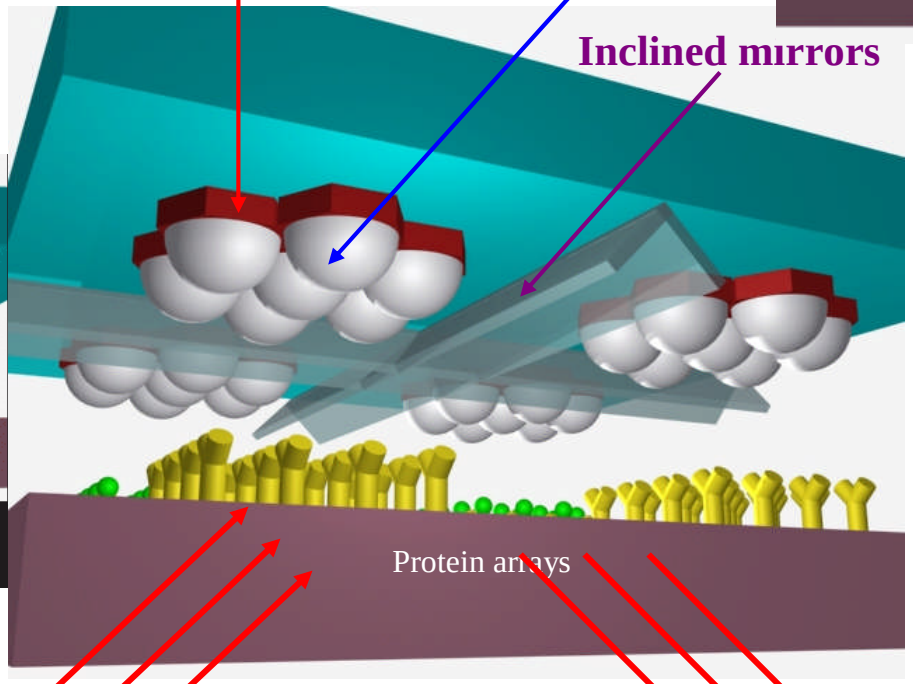

Characteristic:

1.In parallel detection

2.Fast

3.Near distance

4.Evanescent wave excitation, low background

Light input

Light output

ELISA of tumor marker test result

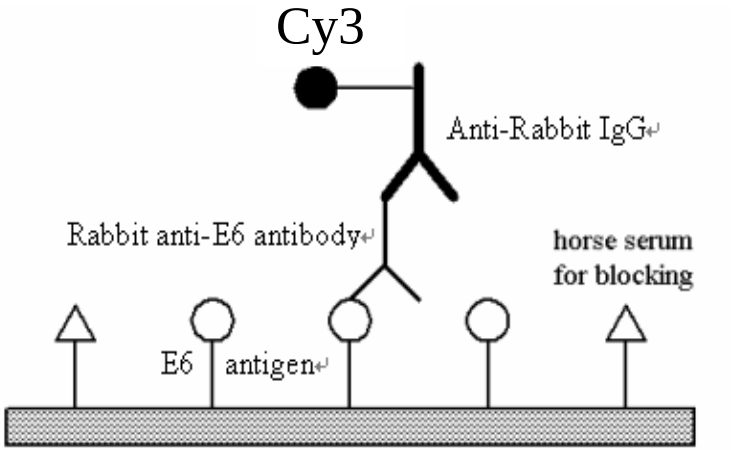

- Hurp: liver cancer antigen
- E6 Papillomavirus antigen

ELISA (Enzyme linked immunosorbent assay) bio-reaction detection.

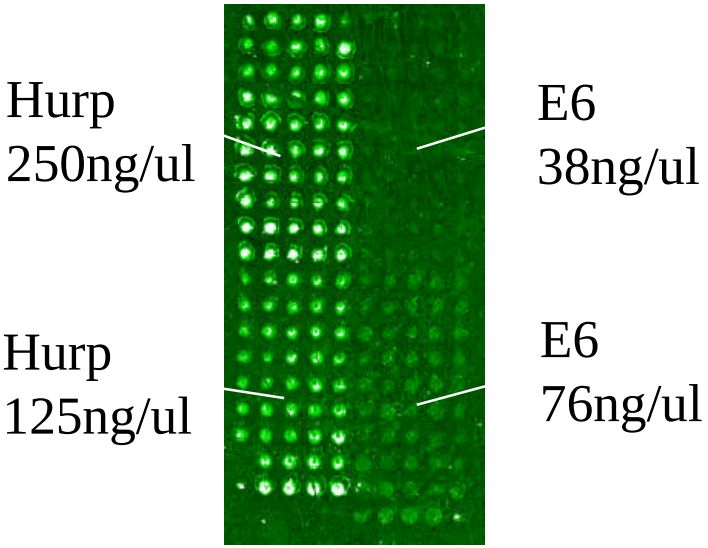

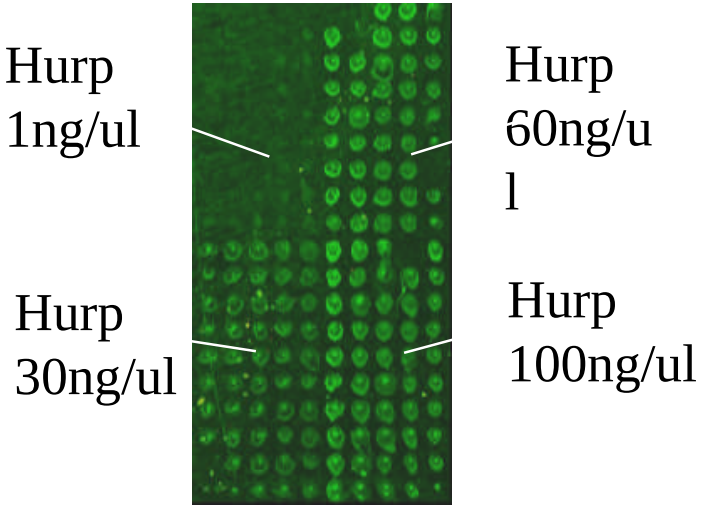

Protein Binding Efficiency Improvement by Mixed SAMs

Single SAMs for Protein binding

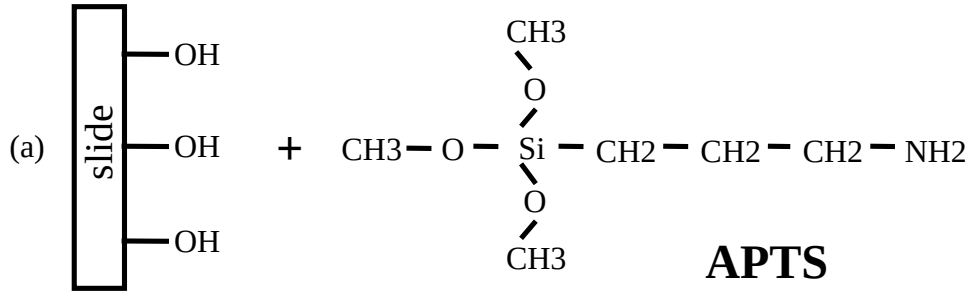

APTS
(aminopropyltrimethoxysilane)

Methoxyl group reacted with hydroxyl group

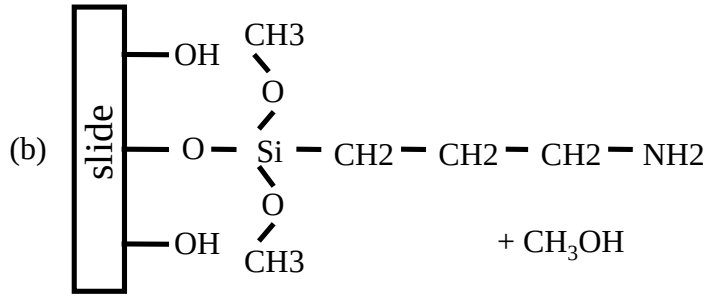

And

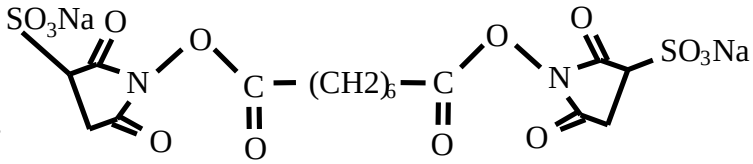

BS3
(bis-sulfo-succinimidyl suberate)

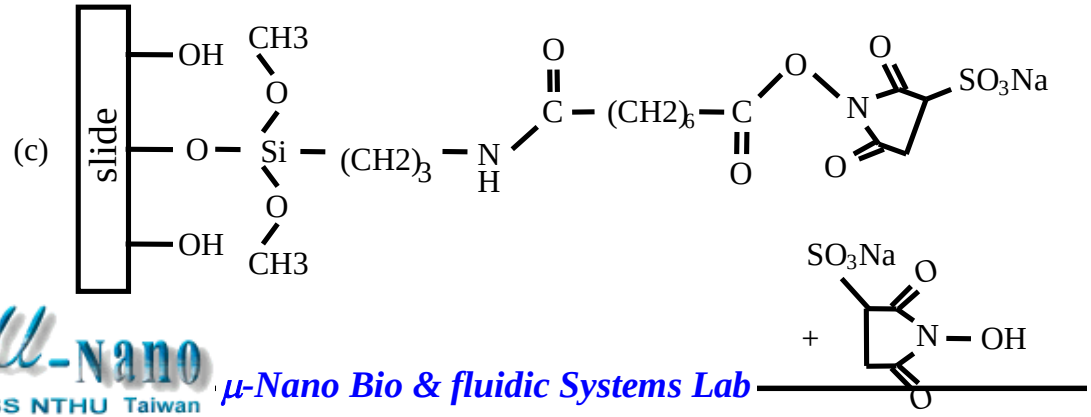

Antibody recognition/binding efficiency on protein chip

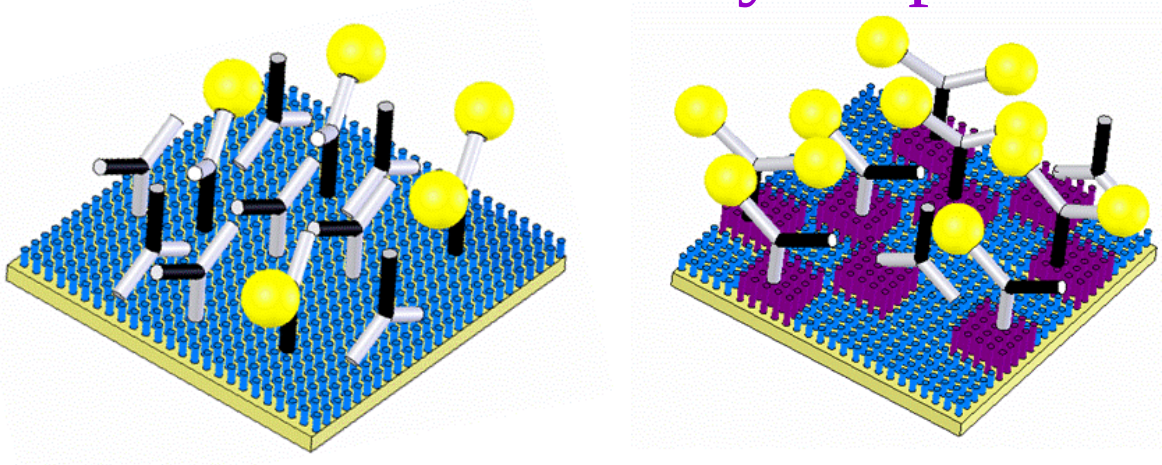

The schematic diagram of the principle for the improvement of recognition efficiency of antibody to antigen by mixed SAMs surface.

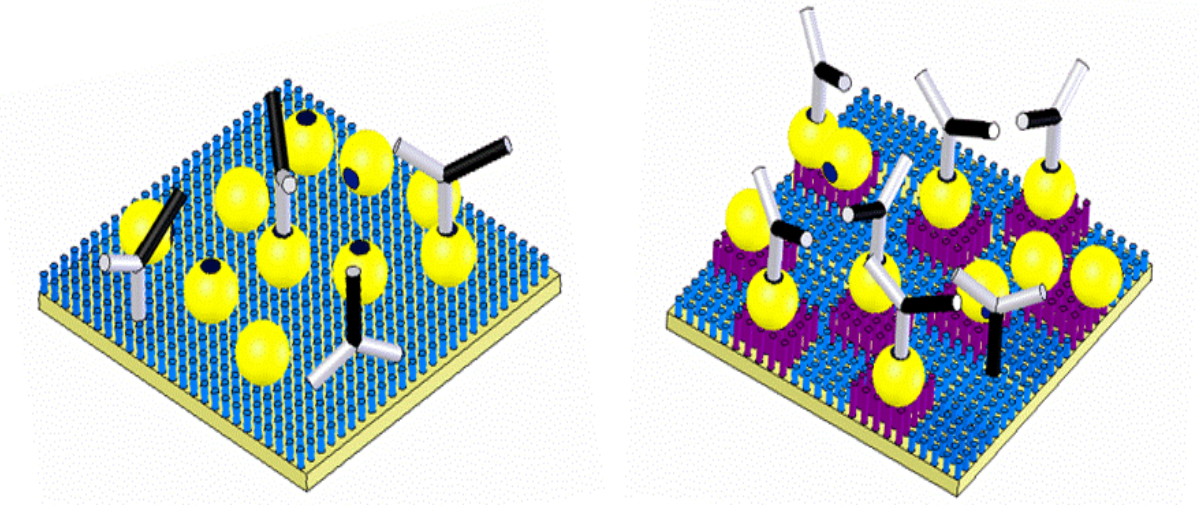

The schematic diagram of the principle for the improvement of binding efficiency of antibody to antigen by mixed SAMs surface

Antibody recognition/binding efficiency measurement by SPR and Fluorescence for different Mixed SAMs

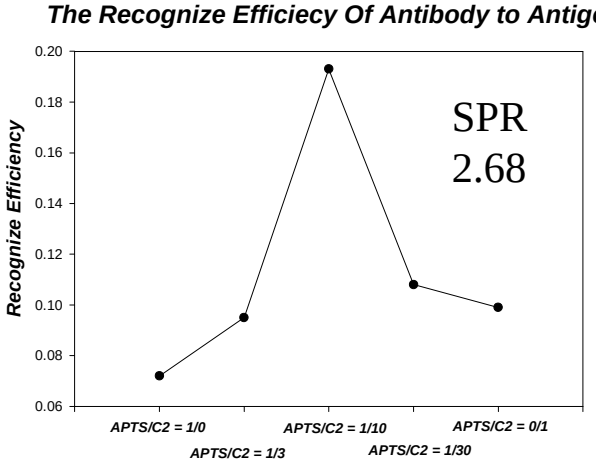

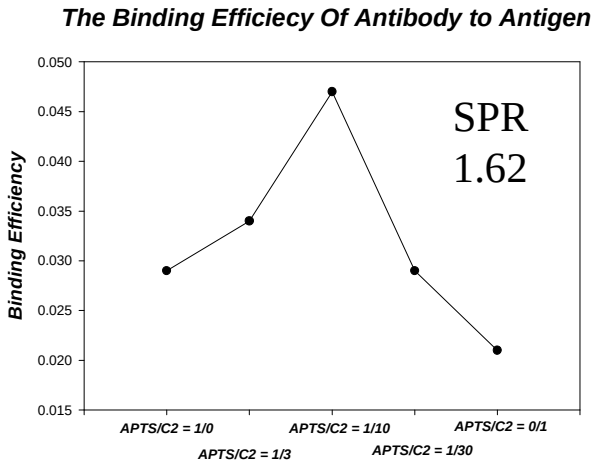

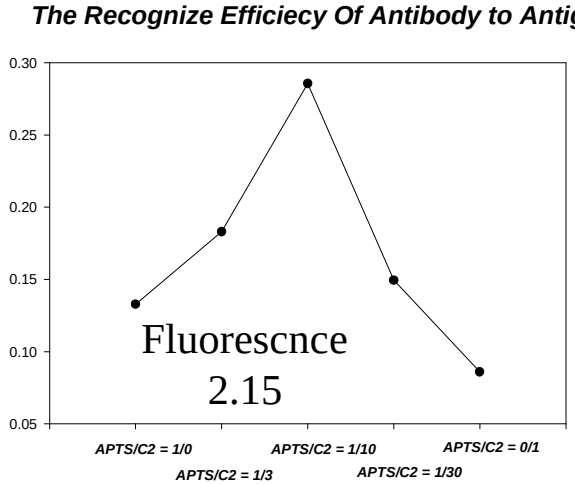

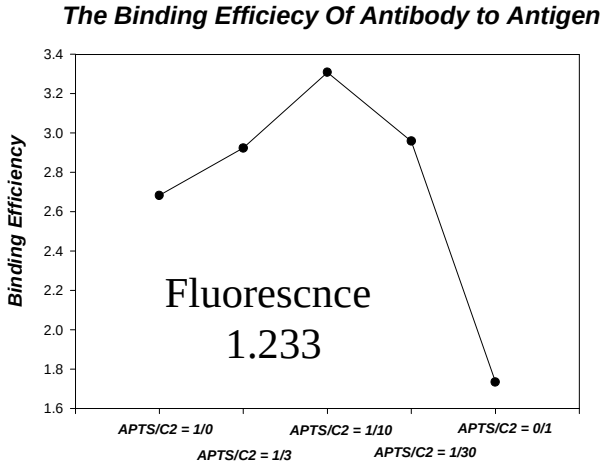

C. Wu, F. Tseng, and C. Chieng, Submitted Langmuir, 2006.

The mixed SAM surface *n*-alkanethiol Surface model

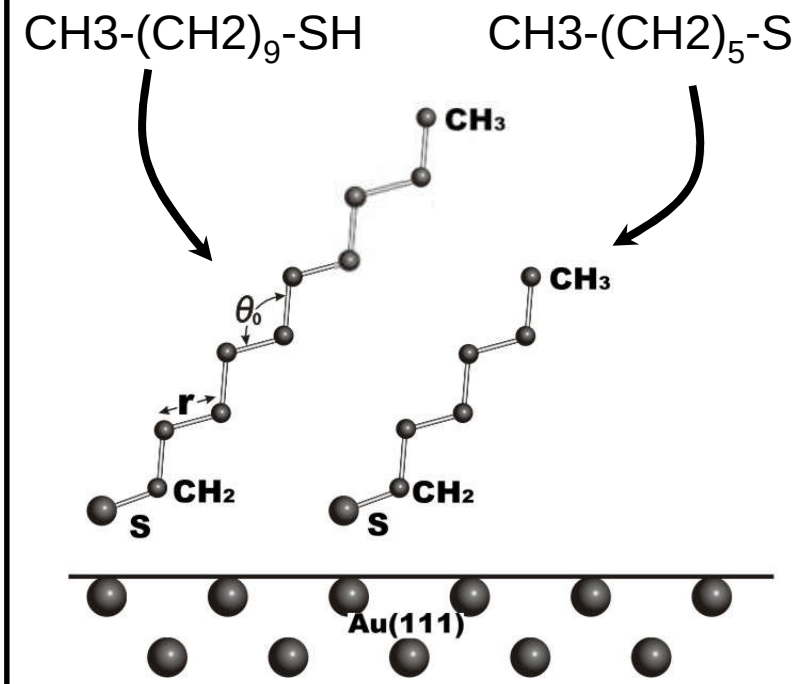

1-decanethiol (C9) 1-hexanethiol (C5)

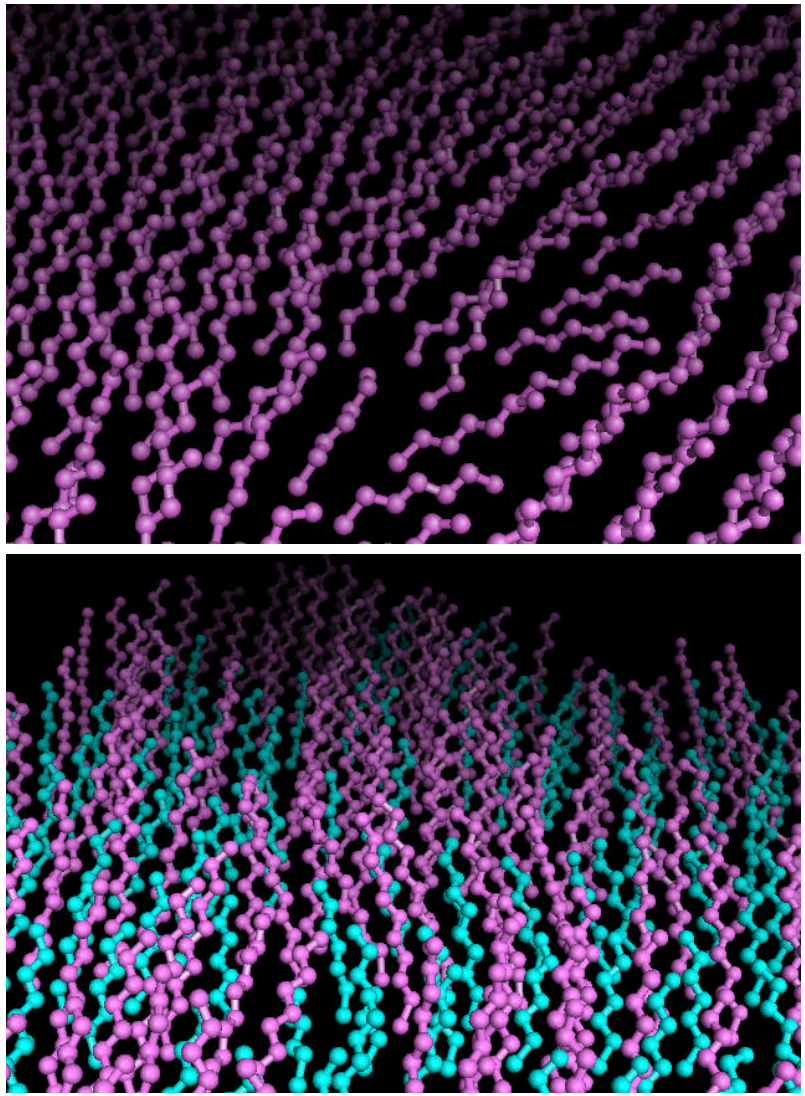

Oncoprotein - E6

- E6 is a 156 amino acid protein
  - MASTSASSQPSTLYQLCKDFGLTLRNLQICCIWCKNHLTSAEAYAYHFKDLHVV WKKGFPYAACAFCLEFYSKVCALRHYDRSAFWHTVEQETGLLLEEQIIRCAICQK PLSPSEKDHHIYNGRHFRFILNRWTGRCTQCRE
- E6 is a oncoprotein of human papillomavirus associated with cervical cancer
- The E6 structure is not yet available.

Predicted structures of E6

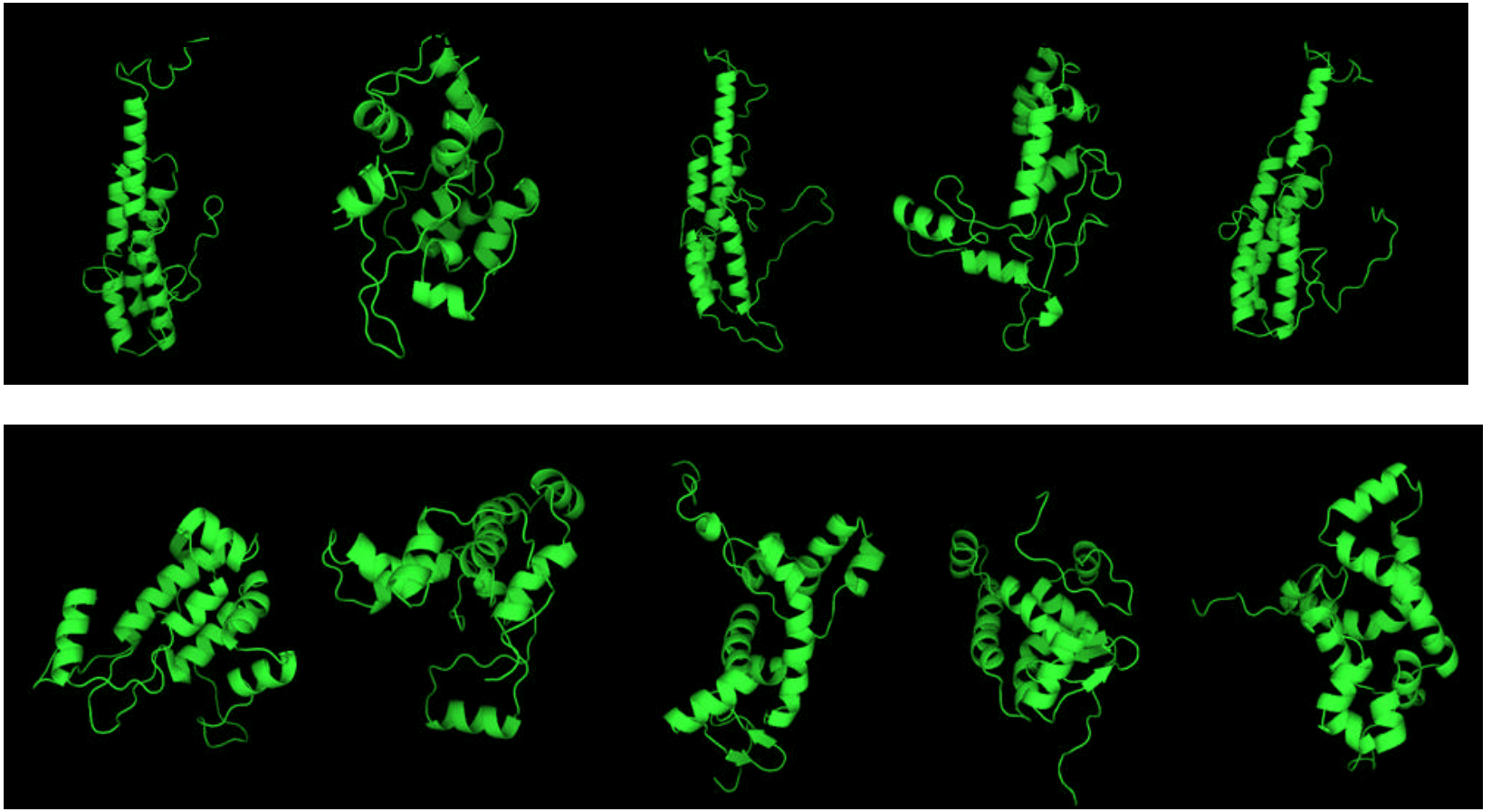

Robetta server : http://robetta.bakerlab.org/

MD simulation on C5:C9=1:1 (Orientation1)

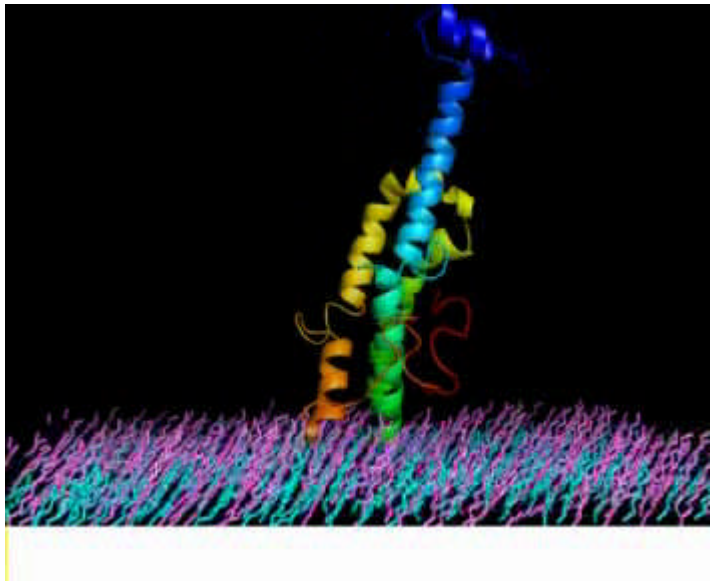

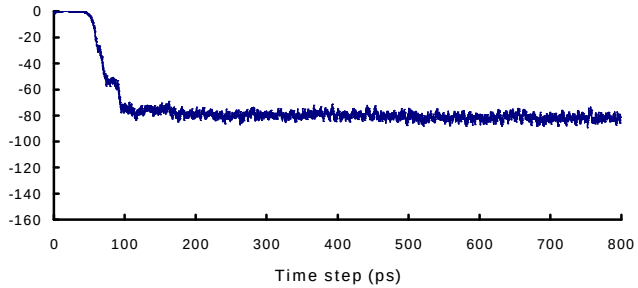

MD simulation on C5:C9=1:1 (Orientation2)

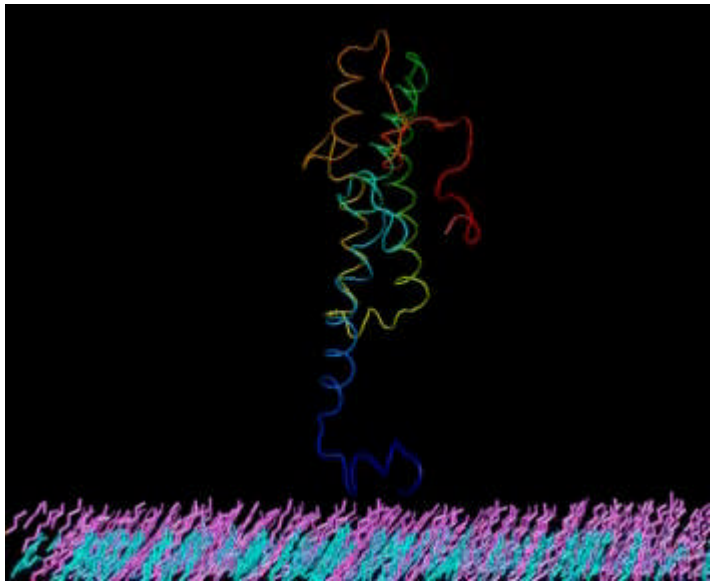

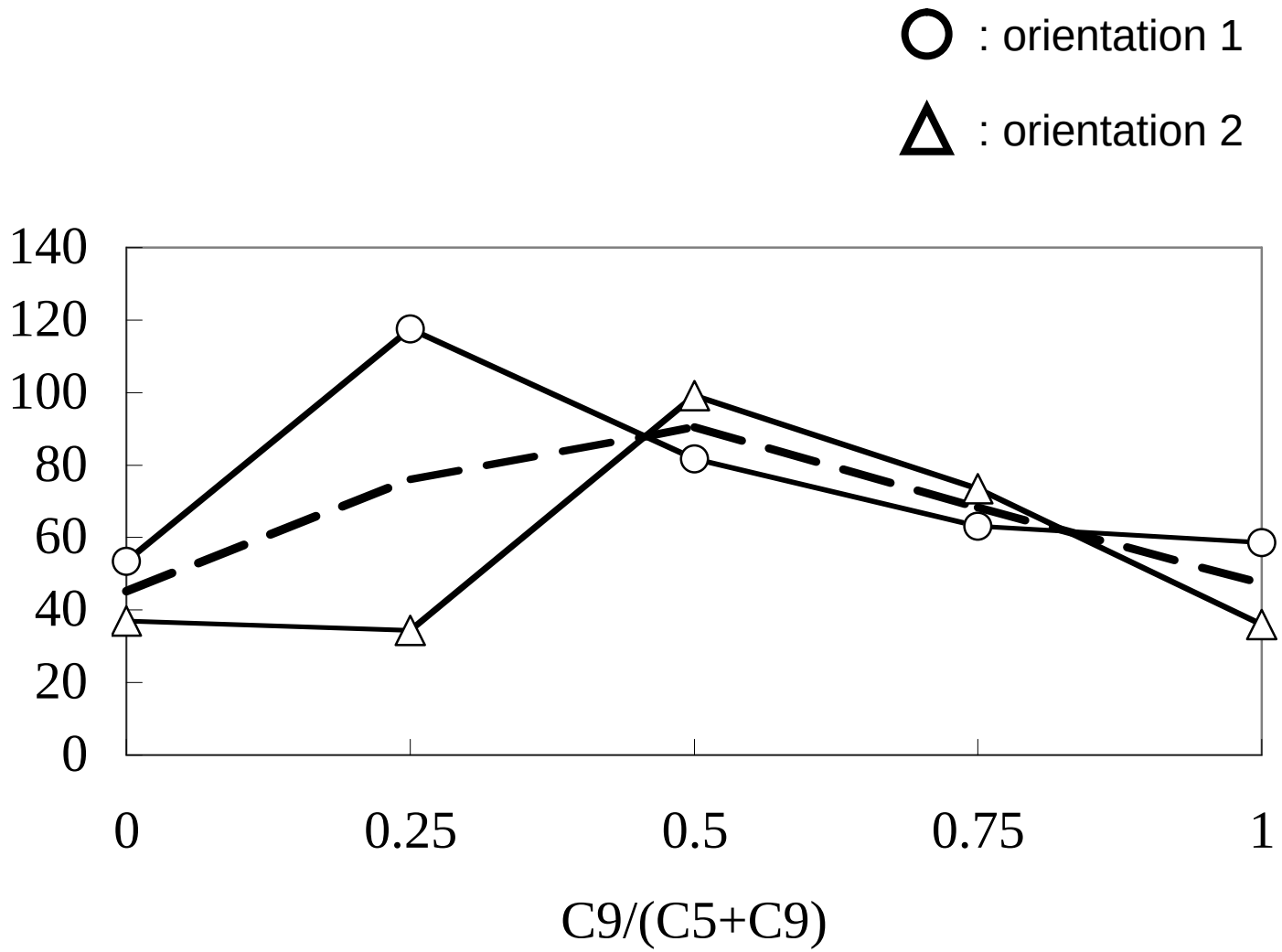
: orientation 1
: orientation 2
140
120
100
80
60
40
20
0
0
0.25
0.5
0.75
1
C9/(C5+C9)

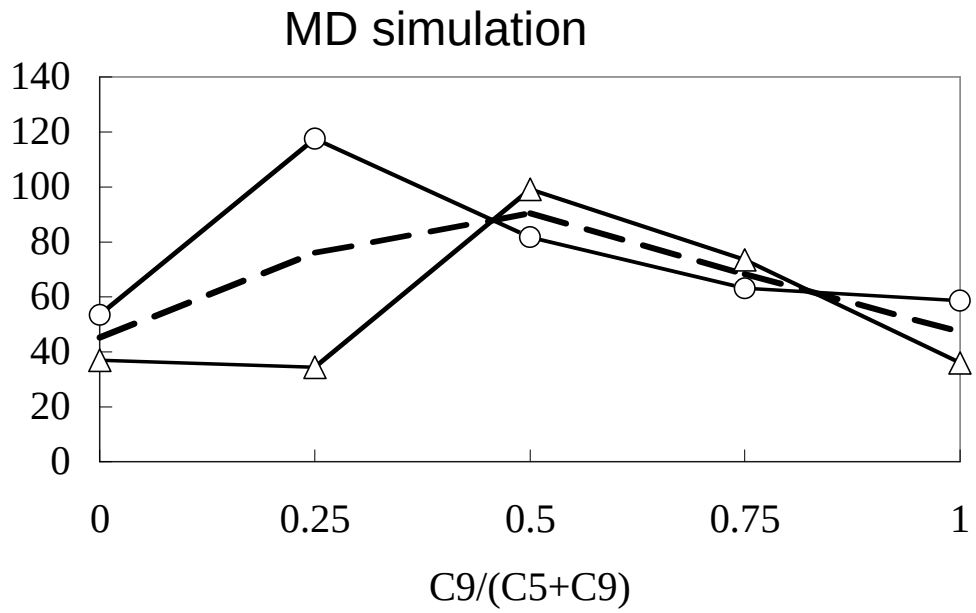
MD simulation
140
120
100
80
60
40
20
0
0
0.25
0.5
0.75
1
C9/(C5+C9)

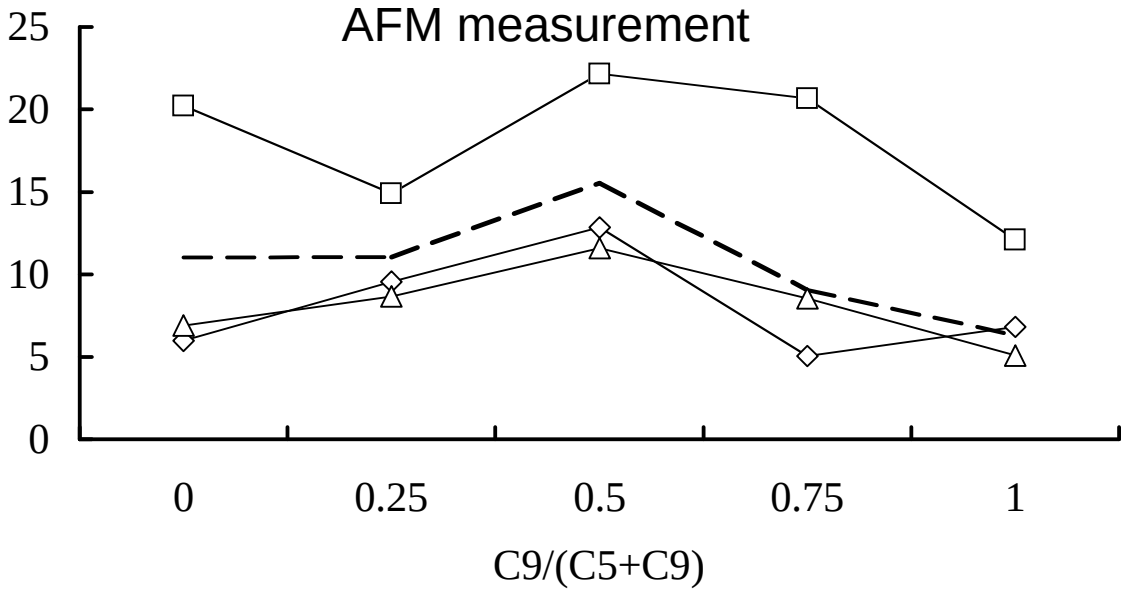
AFM measurement
25
20
15
10
5
0
0
0.25
0.5
0.75
1
C9/(C5+C9)

傳統採用生物血清於晶片上之鍵結阻絕實驗流程

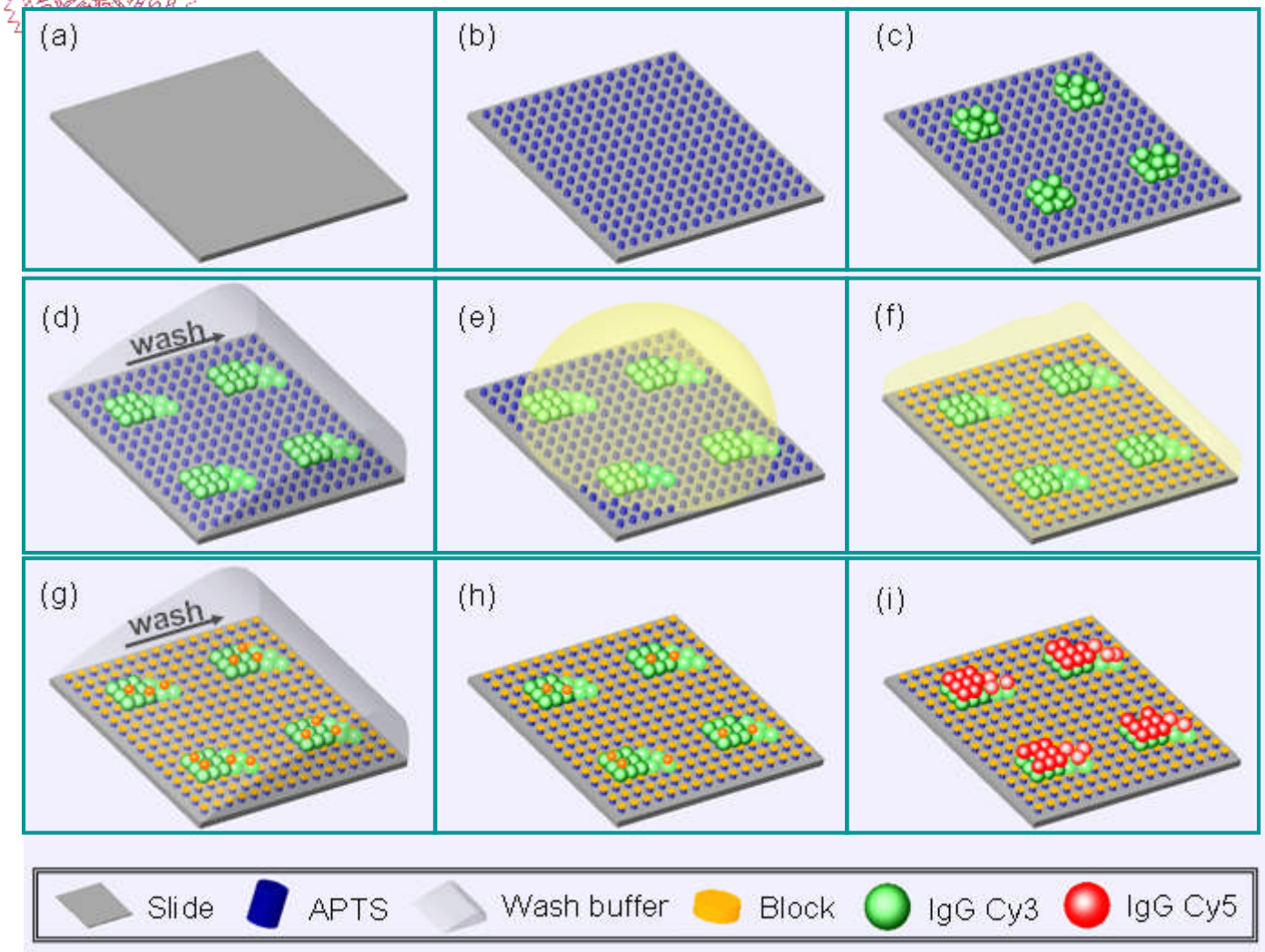

(a) 清潔載玻片

(b) 生長APTS

(c) 點上過量濃度的第一級抗體

(d) 清洗試片

(e) 加入生物血清鍵結阻絕試劑

(f) 鍵結阻絕完成

(g) 清洗試片

(h) 露出受生物血清分子沾黏的第一級抗體

(i) 加入第二級抗體作辨識接合

IgG Cy3 (第一級抗體)：Rabbit anti-mouse IgG Cy3

IgG Cy5 (第一級抗體)：Goat anti-rabbit IgG Cy5

Prof. Fan-Gang Tseng

Vapor phase bio-blocking

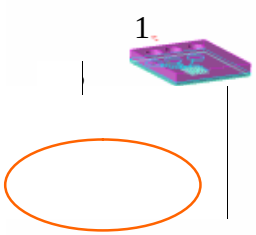

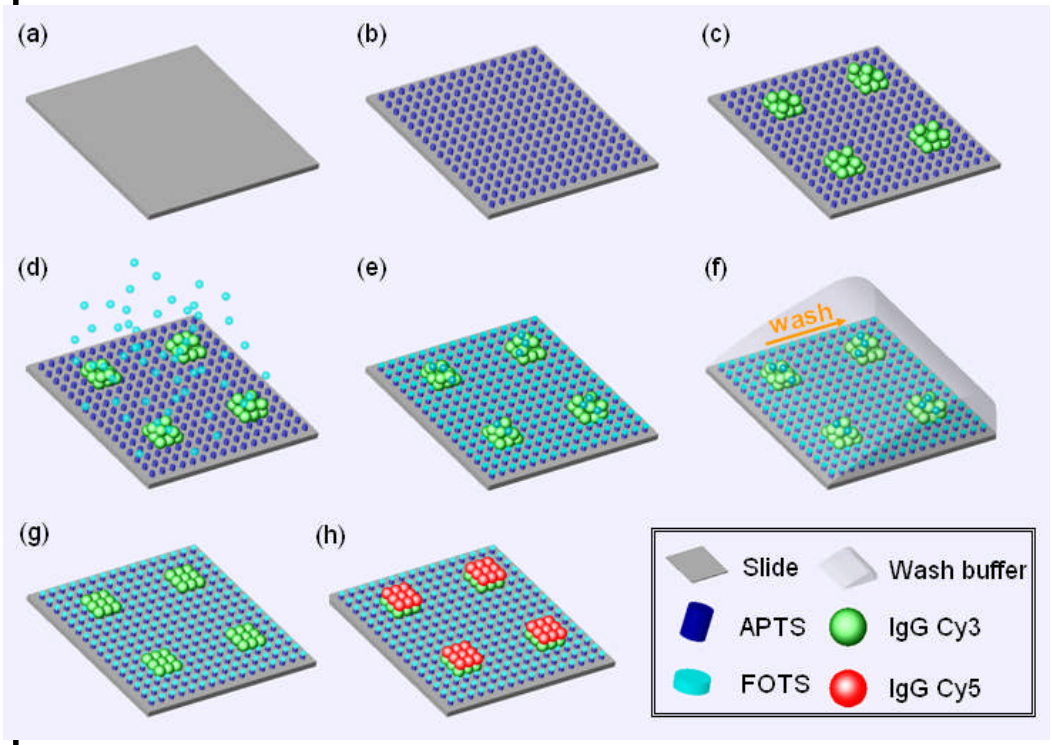

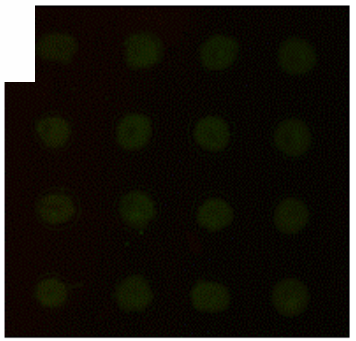

SiO2_no block

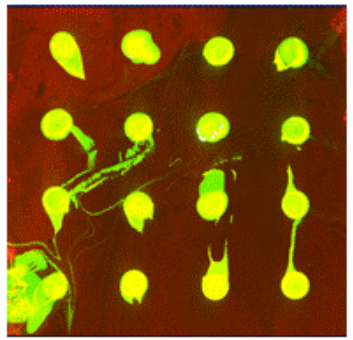

APTS_no block

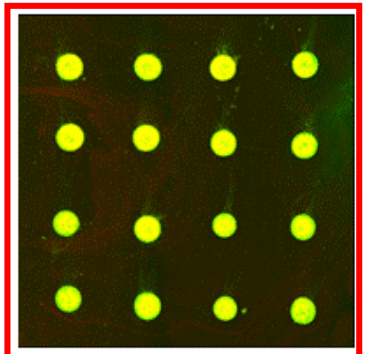

FOTS

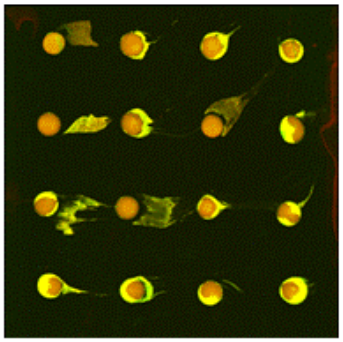

BSA

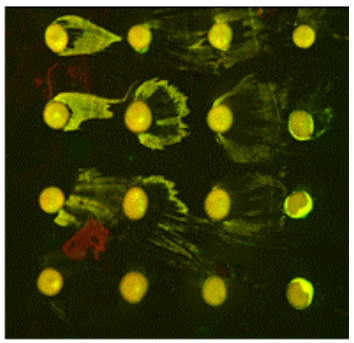

MILK

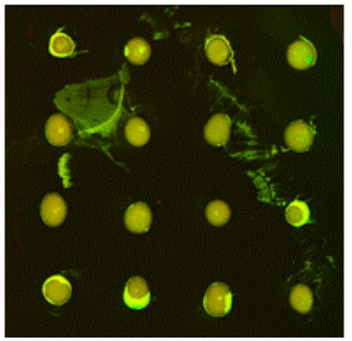

HS

Binding time improved from hours to 5 minutes, efficiency improved by 2-4 folds!!!, no tailing issue!

奈米國家型科技計畫學術卓越創新研究計畫構想

分升侷限空間激發及表面張力高度分子集中之單一分子奈米陣列酵素動力分析

The Kinetics/Dynamics of Single Enzyme Molecule Array Excited in fL-Confined Volume with Surface Tension Driven Concentration

計畫主持人：曾繁根 教授，國立清華大學/工程與系統科學系

奈微米生醫系統，奈微米流體物理(總計劃及子計畫一)

計畫共同主持人：潘榮隆 院長/講座教授,國立清華大學生命科學院

單一分子奈米陣列之酵素動力學研究(子計畫二)

計劃共同主持人：魏培坤 副研究員，中央研究院應用科學中心

近場侷限空間螢光激發及單分子遠場觀測(子計畫三)

12.06.2006

Importance and Limitation of SMD

Advantages:

1. Single molecule events possible
2. Low background noise
3. Low-middle concentration
4. High parallelism

Disadvantages:

1. Ambiguity of single molecule immobilization/reaction
2. Random distribution
3. Low possibility of single molecule event-huge effort to obtain statistically meaningful data
4. long observation time -not easy for dynamic observation
5. Numbers of proteins on a cite (chamber, bead)
6. Low dynamic range

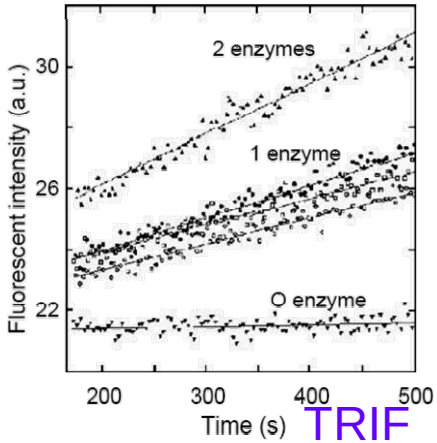

TRIF

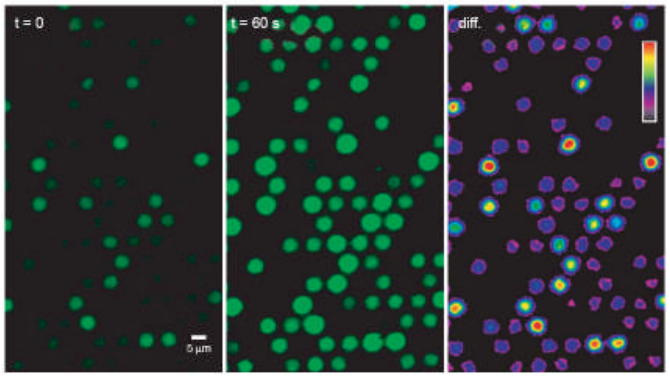

Nature Biotechnology, 2005

Confocal

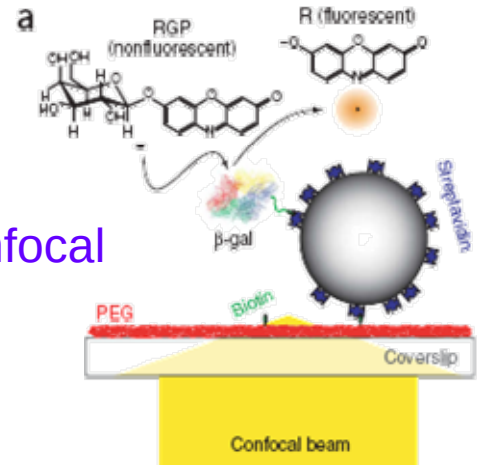

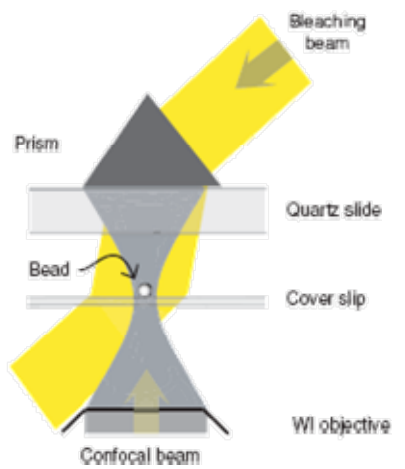

Nature Chemical Biology, 2006

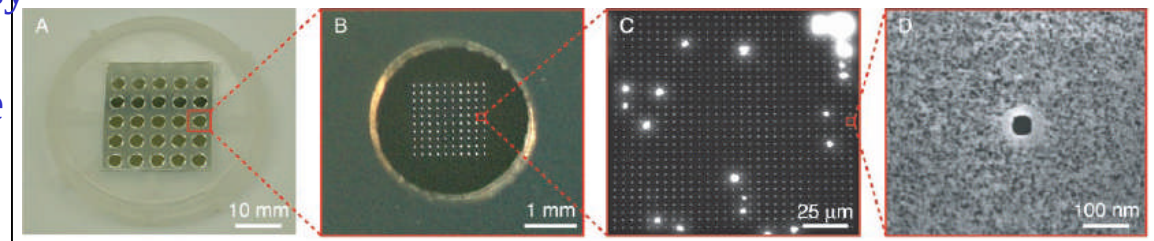

1D wave guide

Science, 2003

Acknowledgements

- **The works were/are supported by National Science Council, Taiwan, through:**

1. National Nanotechnology project, NSC
2. Biomedical and Pharmaceutical National Project Program, NSC
3. NSC Research Program
4. 榮台聯大跨領域計劃

- **Collaborators:**

Prof. C. C. Chieng(錢景常), ESS Dept., NTHU
Prof. P. K. Wei(魏培坤), Applied Science, Academia Sinica
Prof. C. C. Yang(楊崇熙), Director/Nanomedicine Center, NHRI
Prof. M. J. Lin(林茂榮), NYMU
Prof. R. L. Pan(潘榮隆), H. M. Huang(黃海美), Life Science Dept., NTHU